Zeitschrift: IABSE reports = Rapports AIPC = IVBH Berichte
Band: 69 (1993)

Rubrik: Theme 4: Structural properties

THEME 4

STRUCTURAL PROPERTIES

Leere Seite
Blank page
Page vide

In-Service Lateral Stiffness of Steel-Framed Buildings

Rigidité latérale des bâtiments avec ossature métallique sous l'effet des charges de service

Seitliche Steifigkeit von Stahlskelettbauten unter Gebrauchsbelastung

Byron J. DANIELS
Researcher
TNO-Bouw
Delft, The Netherlands

Peter de WINTER
Researcher
TNO-Bouw
Delft, The Netherlands

Piet van STAALDUINEN
Researcher
TNO-Bouw
Delft, The Netherlands

Paul WAARTS
Researcher
TNO-Bouw
Delft, The Netherlands

SUMMARY

This article summarises theoretical and experimental work undertaken as part of a research project entitled «Serviceability Deflections and Displacements in Steel Framed Structures». The objective of this study is to examine the static stiffness of steel-framed structures under working loads. Experimentally this is done using a pulse load induced by a hammer blow. Numerical models of the structure include structural components, exterior cladding and interior partitions.

RESUME

Cet article représente un résumé des travaux théoriques et expérimentaux dans le cadre d'un projet «Serviceability Deflections and Displacements in Steel Framed Structures». L'objectif de ces études est d'examiner la rigidité statique des bâtiments avec ossature métallique soumis à des charges de service. Expérimentalement ceci est fait in situ au moyen d'excitations dynamiques. Des modèles théoriques sont construits qui tiennent compte d'éléments structuraux classiques, de panneaux extérieurs et de murs intérieurs.

ZUSAMMENFASSUNG

In diesem Artikel werden die Ergebnisse theoretischer und experimenteller Arbeiten zusammengefasst, die im Rahmen des Programms «Serviceability Deflections and Displacements in Steel Framed Structures» durchgeführt wurden. Ziel einer Teilstudie war die Untersuchung der statischen Steifigkeit von Stahltragwerken unter Gebrauchslast. Dazu wurde die Tragwerksantwort auf die Anregung mit einem Impulshammer gemessen. Numerische Modelle der Konstruktion berücksichtigen die Stahlbauteile, Fassaden und inneren Trennwände.

1. INTRODUCTION

Increasing adoption of limit states based approaches to the design of steel structures has tended to concentrate researcher's attentions on the need to reliably predict load levels corresponding to the attainment of the structure's ultimate static strength. Thus design is based on scientific studies that ensure a suitable margin against plastic collapse, buckling, fatigue failure etc. Although codes and specifications also call for checks at serviceability, these are usually couched in rather simple terms and little real guidance on exactly how such checks be conducted or exactly what they are intended to achieve is provided. There is thus at least the suspicion of a considerable imbalance between the qualities of design for the ultimate condition and design for the serviceability condition.

It was in recognition of this that a three-part programme of research, focussing on static deflections of steel framed buildings, funded by the European Coal and Steel Community (ECSC), was stated in late 1990. It comprised:
-Investigation of the in-service performance of steel buildings (TNO-Bouw)
-Review of existing code requirements and their basis (University of Nottingham)
-Numerical studies and consideration of design models (University of Trento)

A report [1] giving the findings of each aspect of the work has been presented to the ECSC. The content of this paper is based on the in-service performance section and is complemented by three other papers at this conference which deal with the other topics.

2 DESCRIPTION OF THE MODELLED STRUCTURE

The building investigated is located at TNO-Bouw, Delft, the Netherlands (Building #11) and may be classified as an office building. This structure is representative of many low-rise steel-framed office buildings recently built in the Netherlands. An isometric view of non-structural components (exterior cladding and interior partitions) is shown in FIGURE 1. Schematic drawings of the structural frames, in the major and minor axes, are shown in FIGURE 2.

Column supports consist of base plates bolted to the caps of existing concrete pilings, which are located in holes in an existing ground slab (subsequently filled with concrete). In the major axis most beam to column connections are provided using half-height connection plates. In the minor axis, most beams are continuous and connected to the columns using cantilevered stud beams. An endoscope was used to check cross-bracing and cross-bracing to column connections.

Exterior cladding consists of minimally reinforced light-weight concrete panels, 15cm thick with openings for doors and windows. Upon close visual inspection no evidence of panel cracking, cracks between panels or cracks at the foundation level were evident.

The first floor slab is made of lightweight precast concrete units with a cast-in-place wearing surface. The roof consists of two dimensional trusses, cross-bracing and a deep-ribbed thin-walled steel decking. Both the first floor slab and roof provide a substantial degree of in-plane shear stiffness to the structure.

All interior partitions consist of 100 mm thick gypsum board. Partitions are glued to the floor slab, no attachment, however, is provided at the lateral or top edges of the partitions to the structural frame. Interior columns are covered with fire protection materials and enveloped in wooden boxes for architectural reasons. Partitions are butted against these boxes.

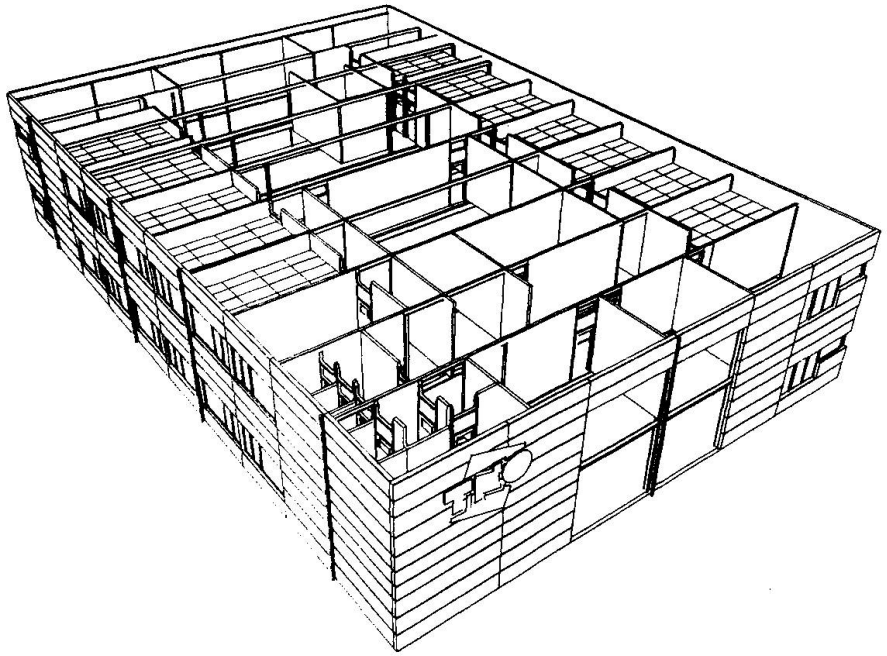

FIGURE 1: Isometrique view of non-structural components for building #11.

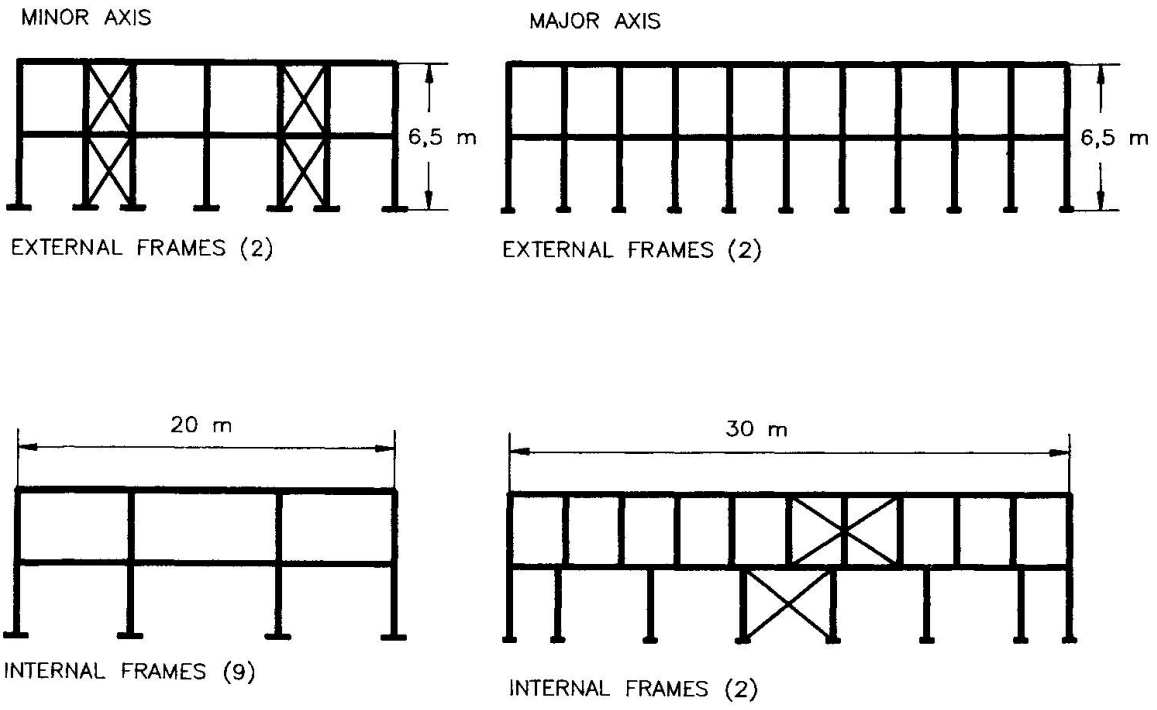

FIGURE 2: Schematic drawings of structrual frames for building # 11.

3. SERVICEABILITY MODELLING

3.1 Introduction

Significant interaction between structural and non-structural components (interior partitions and exterior cladding) may be present. The importance of this interaction depends upon the building type (office, industrial, low-rise, high-rise, etc.) the choice of non-structural components (wood, masonry, stone, glass, sandwich panels, profiled sheeting, etc.) and the type of connection between structural and non-structural components.

At service loads, some simplifications may be used to reduce model complexity. First, existing models describing the behaviour of the structural system at ultimate load levels are used. Second, non-structural components are described using their initial (un-damaged) stiffness. Past research on such components has tended to concentrated on predicting failure loads and in many cases the initial stiffness is reported. Lastly, connections between structural and non-structural components should remain un-damaged at service load levels. Connection types are categorised and their behaviours simplified (full moment connection, pin-ended, etc.). Upon close inspection no evidence of previous movements between structural frame and panel was observed. Connections have received even less attention in the literature than the in-service behaviour of non-structural components.

3.2 Modelling of building #11

Two-dimensional linear finite element structural models were constructed (major and minor axes). This is the same level of sophistication which was used for ultimate limit design calculations. Static and dynamic analyses based upon these models were performed. This provides two checks between measurements and predictions: the lateral stiffness and the lowest side-sway natural frequency.

Standard six-node beam elements and point mass elements were chosen to model structural components. Nominal section properties (cross-sectional area and moment of inertia) were used. A modulus of elasticity, E, of 210'000 N/mm2 and Poisson's ration, μ, equal to 0.3 were used to define basic steel characteristics. No plastification is expected thus plastification post yield criteria were not specified.

An upper bound estimation for cladding stiffness was assumed in the model: no movement is allowed between individual cladding panels or between panels and their foundation. Eight-node plate elements were used to model the exterior cladding. A nominal thickness of 15 cm for all elements was assumed. A modulus of elasticity, E, of 20'000 N/mm2 and Poisson's ratio, μ, equal to 0.25 were used to define basic concrete characteristics. No concrete cracking or crushing is expected. The exterior cladding is connected to the structural system (exterior columns) using structural angels (clips), which are bent to fit. Interior partitions were not included in the static model due to the lack of available connection to other components.

A nominal lateral load (equal to1N) was applied at the first floor and roof levels. The predicted values of horizontal drift were used to calculated side-sway stiffness using the following expression:

$$K = F / \delta$$

where:

K is the side sway stiffness
F is the applied lateral force
δ is the predicted lateral displacement

Static and dynamic analyses are performed for the following cases:

1.The entire building, assuming full interaction between cladding and the structural frame with cross-bracing. All columns are assumed to be fixed-ended ground level. *This represents the base case from which individual parameters are studied.*
2.The base case without cross-bracing.
3.The base case with columns pin-ended at ground level.
4. The base case with all connections between beams and columns pin-ended.
5.The structural frame only (including cross-bracing).

3.3 Summary of model predictions

A detailed summary of modelling results is available in the full ECSC report [1]. Based upon the results the following observations may be made based upon the static analyses:

-*Cladding vs. the structural frame.* The model predicts that the cladding is stiffer than the structural frame.
-*In-plane vertical cross-bracing.* Cross-bracing in the structural frame has a small but detectable influence at service load levels (cross-bracing, however, often is of greatest importance during the construction phase).
-*Beam to column connections.* The influence of beam-to-column fixity (fix-ended or pin-ended) is of secondary importance.
-*Column base fixity.* The influence of column base fixity (fix-ended or pin-ended) is of no practical importance.

The results of the dynamic analyses tend to support the conclusions of the static analyses.

4. TESTING

4.1 Introduction

The building tested is the same as that described in Chapter 2 and modelled in Chapter 3. The objective of these tests is to derive in-situ values of natural frequency and static lateral stiffness. This is achieved by exciting the building using an impact hammer and measuring the response (both displacement and acceleration). This testing method has been extensively researched at TNO-Bouw. A shaker (eccentric counter-rotating masses) were used to obtain a independent check of the hammer test results.

Structural properties (static stiffness and natural frequency) can be derived by measuring the time functions of both excitation and response. Time functions are converted into frequency response functions. Comparing the frequency response functions with mathematical models, structural parameters as stiffness, mass, natural frequency and damping can be derived. The full procedure behind the derivation of structural properties is beyond the scope of this paper, but is contained in the final ECSC report [1].

4.2 Field measurements

Impact hammer field measurements were made using the field testing equipment listed in TABLE 1. Excitation was applied by means of a 10 kg instrumented hammer or a 400 kg mechanical shaker. In both cases the structure was excited on the first floor in both major and minor axis several times to obtain statistically significant values.

Theoretically when the structure is excited by a hammer impulse all frequencies have the same magnitude in the frequency domain. In practice, higher frequencies can be suppressed by mounting a rubber tip on the hammer. In this manner more energy is input at lower frequencies. The hammer was instrumented with an accelerometer, thus the impact load is determined using the hammer mass and measured accelerations.

When using a shaker, measurements were made using frequency steps (1 Hz). In this way the frequency response function could be derived and the natural frequency estimated. Applied force was not measured directly but is calculated using rotating mass eccentricity and rotation frequency.

The response of the structure was simultaneously measured on the ground floor, first floor and roof level by means of acceleration and displacement transducers in the same direction as the applied force. Typically, displacement transducers give better results in very low frequency ranges ($1 < f <$ 20 Hz) and acceleration transducers give better results in the higher frequency range ($f > 20$ Hz).

Table 1: Field testing equipment.

Number	Description	Make	Type
6	Accelerometers	Sunstrand	S-700
6	Conditioner for Sunstrand	TNO-Bouw	C-S-700
6	Displacement transducers	Hottinger	B-3
6	Conditioners for Hottinger	Hottinger	KWS 3073
6	Amplifiers	Hottinger	Z 3576
1	Data acquisition system	Bakker	2570
1	Pulse hammer	TNO-Bouw	10 kg
1	Conditioner for hammer	B & K	2626
1	Mechanical exciter	TNO-Bouw	400 kg

4.3 Data reduction and test results

All signals were digitized and recorded using a data acquisition system. Afterwards the signals were converted to the frequency domain. This results in a complex frequency response function and in a coherence function between excitation and response.

For all locations and directions the natural frequency and static stiffness of the building are derived using a circle fit procedure assuming viscous damping. In the derivation of the stiffness the influence of higher order modes has been calculated. The fit procedure was carried out using the acceleration and displacement response signals.

The lateral load response, static stiffness, natural frequency and damping ratio of an entire as-build steel-framed building is thus measured using a hammer excitation. When measuring displacements response instead of acceleration response, the stiffness at ground floor level can be derived even when exciting at first floor level.

The coefficients of variation for stiffness estimations, per hammer blow, are in the order of 0.02. Average coefficients of variation (obtained by averaging all hammer blows at one specific location and direction) are approximately 0.20.

4.4 Comparison of testing methods

The determination of the natural frequency and static stiffness is potentially as accurate using a shaker as when using a hammer blow. With a hammer blow, however, measurements are both accurate and quickly obtained. Using a shaker, measurements must be made at many different speeds to obtain the buildings frequency response spectrum.

Irregardless of measurement quality, installation and measurement times for the hammer blow technique are much shorter than for the rotating mass. The rotating mass itself is heavy, requiring

special equipment to move it into location. In the case of the TNO building, it was necessary to install the rotating mass using a fork lift truck through a first storey window.

As the size of the structure increases so does the necessary energy input. For very large structures it may become difficult to supply sufficient energy in the low frequency range using a hand-held hammer.

5 COMPARISON OF TEST RESULTS AND MODEL PREDICTIONS

5.1 Introduction

An existing steel-framed building was modelled and tested under service load conditions. Static lateral stiffness and natural frequency were calculated and measured. A simple finite element model was used (two-dimensional, linear and consisting of beam and plate elements). This model is similar to the model used by the designer to predict the ultimate load carrying capacity of the structural system alone. Simple assumptions are used for parameters such as column fixity, joint stiffness, cladding stiffness and the interaction between structural and non-structural components.

Test values are reported for a statistically significant population, thus the mean and standard deviation have been estimated. All comparisons are given for mean values (for one particular structure) between typical design models including non-structural components and real structural behaviour at service load levels.

5.2 Summary

A comparison of measured and predicted values are shown in TABLE 2. Finite element model predictions and test results differ by 10% to 25%. Measured values are given for a confidence level of 90%, which implies the following:
-A 10% uncertainty in the major axis.
-A 25% uncertainty in the minor axis.

Table 2: Comparison of measured and predicted values.
(Lateral load applied at the 1st floor)

Value	Test (Real structure)	F.E.M. (Real structure)	F.E.M. (Bare steel frame)
MAJOR AXIS			
Natural frequency	7.7 Hz	8.4 Hz	3.1 Hz
1st floor stiffness	640×10^6	720×10^6 N/m	99×10^6 N/m
Roof stiffness	430×10^6	560×10^6 N/m	95×10^6 N/m
MINOR AXIS			
Natural frequency	8.4 Hz	7.1 Hz	3.1 Hz
1st floor stiffness	710×10^6 N/m	650×10^6 N/m	130×10^6 N/m
Roof stiffness	420×10^6 N/m	520×10^6 N/m	110×10^6 N/m

The larger uncertainty in the minor axis is due to a rotational component of buildings response. This component was not further investigated as it could not be predicted using the two dimensional finite element model. This influence, however, is negligible when compared to the difference between the basic steel frame and models including non-structural components: between 250% and 650%. These gains can be obtained using *existing* calculation techniques and *without adding* material to the existing structure.

Experimental errors at service load levels are generally larger than those that may be expected at ultimate load levels. This is due to the participation of many building components that normally fail before ultimate loads are applied and the simplicity of the model approximating their behaviour. The implications of slightly overestimating service load level stiffness and ultimate load capacity, however, are quite different.

6. CONCLUSIONS AND RECOMMENDATIONS

6.1 Conclusions

An economic method of obtaining static lateral stiffness and natural frequencies at service load levels is presented: an impact hammer. Installation and measurement times of impact hammer tests are greatly reduced in comparison with shaker tests.

Measured and predicted values of lateral stiffness correspond reasonably well for the structure modelled. This is encouraging as it suggests that models used to predict the ultimate load carrying capacity of the bare structural frame may be modified to include non-structural components at service load levels. Simple assumptions can be used to define column base fixity, beam to column connection behaviour and the behaviour of connections between structural and non-structural building components. Substantial increases in lateral stiffness may be justified.

6.2 Recommendations

This work must be generalised through the testing and modelling of a range of steel-framed structures. Future testing should give preference to classes of steel-framed structures where existing codes suggest that serviceability problems may occur.

Parallel to future testing, a concentrated effort should be made to improve existing data bases containing lateral stiffness and strength limits for non-structural components commonly used in steel-framed construction. Much work remains to be done to classify and model the service behaviour of connections between structural and non-structural components.

Lastly, the results of these exercises should be used to replacing existing serviceability limits with more rational and statistically significant limits in future steel design codes.

ACKNOWLEDGEMENTS

The work reported in this paper was undertaken as part of the ECSC financed project "Serviceability deflections and displacements in steel framed structures" conducted jointly by the University of Trento, the University of Nottingham and TNO-Bouw and coordinated by Centrum Staal. Specific support to TNO-Bouw were provided through contract No.7210-SA/613.

REFERENCES

1.Serviceability requirements for steel framed structures. European Coal and Steel Community, ECSC project no. SR 92029. To be published.

Evaluation of Structural Behaviour by In-Situ Dynamic Tests

Evaluation du comportement structural au moyen d'essais dynamiques in-situ

Bewertung des Tragwerkverhaltens bei dynamischen In-situ-Versuchen

Marco BALLERINI
Researcher
Univ. of Trento
Trento, Italy

Maurizio PIAZZA
Professor
Univ. of Trento
Trento, Italy

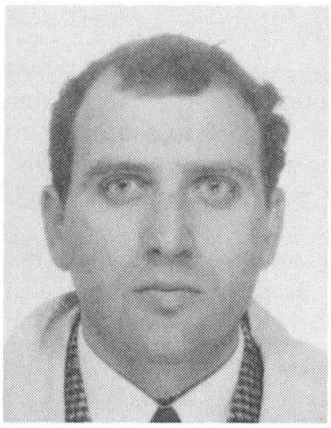

Marco Ballerini, born in 1960, engineer, is researcher at University of Trento (Dep. of Structural Mechanics). He carried out research on timber structures and composite structures with semi-rigid joints.

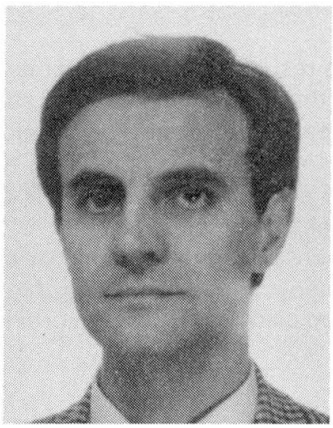

Maurizio Piazza, born in 1953, engineer, is professor at University of Trento (Dep. Structural Mechanics). He carried out research on steel structures, timber structures and numerical analysis techniques in the structural field.

SUMMARY

This paper reports the comparisons between the results of in-situ dynamic tests, carried out on mixed reinforced concrete and steel structures, and the results of the related numerical models. The study is directed towards verifying the possibility of evaluation of some parameters caracterizing the structural behaviour at service load levels. This article summarises the experimental and numerical work undertaken at the University of Trento, as part of a research project entitled «Serviceability Deflections and Displacements in Steel Framed Structures».

RESUME

Dans ce rapport on a exposé les résultats des essais dynamiques in-situ, exécutés sur des structures de bâtiments, en béton armé et en acier, comparés aux résultats des modèles numériques correspondants. On a cherché à évaluer certains des paramètres qui caractérisent le comportement structural pour des charges réelles. Ce rapport résume les recherches expérimentales et numériques menées à l'Université de Trento, faisant partie d'un projet de recherche «Serviceability Deflections and Displacements in Steel Framed Structures».

ZUSAMMENFASSUNG

Der Beitrag enthält einen Vergleich zwischen den Ergebnissen von dynamischen In-situ-Versuchen und den entsprechenden numerischen Modellen. Zweck der Studie ist die Untersuchung der Bewertungsmöglichkeit einiger Parameter, die das Tragverhalten unter Nutzlast charakterisieren. Es werden hier die experimentellen und numerischen Untersuchungen des Forschungsprojekts «Serviceability Deflections and Displacements in Steel Framed Structures» zusammengefasst, die an der Universität Trient durchgeführt wurden.

1. INTRODUCTION

The capability of evaluating the actual structural behaviour of ancient [1], old and new buildings is a significant research item particularly referring to serviceability limit states. Furthermore, the evaluation of the influence of internal and boundary connections on the global behaviour is relevant in order to establish simplified design and optimization criteria for the checks at service load levels.
To this purpose a three-part programme of research, focusing on static deflections of steel framed buildings, funded by the European Coal and Steel Community (ECSC), was started in late 1990.
It comprised:

- Investigation of the in-service performance of steel buildings (TNO-Bouw);
- Review of existing code requirements and their basis (University of Nottingham);
- Numerical studies and considerations on design models and in-situ dynamic tests on steel and steel-concrete buildings (University of Trento).

A report [2] giving the findings of each aspect of the work has been presented to ECSC. The content of this paper is complemented by three other papers at this conference which deal with the other topics of the research [3, 4 and 5].

This paper reports some results of in-situ dynamic tests and numerical analyses regarding two different types of new buildings, the first one made with steel columns and steel-concrete floors, the second one entirely realized with steel. Two kinds of dynamic exciter have been used with regard to the different masses of the two buildings. Physical results (in terms of acceleration and power spectrum) have been compared with those of some numerical models obtained assuming different boundary conditions and internal continuity between the elements.
Conclusions are drawn concerning the capability of in-situ dynamic test methods to correctly estimate the structural behaviour at service load levels; on the basis of the test results the problem of the choice of test methodologies will be discuss, in order to provide meaningfully results for the evaluation of the actual behaviour.

2. INVESTIGATED STRUCTURES

2.1 The mixed structure

The first structure investigated, briefly described in figure 1, is a part of the extension of passengers aerostation of Milan-Linate Airport.
It is essentially a rectangular mixed r.c.-steel building with a basement and one above-ground floor.
The floor thicknesses are of 0.45 and of 0.50 m respectively for spans of 8 and 12 m. The floor structure consists of reinforced concrete predalles with load-reducing polystyrene blocks, supported by in pairs 8 m span steel beams which are included into the final layer of concrete (see Sec. A-A, Fig.1). The beams have no continuous steel reinforcement at the column lines.

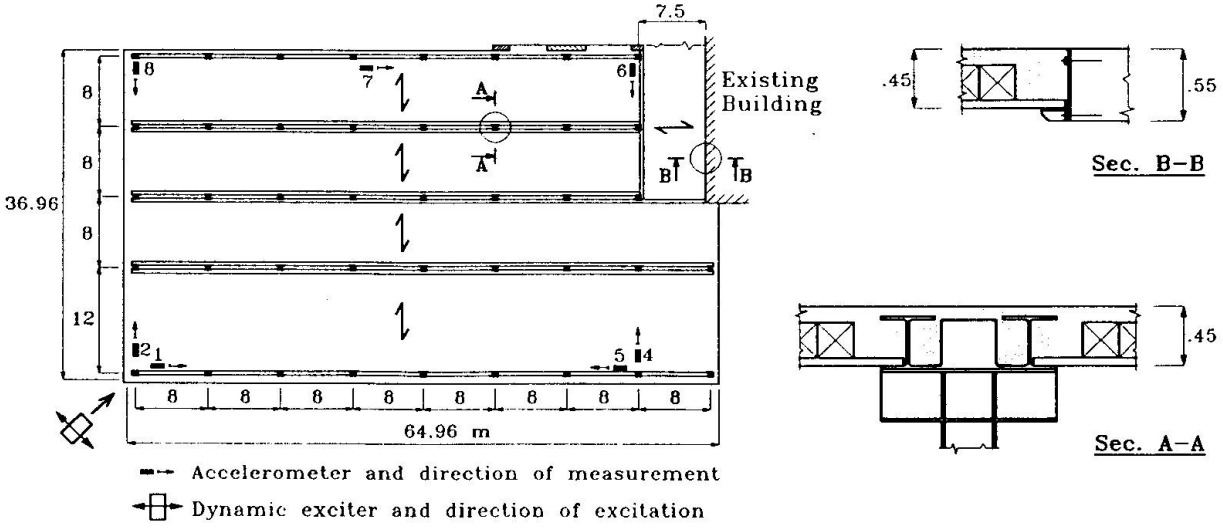

Fig. 1 - Mixed RC-steel structure: roof floor plan and location of instruments

2.2 The steel structure

The second structure investigated, briefly described in figure 2, is a part of the roofing steel structure of the extension of passengers aerostation of Milan-Linate Airport.
The roofing structure, based on the r.c.-steel part of the buiding, is realized with longitudinal HE 300 B and IPE 400 main beams, for the 8 m spans, and with welded beams for the 12 m spans; the transversal secondary beams are 8 m long IPE 270. The columns are realized with HE 240 A and HE 400 B sections.
The horizontal deflections are limited by nominally pinned portal frames in the transversal plane, realized with HE 260 B beams and welded columns, and by a brick wall along the A alignement.
In the roof plane a cross-bracing system, realized with 28 mm diameter steel bars, provides the necessary in-plane stiffness (see Fig. 2).
The roofing is made by profiled steel sheeting riveted to the structure.

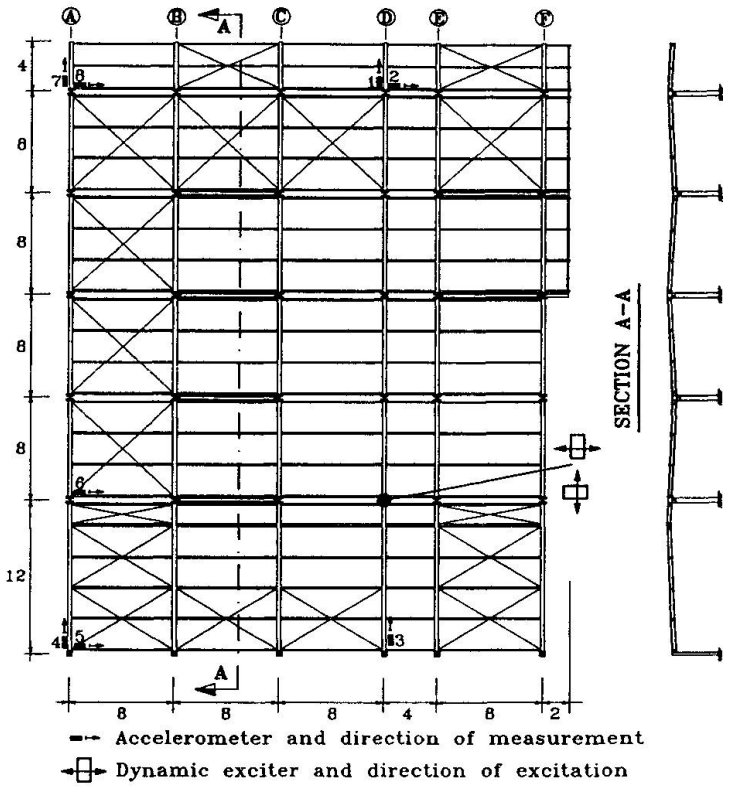

Fig. 2 - Steel roofing structure: plan and location of instruments

3. NUMERICAL ANALYSES AT SERVICE LOADS

3.1 The mixed structure model

Finite element models, entirely realized with beam type elements only, have been set up to evaluate the fundamental vibration frequencies of the structure as a whole. Numerical analyses have been carried out for different internal continuity degrees between the elements. The following cases are here reported:

- structure with base pinned columns and full continuity for all internal joints;
- structure with base fixed-end columns and pinned beams;
- as the previous but with full continuity for all internal joints.

Case #	Fundamental Frequencies [Hz]		
	Mode 1	Mode 2	Mode 3
1	1.87	4.37	4.96
2	2.10	4.18	4.79
3	3.48	5.08	5.81

Table 1

The three fundamental free vibration frequencies for the described cases are reported in table 1; the three modes are the same for the three cases considered and are horizontal vibrations.

3.2 The steel roofing structure model

A finite element model, which also make use of beam elements only, has been adopted for the numerical study of the steel roofing structure.
In the analyses the full continuity has been considered at the top end of the columns, at the ends of the main longitudinal beams and at the ends of beams of pinned portal frames. On the contrary the secondary beams have been considered as simply supported.
The numerical analyses have been carried out for three different cases:

- with base pinned columns;
- with base pinned columns and with the contributions of the brick wall and of the steel sheeting;
- as the previous but with base fixed-end columns.

The three fundamental free oscillation frequencies for the described cases are reported in table 2.

The first two modes are the same for the three cases considered and are essentially horizontal vibrations along transversal direction: these two modes, for case 3, are reported respectively in figures 4 and 5. For cases 1 and 2 the third mode is again an horizontal vibrating mode while it is a vertical one of the cantilever part of the structure for case 3.
By comparison between cases 1 and 2 it is possible to note that for this structure the brick wall doesn't play an important role on the fundamental frequencies: this is due to the fact that vibrations related to the fundamental frequencies are essentially orthogonal to the plane of the wall, even for case 1.

Case #	Fundamental Frequencies [Hz]		
	Mode 1	Mode 2	Mode 3
1	2.27	3.08	4.27
2	2.44	3.32	4.58
3	4.39	5.95	6.62

Table 2

4. IN-SITU DYNAMIC TESTS

The tests on both structures have been performed applying at a pre-established point a sinusoidal force (with known intensity, direction and frequency) by a dynamic exciter, and acquiring the accelerations at significant points of the structures by means of some piezometric accelerometers, which were connected to a recording system and a function analyser allowing on-line check of structural response.
For the mixed structure a 200 Kg counterrotating masses dynamic exciter has been used; the exciter and accelerometers location are showed in figure 1.
For the steel roofing structure, due to the lower total mass, a 50 Kg dynamic exciter has been used; the location of the instruments is showed in figure 2.
The tests were performed arranging the dynamic exciter so as to provide horizontal forces in the top floor of the mixed building and in the plane of the roof for the steel structure.
Accelerations have been recorded in correspondance of the stationary response of the structure for several forcing frequencies and for the free final vibrating transients.
The investigated frequencies range from 1 to 8 Hz for both structures.

5. COMPARISONS

5.1 Results and comparisons for the mixed structure

Figure 3 shows the spectra of the accelerations recorded by accelerometers 1 and 2 (see fig. 1) during the free vibration transients: the values observed for the fundamental frequencies are respectively 3.25 and 6.25 Hz. By comparison with table 1 it can be noticed that the first fundamental frequency is satisfactorily consistent with the numerical one for case no. 3, while the second one is underrated in the same numerical model.
The consistency of the fundamental numerical and physical frequency only for model no. 3 states that the structure behaves like a frame with full continuity at least for moderate applied forces.

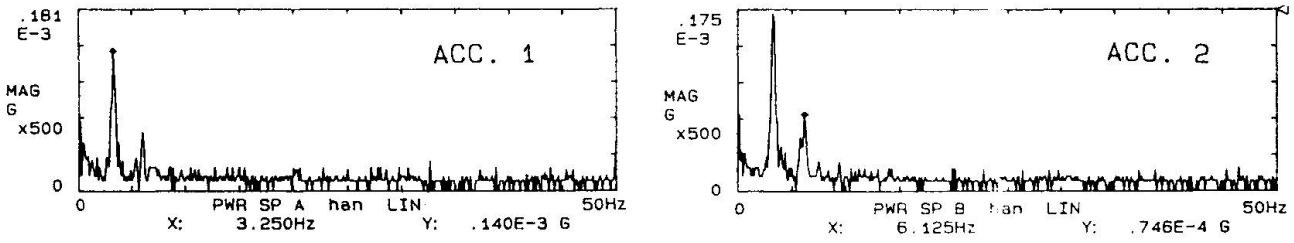

Fig. 3 - Mixed structure: power spectra

5.2 Results and comparison for the steel roofing structure

The main numerical and test results are reported in figures 4÷6. Figures 4 and 5 show the two fundamental theoretical vibrating modes of the structure for case no. 3, related to frequencies of 4.39 and 5.95 Hz, and the accelerations of the more interesting points recorded respectively at 4.5 and 5.5 Hz.

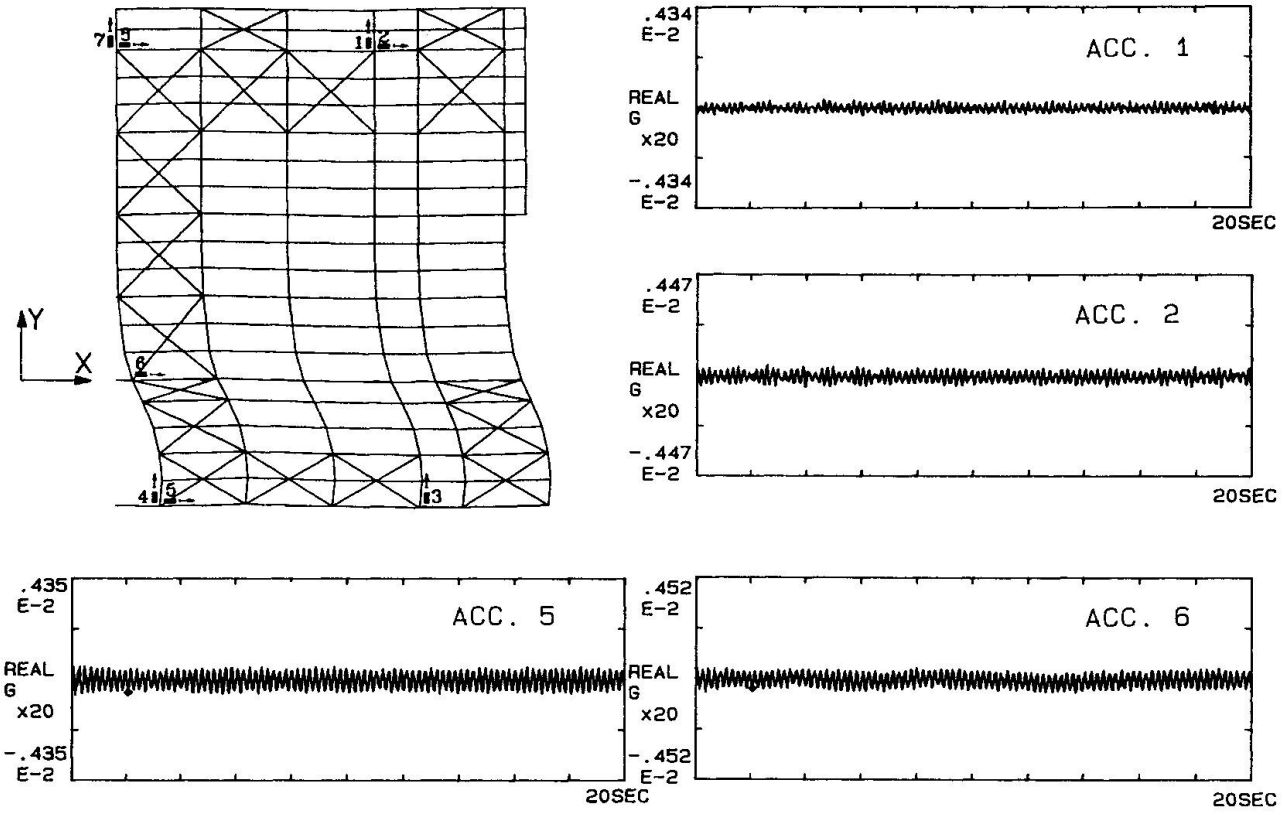

Fig. 4 - Mode 1 of the numerical model (4.39 Hz) and recorded accelerations at 4.5 Hz.

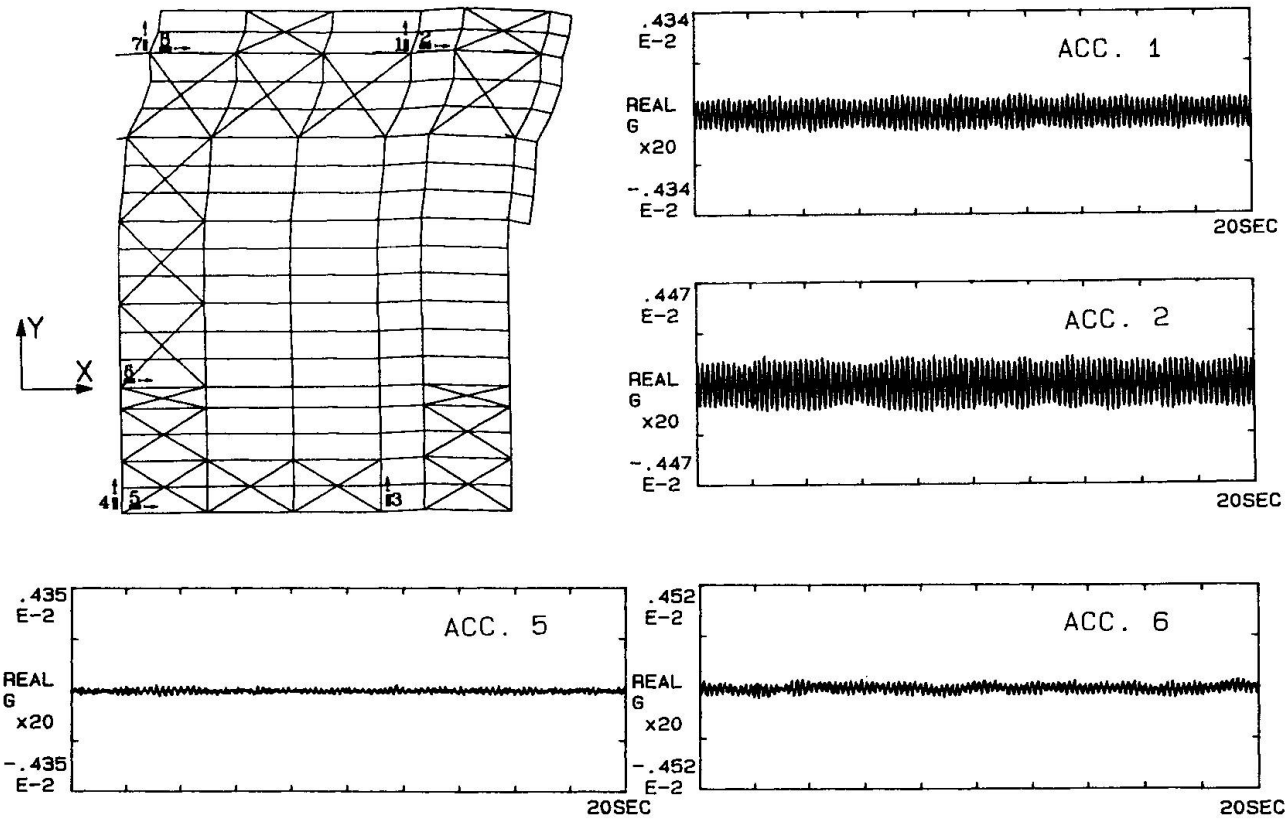

Fig. 5 - Mode 2 of the numerical model (5.95 Hz) and recorded accelerations at 5.5 Hz.

By comparison between the amplitude of the recorded accelerations and of the theoretical vibrating modes, it can be noticed that at 4.5 Hz the structure moves approximatively like the first fundamental numerical mode, while at 5.5 Hz it vibrates like the second one.
Figure 6 shows the response spectra of the free vibrating accelerations recorded by accelerometers 2 and 5 and states that the most energy contents are at 4.45 Hz and 5.45 Hz respectively for accelerometer 5 and 2.
These results are fully consistent with the first two modes of the numerical analyses: indeed, accelerometer 5 doesn't show the second frequency because it hasn't an appreciable vibration in the second mode and accelerometer 2 shows the same behaviour but regarding the first mode.

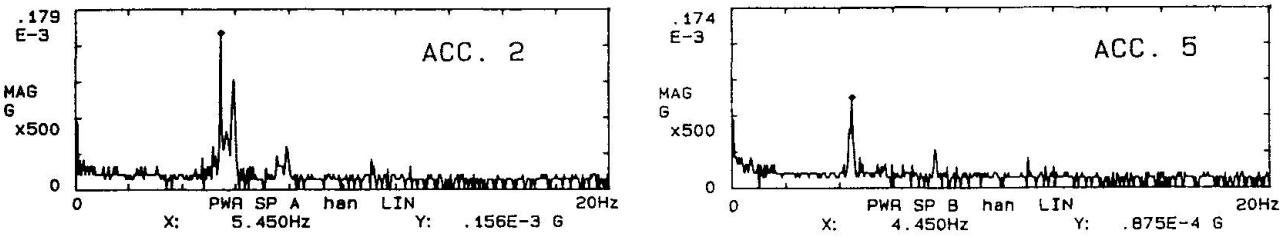

Fig. 6 - Steel roofing structure: power spectra

The described figures of the recorded data show that observed fundamental frequencies are close with those obtained by numerical analysis in the case of base fixed-end columns (case no. 3), and also the actual vibrating modes are consistent with those obtained by the same model.

6. CONCLUSIONS

The capability of evaluating the actual structural behaviour of buildings at service load levels by means of simple in-situ dynamic tests has been investigated.
It has been pointed out that in-situ dynamic tests could supply useful informations about the actual restraint of building connections; these informations, if properly recognized in very simple numerical models, allow the global structural behaviour for "service load levels" to be evaluated. It is important to stress that these models must be able to decribe the full set of nodal displacements and correctly evaluate the mass distribution on the structure: therefore, generally, 3-D numerical models are necessary.
Finally, the correct interpretation of the results of in-situ dynamic tests is directly related to the energy supplied to the structure; due to this fact only in the case of buildings with very simple mesh and with low total masses the hand-held hammer method can be usefully used [4].

ACKNOWLEDGEMENTS

The work reported in this paper was undertaken as part of the ECSC sponsored project "Serviceability Deflections and Displacements in Steel Framed Structures", conducted jointly by the University of Nottingham, the TNO-Bouw, the University of Trento and coordinated by Centrum Staal.
The authors wish to express one's thanks to the Fratelli DIOGUARDI S.p.A., the firm responsible for the construction work, which co-operation have made possible the execution of the tests.

REFERENCES

1. CASTOLDI A., CHIARUGI A., FANELLI M., GIUSEPPETTI G., *In-Situ Dynamic Tests on Ancient Monuments,* "Monitoring of Large Structures and Assessment of their Safety", IABSE, Vol. 56, 1987.
2. ECSC Report, *Serviceability Deflections and Displacements in Steel Framed Structures,* Contract no. 7210-SA/418, 1992.
3. NETHERCOT D.A., SAIDANI M., *Serviceability Requirements for Steel Framed Structures,* Int. Colloquium on "Structural Serviceability of Buildings", Göteborg, Sweden, June 9-11, 1993.
4. DANIELS B.J., DE WINTER P., VAN STAALDUINEN P., WAARTS P., *The In-Service Lateral Stiffness of Steel-Framed Buildings,* Int. Colloquium on "Structural Serviceability of Buildings", Göteborg, Sweden, June 9-11, 1993.
5. BERNUZZI C., ZANDONINI R., *Serviceability and Analysis Models of Steel Buildings,* Int. Colloquium on "Structural Serviceability of Buildings", Göteborg, Sweden, June 9-11, 1993.

Serviceability and Analysis Models of Steel Buildings

Aptitude au service et modèles d'analyse en construction métallique

Gebrauchstauglichkeit und Berechnungsmodelle im Stahlbau

Claudio BERNUZZI
Research Associate
Univ. of Trento
Trento, Italy

Riccardo ZANDONINI
Professor
Univ. of Trento
Trento, Italy

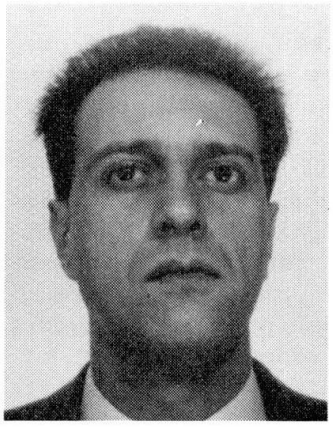

Claudio Bernuzzi, born in 1962, received his degree at the University of Pavia, Italy. Since 1987 he has been at the University of Trento. His research work is focussed on the behaviour of beam-to-column joints and on the stability of semi-continuous frames both for steel and steel-concrete composite structures.

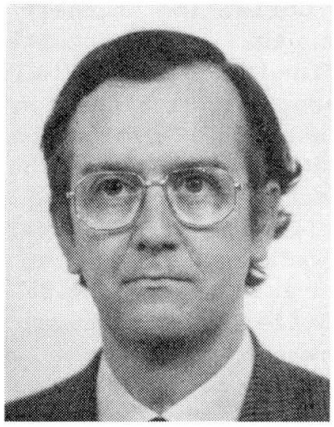

Riccardo Zandonini, born in 1948, received his engineering degree at the Technical University of Milan, where he served as a faculty member from 1972 to 1986. He has been on the faculty of Engineering in Trento since 1986. His research work is devoted to the study of the response of steel and steel-concrete composite structures.

SUMMARY

Recent trends of modern construction are likely to make in-service performance the governing design parameter. More and more refined models are used in structural analysis, allowing the response to be approximated quite closely. However, code serviceability checks still refer to traditional criteria, based on the elastic analysis of rather simple models of the bare structure. A review of such a philosophy seems necessary. This paper intends to emphasize the role of a link between analysis models and in service drift criteria.

RESUME

La tendance actuelle en construction métallique est de faire des conditions de service le paramètre prédominant lors du dimensionnement des cadres. Pour les analyses structurelles, on a recours à des modèles de plus en plus sophistiqués qui permettent d'approcher de manière très précise le comportement réel de la structure. Les codes pourtant continuent à s'appuyer, pour les vérifications en service, sur des critères traditionnels qui se fondent sur l'analyse élastique de systèmes idéalisés. Il semble nécessaire de revoir cette philosophie. Le présent article se propose de souligner le rôle de la liaison entre le modèle d'analyse et les limites des déplacements sous charges de service.

ZUSAMMENFASSUNG

Die neuesten Entwicklungen im Stahlbau zeigen, dass die Gebrauchstauglichkeit ein entscheidendes Kriterium im Entwurf ist. Immer präzisere Berechnungsmodelle erlauben es, dem tatsächlichen Verhalten des Tragwerkes näher zu kommen. Trotzdem stützen sich die Baunormen weiterhin auf althergebrachte Kriterien, welche auf dem elastischen Verhalten von vereinfachten Modellen gründen. Dieses muss kritisch betrachtet werden. Der Artikel bezweckt, die Wichtigkeit der Relation zwischen Berechnungsmodellen und den Kriterien für die Begrenzung der Verschiebungen unter Dienstlasten hervorzuheben.

1. INTRODUCTION

Limit state design is nowadays accepted by the vast majority of National and International Codes. This design philosophy stresses the link between structural reliability and performance of the system with respect to both service and ultimate loading conditions. Although the theoretical background of the method is well established, some of the problems related to its implementation in design practice have not yet been fully solved. Among these, an important question, requiring further studies, arises from the existing imbalance in the state of knowledge of the performance of the structure in different loading conditions. Research activity has been focussed mainly on the ultimate resistance of the structure, despite the fact that the performance under service loads is the critical requirement for many structural forms and materials. As a result of this limited research interest, a comprehensive information on in service responses of buildings is lacking, even for the most popular forms of construction. Furthermore, no criteria are available for an effective selection of the parameters to be used in serviceability checks and for a realistic definition of their limit values. Finally, the performance of the construction is usually investigated via numerical analyses, which make use of more or less refined models to simulate the response of the structural system as well as its interaction with the non structural components. Figure 1 provides a schematic representation of typical components with reference to a building with a steel braced framework as main structural system. Traditionally, the complexity of the many interactions determining the performance of the construction is substantially simplified in design analyses. However, the sophistication of the computing tools nowadays available to practising engineers permits increasing refinement of design analyses, which is more and more exploited, due to the strong competition among different structural materials. A relationship exists between the degree of refinement of the model adopted and the performance "required" of the model. This relation is clearly recognized for ultimate limit states, whilst even guidelines for a practical appraisal of this relationship with reference to serviceability are lacking. This condition is clearly reflected by recent structural Codes, even advanced ones, such as the Eurocodes [1,2]: they are still based on the traditional philosophy. This approach contrasts with the remarkable refinement of the prescriptions related to the ultimate limit state.

This situation represents a heavy burden for the design, in particular, of steel and composite steel-concrete buildings, for which the current trend towards larger spans and lighter systems makes serviceability increasingly important. Recognition of this significant imbalance in the design quality for the ultimate condition and for the serviceability condition has lead the European Coal and Steel Community (ECSC) to fund a research programme focussing on the static deflection of steel framed buildings. The research project, which was started in late 1990, comprised: (1) Investigation of the service performance of buildings (TNO-Bouw), (2) Review of existing Code requirements and their basis (University of Nottingham) and (3) Numerical studies and consideration of design models (University of Trento). A report giving the findings of each aspect of the work has been presented to ECSC. The content of this paper is based on the section on numerical studies and design models and is complemented at this Conference with three other papers which deal with the other topics.

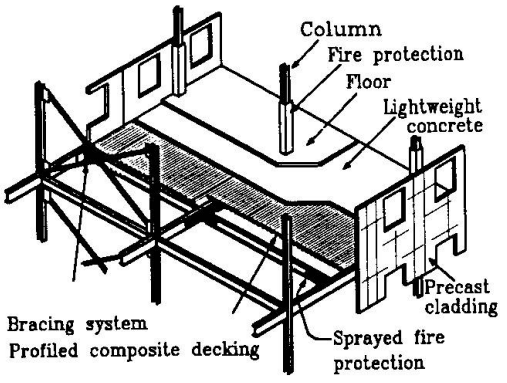

FIGURE 1

2. THE NUMERICAL STUDIES

The influence of the design model adopted for assessing the performance under service loads has been appraised through numerical studies on the two frame configurations shown in fig. 2. The figure reports as well the member sizes and the reference loads q and F. The main parameters considered were: (1) the joint action, (2) the cladding

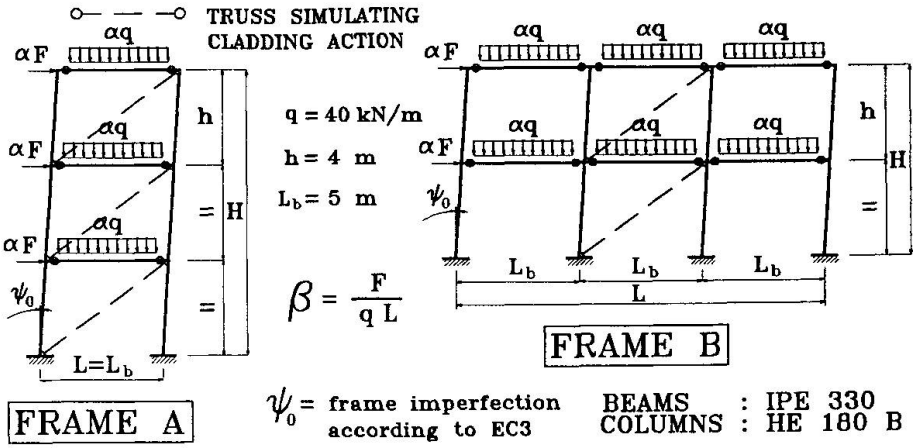

FIGURE 2

action and (3) the ratio ß between the vertical and horizontal loads at each storey. The M-ϕ curves in figure 3, from available test data on end plate and cleated connections [3,4,5], were selected to represent typical responses of flexible and semi-rigid joints. Besides these curves, the upper and lower bounds of the semi-rigid range defined by the Eurocode 3 [1] were also used as moment-rotation relations. The cladding stiffness and strength vary within a fairly wide range due to the very different cladding forms (ranging from glass to reinforced concrete panels) and cladding-to-structure interface connections [6,7]. It was then decided to make reference, in this first phase of the study, to the simple metal deck panel in figure 4, for which the shear response was determined experimentally for an aspect ratio very close to the bay span-to-height ratio of the frames considered [8]. An additional series of analyses permitted determination of the minimum value of the cladding stiffness required to meet the serviceability drift limits. The ratio ß was varied from 0.0125 (low to medium wind load) to 0.10 (high wind load or low seismic forces). The analyses incorporated both geometric and material nonlinearities; the limited aim of the study permitted simulation of cladding action through an equivalent diagonal bracing member [7]. All loads were increased proportionally through a common load multiplier α up to collapse. First order analyses were also conducted in selected cases in order to investigate the importance of the P-Δ effect. The serviceability limits specified by Eurocode 3 were assumed in the evaluation of the results (i.e. H/500 and h/300).

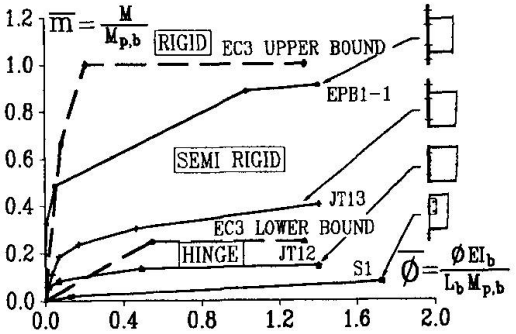

FIGURE 3

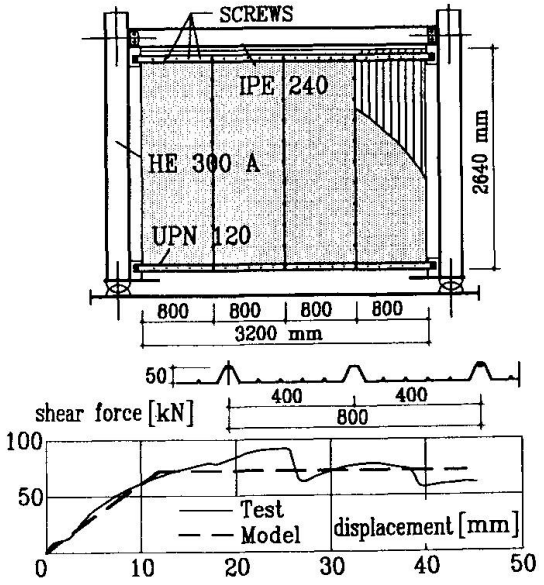

FIGURE 4

3. INFLUENCE OF JOINT ACTION

Traditional design of steel frames assumes that connections behave according to the ideal models of hinge and rigid joints. The present knowledge of joint response enables use of models closer to the actual behaviour, i.e. it permits designers to incorporate joint action in a fairly accurate way. A first series of analyses aimed at assessing the "effect" of this finer numerical simulation on the evaluation of the frame performance in service. To this purpose, the frames were first analysed for the limit cases of hinged and rigid joints. The service loads (i.e., $\alpha_{s,h}$ and $\alpha_{s,r}$ respectively) were defined by dividing the ultimate load multiplier α_u by

an "average" safety factor equal to 1.43; sway indexes H/V were then determined at these load levels. The responses of the frames were subsequently determined incorporating the "actual" joint behaviour, and the sway indexes were evaluated for the service loads defined for the corresponding ideal case (i.e., the rigid frame for frames with EPB1-1 and EC3 upper bound joints and the "hinged" frame for frames with S1, JT12, JT13 and EC3 lower bound joints). The significant influence of joint action is apparent from figure 5 and table 1. The degree of continuity provided even by the most flexible connections substantially increases the stiffness of the frame (up to 30 times for frame A and ß=0.0125). The ultimate frame strength also improves remarkably, hence higher service loads might be admissible ($\alpha_{s,j}$). The frame stiffness, however, is not sufficient to allow this potential increase

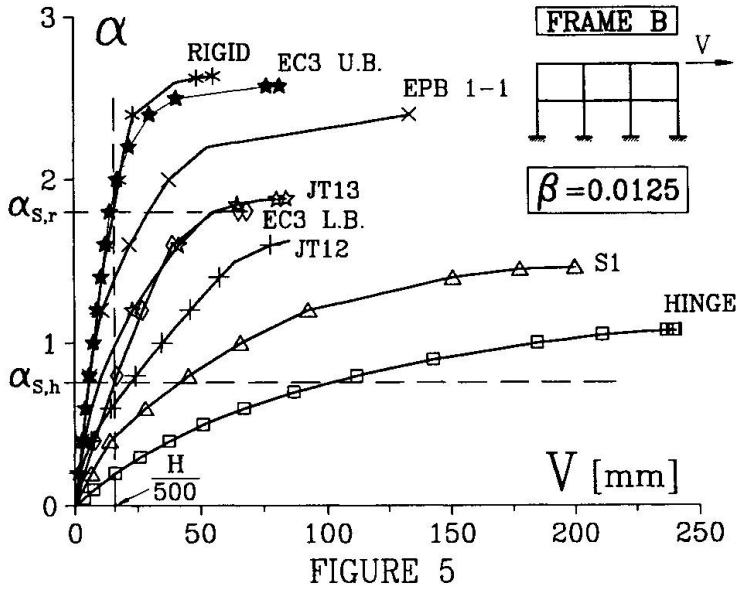

FIGURE 5

of resistance to be fully exploited (see the values of sway index determined at $\alpha_{s,j}$). Frame response is far less sensitive to a variation of joint flexibility with respect to the rigid joint model. This applies to both ultimate strength and stiffness in service. However, the recognition of the semi-rigid behaviour of joint EPB1-1 implies a remarkable increase in the flexibility of the frame model. Appraisal of frame performance in service based on this model would lead to regard the frame as inadequate also for ß = 0.0125. Since extended end plate joints are traditionally considered "rigid", frames accepted in the past on the basis of a rigid frame analysis would be rejected now if joint action is incorporated in the design analysis.

TABLE 1 - LATERAL DRIFT: FRAME A WITHOUT CLADDING

JOINT	ß	S.I. at $\alpha_{s,h}$	$\frac{S.I._h}{S.I._j}$	$\frac{\alpha_{s,j}}{\alpha_{s,h}}$	S.I. at $\alpha_{s,j}$
Hinge		60	1.00	1.00	60
S1	1	203	0.30	1.43	118
JT12	——	655	0.09	2.33	163
EC3 L.B.	80	583	0.10	2.58	188
JT13		1784	0.03	2.69	265
Hinge		39	1.00	1.00	39
S1	1	56	0.70	1.36	41
JT12	——	347	0.11	2.09	136
EC3 L.B.	20	266	0.15	2.72	89
JT13		645	0.06	3.09	141
Hinge		34	1.00	1.00	34
S1	1	71	0.48	1.33	44
JT12	——	387	0.09	1.93	106
EC3 L.B.	10	214	0.16	2.59	77
JT13		599	0.06	2.94	135

JOINT	ß	S.I. at $\alpha_{s,r}$	$\frac{S.I._r}{S.I._j}$	$\frac{\alpha_{s,j}}{\alpha_{s,r}}$	S.I. at $\alpha_{s,j}$
RIGID	1	677	1.00	1.00	677
EC3 U.B.	——	662	1.03	1.01	656
EPB1-1	80	308	2.19	0.99	295
RIGID	1	259	1.00	1.00	259
EC3 U.B.	——	251	1.03	1.02	217
EPB1-1	20	197	1.32	0.98	204
RIGID	1	192	1.00	1.00	192
EC3 U.B.	——	185	1.04	1.00	183
EPB1-1	10	154	1.25	0.94	175

S.I. = Sway Index (= H/V)

4. INFLUENCE OF CLADDING ACTION

Interaction between the frame skeleton and the cladding elements is fairly complex, as it depends on the responses of these two systems as well as on the type of interface connection. For the limited scope of this study a very simple model was adopted, which uses an equivalent concentric diagonal strut (Fig. 2). The cross section area of this strut can be easily computed when the elastic shear stiffness of the panel is known [8]. The first series of analyses considered that all storeys were "stiffened" by the metal sheeting panel in fig.4. Comparing fig. 6 and fig. 5, it is readily apparent that cladding action is the prime factor affecting the

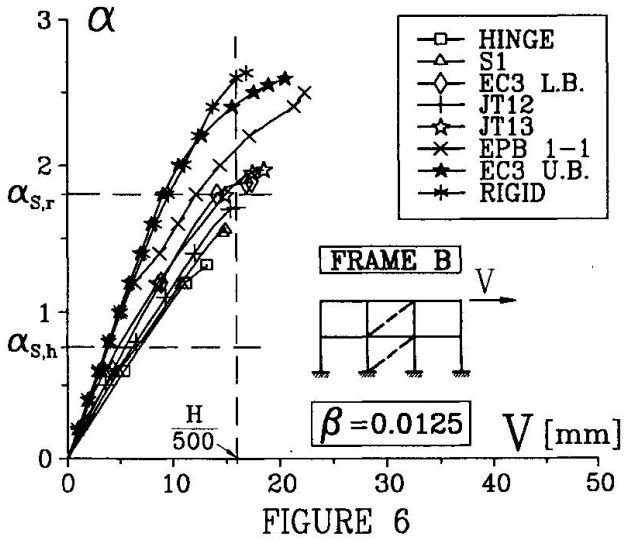

FIGURE 6

frame stiffness. Drifts at the service load levels $\alpha_{S,h}$ and $\alpha_{S,r}$, determined for the hinged and for the rigid frame neglecting cladding action, vary only moderately with the type of joint (less than 30% difference between the frames with hinge and semi-rigid (JT13) joints). Moreover, the simple panel considered provides in many cases sufficient stiffness to make the ultimate limit state govern design. In other terms the potential strength of the framework can be fully utilized, at least in the presence of low to moderate horizontal forces. Fairly high horizontal forces (ß = 0.10) still make serviceability limits critical. Shear forces in the panel "in service" are well within the elastic range of its response. It should be also considered that the stiffening action of cladding substantially reduces the geometrical (P - Δ) effects, enabling the designer to use a first order analysis, at least for serviceability checks: lateral drifts determined via first and second order analysis differed less than 8%.

It is interesting to note that for joint EPB1-1 second order analysis should be required if the analysis were conducted on the frame skeleton incorporating the joint response.

A further series of analyses considered the different conditions raising when panels were not present at all storeys. The results indicated that a substantial improvement of the frame model performance is associated even with the presence of the cladding in only one storey. For frame A the maximum influence of a single panel is achieved when this is located at the third storey.

Finally, the minimum shear stiffness K_{cl} required of the cladding to make the frame

TABLE 2 - LATERAL DRIFT: FRAME A WITH CLADDING

JOINT	ß	S.I. at $\alpha_{S,h}$	$\frac{S.I._h}{S.I._j}$	$\frac{\alpha_{S,j}}{\alpha_{S,h}}$	S.I. at $\alpha_{S,j}$
Hinge		3659	1.00	2.05	2483
S1	1	3703	0.99	2.25	1617
JT12	——	4013	0.91	2.56	1440
EC3 L.B.	80	4013	0.91	2.83	1378
JT13		4761	0.77	2.95	1333
Hinge		1980	1.00	3.11	610
S1	1	2000	0.99	3.53	558
JT12	——	2091	0.95	3.87	494
EC3 L.B.	20	2091	0.95	4.28	471
JT13		2490	0.79	4.47	461
Hinge		1509	1.00	4.52	326
S1	1	1548	0.95	5.12	291
JT12	——	1633	0.92	5.60	265
EC3 L.B.	10	1617	0.93	6.19	256
JT13		1881	0.80	6.45	253

JOINT	ß	S.I. at $\alpha_{S,r}$	$\frac{S.I._r}{S.I._j}$	$\frac{\alpha_{S,j}}{\alpha_{S,r}}$	S.I. at $\alpha_{S,j}$
RIGID	1	1536	1.00	1.00	1528
EC3 U.B.	——	1490	1.03	1.01	1477
EPB1-1	80	1488	1.03	0.98	1460
RIGID	1	674	1.00	1.26	533
EC3 U.B.	——	630	1.07	1.26	508
EPB1-1	20	561	1.20	1.26	501
RIGID	1	506	1.00	1.74	284
EC3 U.B.	——	490	1.03	1.74	271
EPB1-1	10	480	1.05	1.74	259

TABLE 3 - MINIMUM VALUES OF THE REQUIRED SHEAR STIFFNESS FOR CLADDING

		FRAME A		FRAME B	
JOINT	ß	K_{cl} at $\alpha_{S,h}$	K_{cl} at $\alpha_{S,j}$	K_{cl} at $\alpha_{S,h}$	K_{cl} at $\alpha_{S,j}$
Hinge		0.38	0.38	1.28	1.28
S1	1	0.04	0.36	0.77	1.54
JT12	——	//	0.46	0.51	1.64
EC3 L.B.	80	//	0.64	//	1.79
JT13		//	0.56	//	1.68
Hinge		1.03	1.03	3.33	3.33
S1	1	0.36	0.89	2.05	3.07
JT12	——	0.10	1.38	1.28	5.12
EC3 L.B.	20	0.34	2.05	1.79	7.68
JT13		//	2.06	//	6.66
Hinge		1.33	1.33	4.61	4.61
S1	1	0.87	1.23	3.69	4.35
JT12	——	0.20	1.54	1.83	7.17
EC3 L.B.	10	0.82	2.66	2.46	11.78
JT13		//	2.46	//	9.73

K_{cl} in kN/mm;

// the frame meets serviceability limit without cladding

model meet serviceability limits was determined. These values, reported in table 3 for the frames with flexible joints, range from 0.04 to 11.8 kN/mm. This range of stiffnesses can be easily provided by metal sheeting panels [6]; the panel in fig. 4 has a shear stiffness equal to 5.4 kN/mm. Masonry and concrete infills do present significantly higher stiffness, also in the presence of openings.

5. CONCLUDING REMARKS

The present approach to the checking of the structural performance in service has no scientific background, and intends to serve merely as an indication that the structure is likely to possess sufficient stiffness to prevent unsatisfactory behaviour. Deflection limits recommended by Codes were empirically established and by no means represent an indication of the actual in service performance. They were basically defined to be compared with frame deformations computed on an elastic model of the bare frame with ideal restraint conditions. The numerical analyses presented in the previous sections show clearly that joint and cladding action have a substantial influence on the response of the system. Incorporation of these actions in design analysis allows in many instances to make serviceability limits less critical and the ultimate strength of the structure to be fully exploited. In particular, the presence of light cladding seems sufficient to wash out the increase of frame flexibility associated to the use of semi-rigid joints in lieu of rigid joints. Noticeable advantages can in effect be achieved just by accounting for the presence of cladding solely for the service conditions. First order elastic analysis under working loads would be adequate in this case.
Knowledge of building behaviour is improving rapidly, and numerical models at hand to designers become more and more sophisticated. It seems hence important and beneficial to revise the present criteria for appraising structural serviceability. A first step in this direction might be represented by the definition of a link between the analysis model and the serviceability limits.

ACKNOWLEDGEMENTS

The work reported in this paper was undertaken as part of the ECSC sponsored project "Serviceability Deflections and Displacements in Steel Framed Structures", conducted jointly by the University of Nottingham, the TNO-Bouw and the University of Trento. The project was coordinated by Centrum Staal.

REFERENCES

[1] European Committee for Standardisation (CEN), Eurocode 3: Design of Steel Structures - Part 1: General Rules and Rules for Buildings, February 1992.
[2] European Committee for Standardisation (CEN), Eurocode 4: Design of Composite Steel and Concrete Structures - Part 1: General Rules and Rules for Buildings, 1992.
[3] Davison J.B., Kirby P.A., Nethercot D.A., Rotational Stiffness Characteristics of Steel Beam-to-Column Connections, Joint Flexibility in Steel Frames, ed. W.F. Chen, Elsevier Applied Science, London, 1987.
[4] Davison J. B., Lam D., Nethercot D.A., Semi-rigid action of composite joints, The Structural Engineer, Vol. 68, No. 24, December 1990.
[5] Bernuzzi C. Zandonini R., Zanon P., Rotational behaviour of End Plate Connections, Costruzioni Metalliche, Vol. 2, 1991.
[6] Bryan E.R., The Stress Skin Design of Steel Buildings., Constrado Monographs, Crosby Lockwood Staples, London, 1972.
[7] Liauw T.C., Steel Frames with Concrete Infills, Stability and Strength series: Steel-Concrete Composite Structures, ed. R. Narayanan, Elsevier Applied Science, 1988.
[8] Mazzolani F.M., Sylos Labini F., Skin-frame interaction in seismic resistant steel structures, Costruzioni Metalliche, Vol. 4, 1984.

Serviceability of Beams with Slender Webs

Aptitude au service de poutrelles avec des âmes élancées

Gebrauchstauglichkeit von Trägern mit schlanken Stegen

Joachim SCHEER
Prof. em.
TU Carolo-Wilhelmina
Braunschweig, Germany

Hartmut PASTERNAK
Dr. Eng.
TU Carolo-Wilhelmina
Braunschweig, Germany

Martin HOFMEISTER
Civil Engineer
TU Carolo-Wilhelmina
Braunschweig, Germany

SUMMARY

Normally static serviceability criteria for beams are given as non-dimensional deflections. In this paper the relations between the non-dimensional deflection and slope, curvature and strain have been derived. One of the results is, that in the case of unsymmetrical end restraints and inner spans, the limitation of the non-dimensional deflection may be insufficient.

RESUME

L'aptitude au service des poutres est généralement exprimée par des flèches rapportées aux portées. Dans cette contribution, les relations de l'inclinaison, courbure et allongement sont présentées. La résistance au cisaillement des poutres est prise en considération. Dans le cas de conditions aux limites asymétriques et de travées centrales, la limitation de la flèche rapportée à la portée peut être insuffisante.

ZUSAMMENFASSUNG

Für Biegeträger gibt es praktisch nur Gebrauchstauglichkeitskriterien in Form von spannweitenbezogenen Durchbiegungen. In diesem Beitrag werden die Beziehungen zu den Verformungsgrössen Neigung, Krümmung und Dehnung unter Berücksichtigung der Schubsteifigkeit dargestellt. Es zeigt sich, dass bei Trägern mit unsymmetrischen Randbedingungen und bei Innenfeldern die pauschale Begrenzung der bezogenen Durchbiegung nicht ausreichend sein kann.

1. INTRODUCTION

For the check of serviceability of beams it is usually requested to limit the relative deflections (δ/L). The limiting values specified in codes are very general values. Therefore they are assumed to be independent from static systems. They should be understood as maximum deflections.

Currently an increasing use of slender beams with plane and profiled webs may be observed. While calculating the deformations of such beams, it is necessary to consider not only the bending stiffness but also the shear stiffness, otherwise the deformations would be underestimated.

It was pointed out very early, that the influence of the shear stiffness has to be taken into consideration while calculating the deformations of beams. Therefore the shear coefficient K was established. The different influences (cross section, static system, type of loading, loading point) on this coefficient K has been discussed in several papers [1 - 4].

Nowerdays in the german literature, the shear deformation is introduced into the differential equation of the elastic curve by means of the coefficient RHO. RHO describes the ratio of the bending stiffness to the shear stiffness and the length of the beam:

$$RHO = \frac{EI}{l^2 GA_Q} \tag{1}$$

where $A_Q = A/K$.

Limit values for RHO have been estimated in [5]. If these values are exceeded, the shear stiffness should be introduced into the calculation of the deflections. These values are valid only for beams with symmetrical end restraints.

In this paper, all relevant characteristics of deformations are investigated as functions of the shear stiffness.

2. (NON DIMENSIONAL) DEFORMATIONS OF BEAMS

2.1 General

In the following, for different static systems, the relationship between the maximum values for the deflection, the slope of the elastic curve and the curvature will be shown. In addition to [6] the shear stiffness will be taken into consideration. Elastic material behaviour is assumed, web buckling is neglected. The considered static systems are shown in Table 1.

2.2 Deflection, Slope, Curvature and Strain

For beams with uniform load wich are handled here, it can be generally stated:

$$\max \frac{\delta}{l} = s_\delta \cdot \frac{q \cdot l^3}{EI}, \quad \max \alpha = s_\alpha \cdot \frac{q \cdot l^3}{EI} = \bar{s}_\alpha \cdot \frac{\delta}{l}, \quad \max æ = s_{æ} \cdot \frac{q \cdot l^2}{EI} = \bar{s}_{æ} \cdot \frac{\delta}{l} \cdot \frac{1}{l} \qquad (2a,b,c)$$

where s_δ is the deflection coefficient, s_α and $\bar{s}_\alpha$ are slope coefficients and $s_{æ}$ and $\bar{s}_{æ}$ are curvature coefficients for the influence of the static system. The related coefficients $\bar{s}_\alpha$ and $\bar{s}_{æ}$ are given to

$$\bar{s}_\alpha = s_\alpha / s_\delta \qquad \text{and} \qquad \bar{s}_{æ} = s_{æ} / s_\delta . \qquad (3a,b)$$

With these related coefficients it is possible to show the influence of the non-dimensional deflection on the other deformations.

For simply supported beams (system 1) they are given as:

$$s_\delta = \frac{5 + 48 \cdot RHO}{384}$$

$$\bar{s}_\alpha = 3.2 \cdot \frac{1 + 12 \cdot RHO}{1 + 9.6 \cdot RHO} \qquad (4a,b,c)$$

$$\bar{s}_{æ} = \frac{9.6}{1 + 9.6 \cdot RHO}$$

In Table 1, these three coefficients are given for RHO = 0.0, i.e. without consideration of the shear stiffness (index 0).

	static system	$s_{\delta,0}$	$\bar{s}_{\alpha,0}$	$\bar{s}_{æ,0}$
1	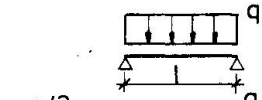	$\frac{5}{384}$	3.20	9.60
2	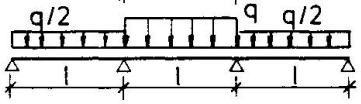	$\frac{1.4}{384}$	2.89	20.6
3	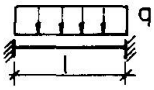	$\frac{1}{384}$	3.08	32.0
4	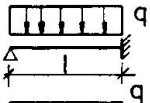	$\frac{2.08}{384}$	3.85	23.1
5	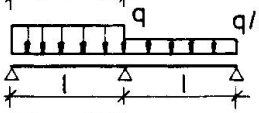	$\frac{2.79}{384}$	3.59	12.9
6	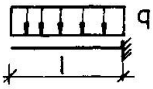	$\frac{48}{384}$	1.333	4.0
7	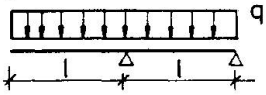	$\frac{96}{384}$	1.167	2.0
8	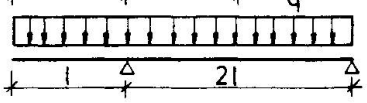	$\frac{48}{384}$	1.333	4.0

Table 1 System coefficients for some static systems

It should be noted, that the ratio EI/GA_Q has to be constant for the regarded system. For beams with cantilevers, l is the length of the cantilever.

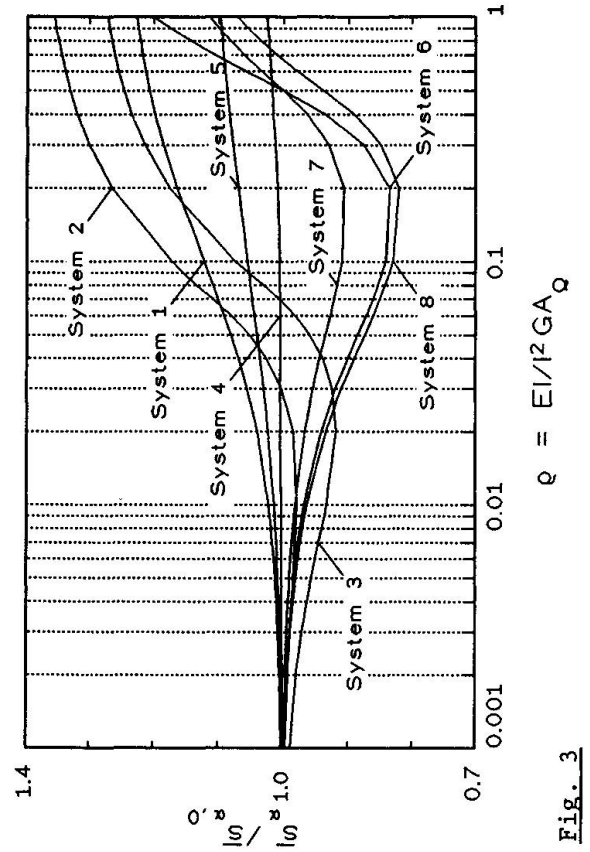

Fig. 3

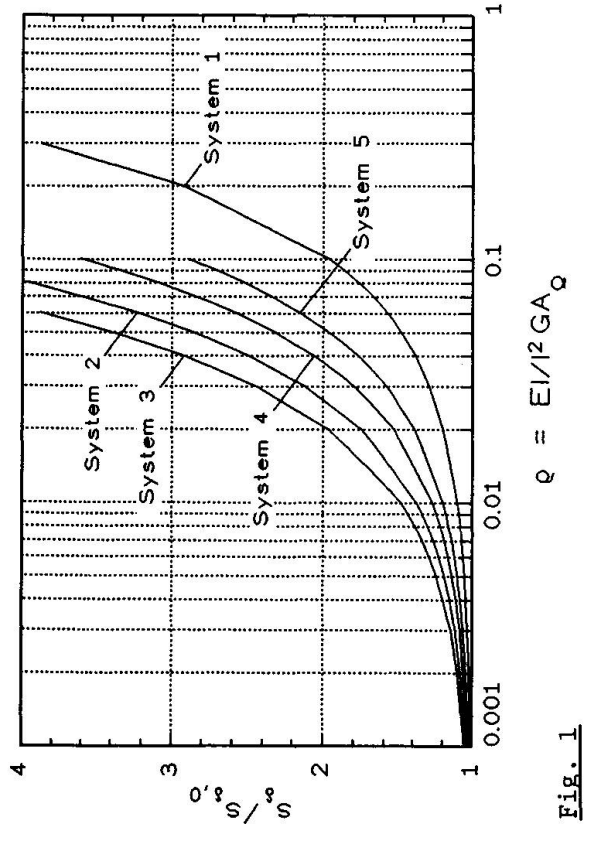

Fig. 1

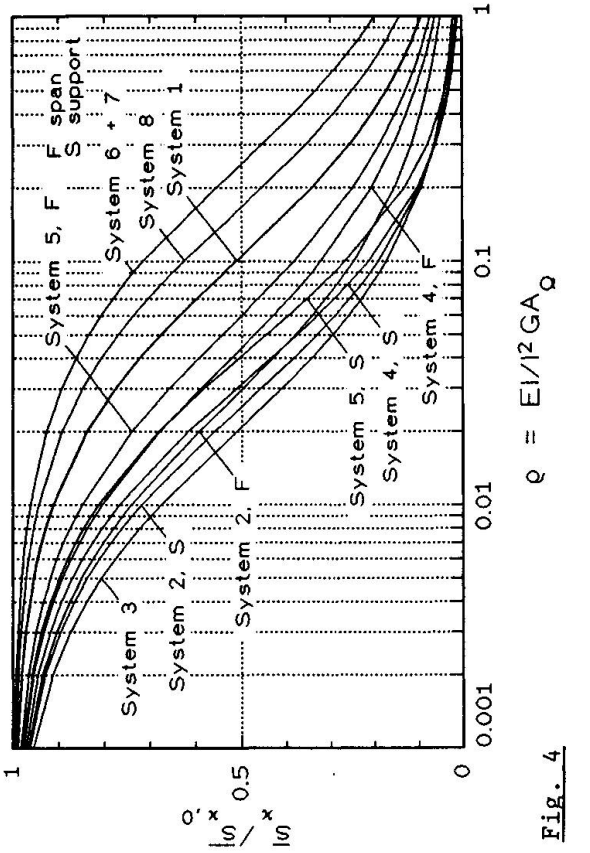

Fig. 4

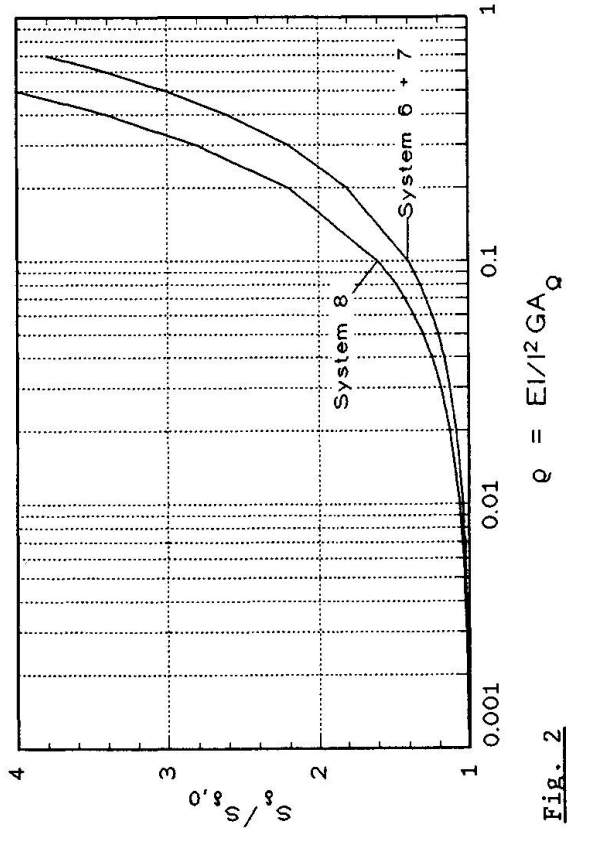

Fig. 2

From Table 1 follows: The advantage of continuous respective fixed beams is due more to their small deflection than to their greater load carrying capacity. The deflection coefficients (under consideration of the shear stiffness) are shown in Fig. 1 and 2. They are presented as related coefficients $s_\delta / s_{\delta,0}$. As expected, the advantage of statically undetermined systems gets lost, in case of large RHO values. The stronger the end restraints of the analysed span, the larger the deflection due to the shear deformation. In case of cantilever beams, this increase is relatively small because of the weak boundary conditions (Fig 2). Normally cantilevers are shorter than simply supported beams. This is the reason for larger RHO values of cantilever beams.

The same is true for the maximum slopes. Regarding the related slope coefficients $\bar{s}_{\alpha,0}$ in Table 1 follows: With beams fixed at one end and simply supported at the other, the slope of the elastic curve with a given non-dimensional deflection is great, whereby it is irrelevant at cantilever beams.

The related slope coefficients (under consideration of the shear stiffness) are shown in Fig. 3. They are presented as related coefficients $\bar{s}_\alpha / \bar{s}_{\alpha,0}$ ($\bar{s}_{\alpha,0}$ from Table 1). Therefrom follows that the advantage of systems with symmetrical end restraints gets lost not before large RHO values are reached. In case of cantilevers this influence may be neglected.

On principle, the advantage of continuous beams with more than two spans are smaller curvatures in comparison with the other systems. From Table 1 follows: Assuming the same non-dimensional deflection, systems with higher stiffness lead to larger curvatures.

The related curvature coefficients (under consideration of the shear stiffness) are shown in Fig. 4. They are presented as related coefficients $\bar{s}_æ / \bar{s}_{æ,0}$ ($\bar{s}_{æ,0}$ from Table 1). Assuming equal non-dimensional deflections, it may be observed, that the curvature decreases with increasing RHO. This is caused by the strong increase of the deflection with increasing RHO. The curvature decreases more at supports than in the spans. In case of cantilevers, the curvature does not depend on RHO.

The strains may be obtained from:

$$\epsilon = æ \cdot e = \bar{s}_æ \cdot \frac{\delta}{l} \cdot \frac{e}{l} \quad . \qquad (5)$$

Shear deformation and finally slopes of the elastic curve occur on both sides of the supports of continuous beams (Fig. 5). Adjacent members get curved additionally (important for brittle members!). Therefore it shouldn't be concluded from Fig. 4, that the problem of strains in coverings decreases with increasing RHO!

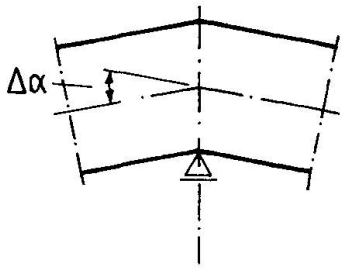

Fig. 5 Shear deformation at the supports of continuous beams

3. SERVICEABILITY CRITERIA

What about the importance of theoretical results for serviceability? According to the authors knowledge, static serviceability criteria for beams are given as absolute values (lim δ) or non-dimensional deflection (lim δ/l). In this paper the relations between the non-dimensional deflection and slope, curvature and strain have been derived. It can be shown that in cases of unsymmetrical end restraints and inner spans, the limitation of the non-dimensional deflection may be insufficient.

The derived relations are valid for all existing beam shapes and materials. If e.g. girders with trapezoidally corrugated webs are used, RHO should be completed by an additional term.

CONCLUSIONS

According to [5], the shear stiffness should be introduced into the estimation of the deflections of spans with symmetrical end restraints, if RHO > $8.5 \cdot 10^{-3}$ for statically determined systems resp. RHO > $2.5 \cdot 10^{-3}$ for statically undetermined systems. The presented investigations lead to the conclusion, that these limit values are not sufficient considering the other relevant characteristics of the deformations. More accurate investigations concerning different building materials are necessary.

The other characteristics of the deformations (slope, curvature and strain) shouldn't get lost.

REFERENCES

1. BACH-BAUMANN, Elastizität und Festigkeit.

2. TIMOSHENKO S. P., On the Correction for Shear of the Differential Equation for Transverse Vibrations of Prismatic Bars. Philosophical Magazine 41 (1921) 744-746

3. STOJEK D., Zur Schubverformung im Biegebalken. ZAMM 44 (1964) 393-396

4. COWPER G. R., The Shear Coefficient in Timoshenko's Beam Theory. Journal of Appl. Mech. 33 (1966) 335-340

5. SCHEER J., PLUMEYER K., Zu Verformungen stählerner Biegeträger aus Querkräften. Bauingenieur 63 (1988) 475-478

6. SCHEER J., PASTERNAK H., HOFMEISTER M., On Serviceability of Steel Structures. 1st Greek National Conference on Steel Structures, Athen 1991, 498-506

Serviceability Requirements for Composite Beams

Exigences d'aptitude au service des poutres mixtes

Gebrauchstauglichkeitsanforderungen an Verbundträger

Paolo E. TRINCHERO
Research Student
Univ. of the Witwatersrand
Johannesburg, South Africa

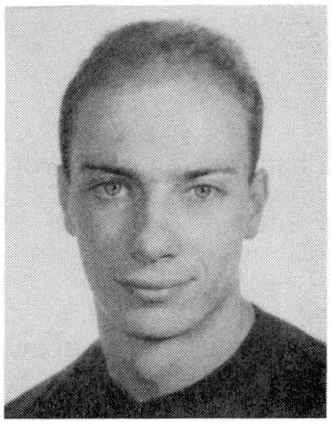

Paolo E. Trinchero, 23, has a BSc from the University of the Witwatersrand and is currently a research student there.

Alan R. KEMP
Prof. of Civil Eng.
Univ. of the Witwatersrand
Johannesburg, South Africa

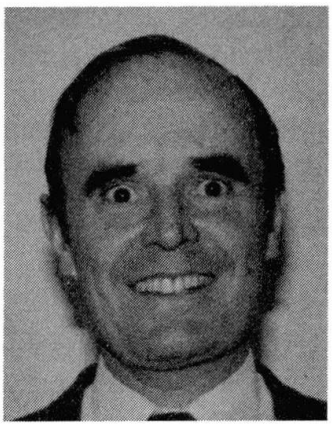

Alan R. Kemp, born 1940, got his BSc and MSc at the University of the Witwatersrand and his PhD from Cambrige University. He was group consulting engineer of Dorman Long (Africa) and Manufacturing Manager of Dorbyl rolling stock before taking the Chair of structural Engineering, University of the Witwatersrand.

SUMMARY

Comparisons are provided between observed serviceability deflections in two composite beams and predictions of the effects of yielding, shrinkage, residual stress and interface slip. The relative importance of these effects is discussed. A prediction of natural frequencies of one of the beams also correlates well with observed behaviour.

RESUME

Les auteurs comparent les flèches observées sur deux poutres mixtes sous charge de service avec les effets préalablement prévus pour l'écoulement plastique, le retrait, la contrainte résiduelle et le glissement dans la surface de contact. Ce faisant, ils analysent l'importance relative de ces influences. La fréquence propre pronostiquée pour l'une des deux poutres correspond bien au comportement observé.

ZUSAMMENFASSUNG

Die beobachtete Durchbiegung zweier Verbundträger unter Gebrauchslast wird mit den vorherberechneten Auswirkungen von Fliessen, Schwinden, Eigenspannungen und Gleiten in der Verbundfläche verglichen. Dabei wird die unterschiedliche Wichtigkeit dieser Einflüsse diskutiert. Die Vorhersage der Eigenfrequenzen eines der Balken stimmt gut mit dem beobachteten Verhalten überein.

1. INTRODUCTION

An analysis of international design codes [1] has indicated that criteria for serviceability differ more significantly than for ultimate load conditions.This particularly applies to the ratio of serviceability to ultimate load; whether elastic stress limits are required and how shrinkage, creep and partial shear connection should be considered.Residual rolling or welding stresses are generally ignored.

The primary objective of the two tests described in this paper was to assess the relative contribution to serviceability deflection of the following effects:

i) short term elastic deflections
ii) yielding of the extreme fibres
iii) residual stresses due to rolling
iv) shrinkage of concrete slab
v) interface slip due to partial shear connection
vi) repeated application of serviceability load
vii) creep under long term load of one beam.

In addition a comparison was made between theoretical and observed natural frequencies of one beam.

2. DESCRIPTION OF TESTS

Two beams were tested to investigate these effects, representing a scaled down version of an unpropped, simply-supported beam and composite slab (or the positive moment region of a continuous beam), as follows:

SF : Sagging (positive) moment (S), unpropped specimen on 6m span with full shear connection (F) and composite deck.
SP : Sagging, unpropped specimen on 6m span with partial shear connection (P) and composite deck.

A distributed 4-point loading was applied (Fig 1) to the composite section to represent the distributed imposed load.The total dead load was achieved through additional weights of 9.8kN hung from the plain steel section.Although unpropped beams would normally be precambered against dead load, it was decided not to precamber these beams because of the unknown strain distribution that would otherwise be induced in the steel section.

The shear connectors are 19mm studs that were welded through the trapezoidal deck.A full shear connection is provided in test SF and 5 studs provide a partial shear connection factor of about 0.5 in beam SP based on the Canadian code.

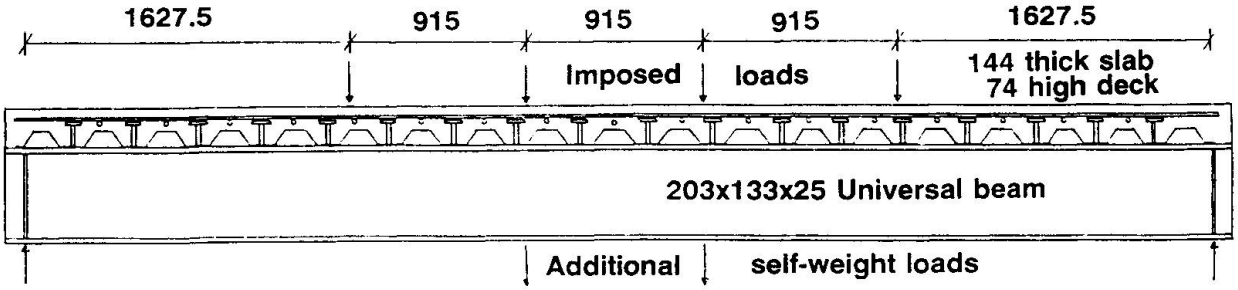

FIG.1.-Arrangement of Test Specimens SF and SP

In these tests the imposed load was applied over a number of load cycles to simulate repeated loading in the region of the load P_y that theoretically causes yielding of the extreme fibre.Although there were residual deflections on unloading, strain hardening ensured that on reloading a similar load-deflection line was followed after yielding (Figs. 2a and 2b).

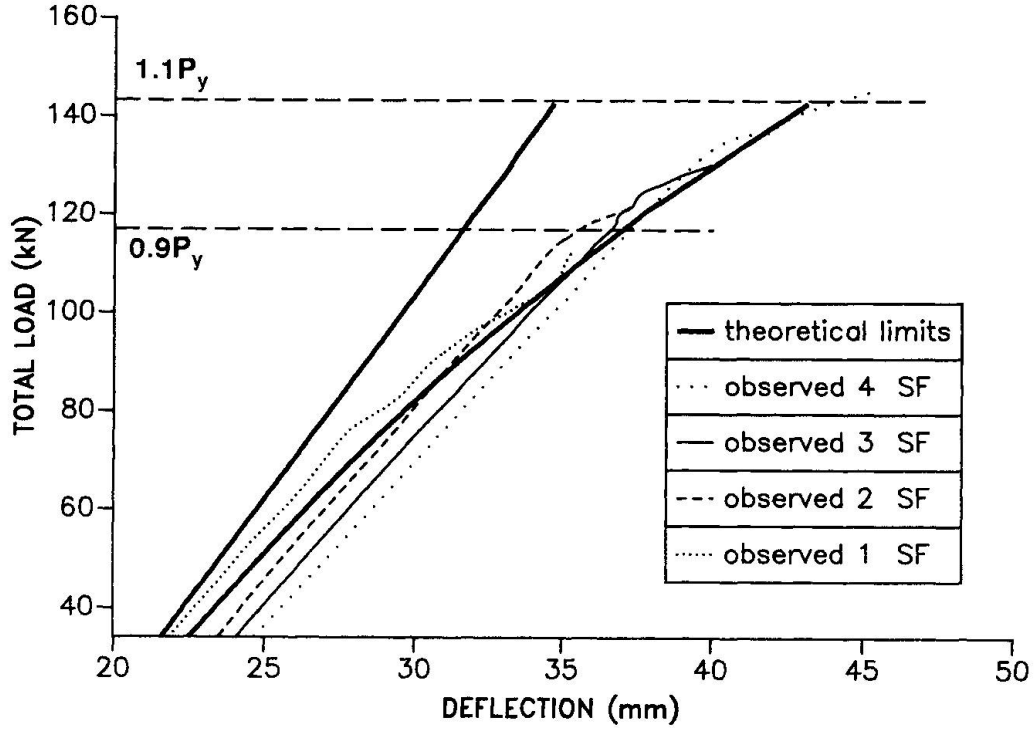

(a) Full Shear Connection Specimen SF

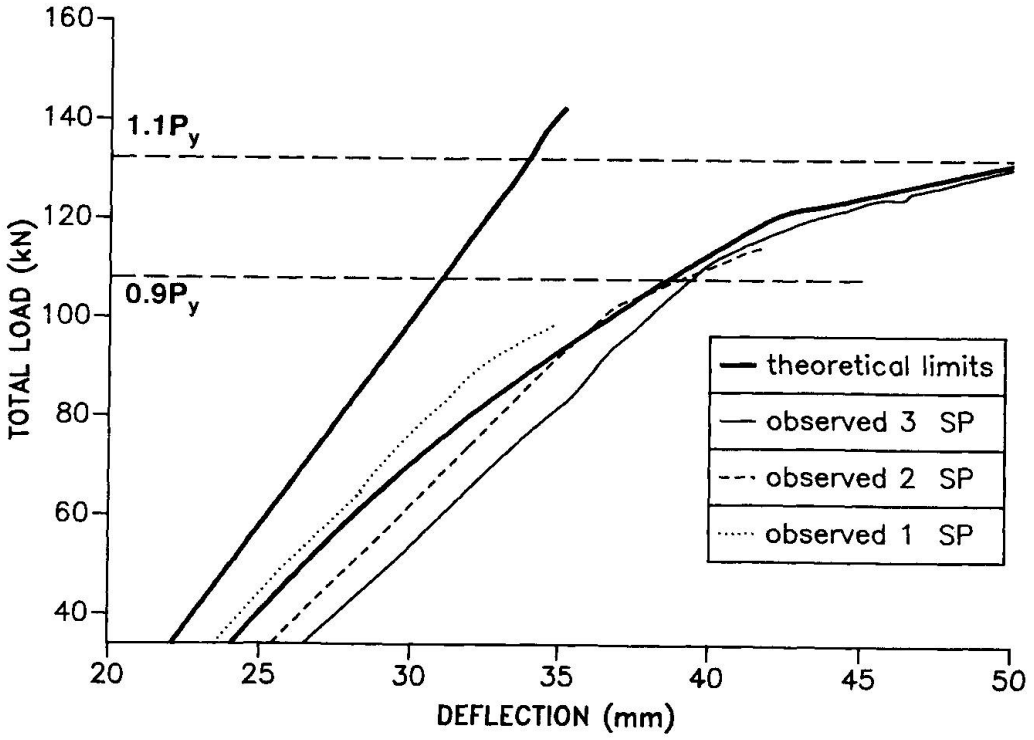

(b) Partial Shear Connection Specimen SP

FIG.2.-Observed & Theoretical Load-Deflection Curves for SF & SP

When the serviceability testing was completed it was decided to monitor specimens SF and SP for further shrinkage.In simply supported composite construction, the effects of shrinkage and creep are generally additive and it is therefore important to consider their contribution when spans are long or beams are shallow.In a paper by Leon [2] it was found that in a typical simply supported composite beam design the shrinkage deflection can vary from five (propped construction) to fifteen times (unpropped construction) the creep deflection.

Creep is important when the ratio of dead to live load is large or when a significant portion of the live load is present for long periods of time.Leon[2] has suggested that 25 % of the live load can be considered to be the long term load.Approximately 20% of the live load was placed on specimen SP after 74 days and the creep effects were observed.Unfortunately due to time considerations the load was removed after 118 days which does not allow an accurate investigation of creep.Annoying floor motion induced by building occupancy is probably the most persistent floor serviceability problem encountered by designers.A series of dynamic tests were therefore performed on specimen SF to determine the natural frequency.

3. TEST RESULTS AND DISCUSSION

Theoretical stresses, strains and deflections for propped and unpropped beams (combining the effect of dead load on the plain steel section with imposed load on the composite section) were assessed at loads up to and beyond yield using a nonlinear, moment-curvature algorithm developed by Kemp [4].Shrinkage deflections were modelled using the model of Chien and Ritchie [3] and creep effects using a creep coefficient determined from specimen tests to obtain a long term concrete modulus.

The observed and theoretical relationships between total load and maximum deflection for tests SF and SP are shown in Figs. 2(a) and (b),starting at a total dead load applied to the unpropped plain steel section of 34.1 kN.The observed deflections under self-weight of the slab are about 19.3 and 20.1mm in tests SF and SP,to which should be added a deflection of 1.8mm for the self-weight of the steel beam and deck in these tests.Additional shrinkage deflections were 0.8 and 1.6mm prior to testing 12 and 19 days respectively after casting.The values of restrained shrinkage strain were included in the theoretical analyses.

The partial shear connection (SP) is modelled by introducing a slip strain at the interface that is proportional to the curvature and that when integrated over the half-span produces an interface slip deflection equal to that observed at the end of the beam.For the theoretical curves in Figs. 2(a) and 2(b) :the upper curve neglects residual stress, shrinkage and slip-strain and the lower curve includes the assumed residual stress patterns based on Young [5],shrinkage and slip-strains.It is apparent from these figures that the pairs of curves reflect the range of stiffness exhibited by the beams during loading and unloading cycles with surprising accuracy.

The test results are summarised in Table 1. and compared at load levels of 90% of the load required theoretically to cause yielding of the extreme fibre and 110% of this load.The following aspects are apparent from these results for unpropped composite beams:
1.Deflections due to shrinkage (associated with the measured values of restrained shrinkage in Table 1) and residual rolling stresses produce significant components of the serviceability deflections.The shrinkage effects may be predicted using Chien and Ritchie's model[3] and the effect of residual stress may be considered based on the distributions proposed by Young [5].

Table 1: Theoretical and Observed Deflections

Specimen		SF (Fig.2a)		SP (Fig.2b)	
Yield stress of flange MPa		317		312	
Yield stress of web MPa		329		336	
Cube strength MPa		32		37	
Mod. of elasticity GPa		27		29	
No. of 19mm studs 115mm high		14/half span		5/half span	
Deflection under self-weight (mm)	Observed	21.1		21.9	
	Theoretical	21.6		22.1	
Restrained shrinkage (ustrain)	Observed	55u @ 12 days		120u @ 19days	
Shrinkage deflection (mm)	Theoretical	0.9		2.0	
		0.8		1.6	
Live load level (kN)		$0.9P_y$	$1.1P_y$	$0.9P_y$	$1.1P_y$
Dead/live load ratio		0.41	0.31	0.46	0.35
Live load deflection effects (mm) Elastic	Theoretical	10.0	12.4	9.0	11.0
Yielding	Theoretical	-	0.7	-	0.9
Residual stress	Theoretical	3.4	6.5	2.4	4.8
Shrinkage	Theoretical	1.1	1.1	2.3	2.4
Connector slip	Theoretical	-	-	1.2	7.8
Total live + Dead load deflection (mm)	Theoretical	37.0	43.2	39.0	51.0
	Observed	35.5	44.7	37.2	51.3
Restrained shrinkage (ustrain)	Observed	307 u @ 89 days		270 u @ 74days	
Shrinkage deflection (mm)	Theoretical	5.2		4.5	
	Observed	4.5		4.2	
Ratio of Total Deflection @ $1.1p_y$/Deflection @ $0.9P_y$	Eqn (1)	1.22		1.26	
	Theoretical	1.17		1.31	
	Observed	1.26		1.38	
Creep deflection due to 18.84kN for 44 days (mm)	Theoretical	-		0.3	
	Observed	-		not significant	
Natural Frequencies (Hz)	Canadian Code	8.1		-	
	Observed	8.0		-	

2.Exceeding the elastic stress limit on the extreme fibre by a small amount ($1.10P_y$ in these tests)does not result in significant increases in deflection, but the interaction of this with residual stress and interface slip in beams with partial shear connection does cause an appreciable non-linear response.Serviceability limits of elastic stress, as in the Canadian and British composite codes, are not justified, particularly because they are considered in isolation of the level of deflection at which they occur [1].

3.The largest increases in deflection at serviceability occur due to interface slip at values of the partial shear connection factor of 0.5.This is not only caused by loss of flexural rigidity, but also by the associated stress distribution that causes premature yielding.Only the American design code refers separately to both of these effects.

4.Creep deflections are unlikely to be large in unpropped beams and may be assessed by using a reduced modulus of elasticity for the concrete based on the Effective Modulus or the Age Adjusted Modulus approach.Little difference was observed due to creep when one of the beams was subjected to an increment of 20 % of the serviceability live load over a prolonged period.

5.The assessment of natural frequency of beam SF using the formulation in the Canadian code provided a reasonably accurate prediction of the actual behaviour.

The composite Eurocode requires account to be taken of creep and shrinkage in the calculation of deflections.The effect of residual stress is neglected as in other codes and partial shear connection is only considered at a shear connection factor below 0.5 which is clearly an unconservative approach when compared to the test measurements.

The following proposal was developed [1] for modelling the non-linear amplification of deflection due to the interaction of shrinkage, yielding, residual stress and interface slip over the range of load from that producing an extreme fibre stress of 90 % of yield ($0.9P_y$) to $1,10P_y$:

"For composite beams in which the total serviceability load P_{serv} exceeds the minimum load P_d required to cause an elastic stress of either $0.9f_y$ in the steel beam or $0.6f_{cu}$ in the concrete (f_{cu} is the cube strength) or a moment of 0.75 M_u,the total serviceability deflection y_{serv} shall be calculated as follows:

$$y_{serv} = y_s(1-EI_s/EI_c) + y_{dc}(P_{serv}/P_d)^2 \qquad .....(1)$$

in which

y_s = elastic deflection due to load applied to plain steel section

EI_s = flexural rigidity of plain steel section

EI_c = flexural rigidity of composite section

y_{dc} = elastic deflection due to total load P_d (self-weight + imposed) applied to composite section and including shrinkage and interface slip

P_{serv} = total serviceability load in the range $P_d < P_{serv} < 1.225\ P_d$."

This empirical proposal reflecting the correct boundary conditions, compares favourably with results of experimental and theoretical analyses in the range of load from first yield at $0.9P_y$ to $1.10P_y$, as shown in Table 1.

4.CONCLUSIONS

The effects of shrinkage, residual stress and interfacel slip have a significant effect on the serviceability deflection of composite beams.Creep effects will commonly be significantly smaller.

Serviceability limits on levels of elastic stress irrespective of whether the deflections are critical at which these stresses occur, can lead to undue conservatism.

The current procedures for determining the natural frequency of composite beams are accurate.

REFERENCES

1.Kemp, A.R. and Trinchero, P.E.,**Serviceability Stress Limits for Composite Beams**,Engineering Foundation Conference or Composite Construction II, Potosi,Missouri, June 15-19, 1992.

2.Leon, R.T.,**Serviceability Criteria for LRFD Composite Floors**,Proc. AISC National Conference, Kansas City ,Missouri, March 1990, pp.18.1-18.23.

3.Chien, E.Y.L. and Ritchie, J.K.,**Design and Construction of Composite Floor Systems**,Canadian Institute of Steel Construction, Willowdale, Ontario, 1984, pp.323.

4.Kemp, A.R., **Simplified Modelling of Material Non-Linearity in Structural Frames**, The Civil Engr. in S.Africa, Vol. 30, No. 9, Sept., 1988, pp.425-432.

5.Young, B.W., **Residual Stresses in Hot-Rolled Sections**, Department of Engineering Tech. Report No. CUED/C-Struct/TR8, University of Cambridge, England, 1971.

Deflection of Composite Slabs Connected with Welded Lattice

Flèches des dalles mixtes avec treillis soudé comme connecteur

Durchbiegung von Verbunddecken mit angeschweissten Stahlmatten

T. Seno ARDA
Prof. Dr.
Istanbul Technical Univ.
Istanbul, Turkey

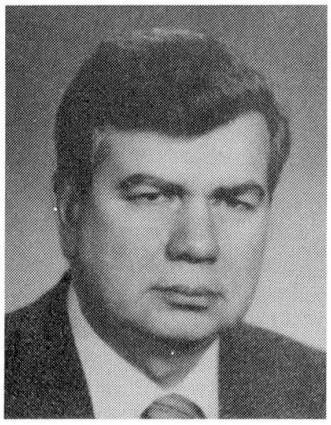

T. Seno Arda, born 1940, received his M.Sc. degree at ITU, the Istanbul Technical University. Research assistant for two years at Liège University Belgium, where he prepared his doctorate thesis. He started his academic career when he returned to ITU, where he is now coordinator of the Steel Structures Group.

Cavidan YORGUN
Dr. Eng.
Istanbul Technical Univ.
Istanbul, Turkey

Cavidan Yorgun, born 1960, received her M.Sc. and Ph.D. degrees at the Istanbul Technical University where she is now research assistant in the Steel Structures Group.

SUMMARY

This paper presents the part of the results related to the serviceability limit states of an experimental research investigation on composite slabs in which the connection between the concrete and the profiled steel sheeting is obtained by a reinforcing lattice welded on the steel sheeting. This type of connection is quite practical and prevents bond failure. The paper is concluded with some design specifications and an interpretation of results.

RESUME

Cet article présente la partie des résultats aux états limites de service, d'une recherche expérimentale ayant pour sujet les dalles de plancher mixtes formées de béton coulé sur des tôles d'acier profilées, la connection entre les deux matériaux étant obtenue par un treillis soudé sur la tôle. Ce type de connection est assez pratique et empêche toute rupture par adhérence. L'article se termine par l'interprétation des résultats et par quelques considérations pour le projet.

ZUSAMMENFASSUNG

In dieser Arbeit werden Versuchsergebnisse zu den Gebrauchsgrenzlasten aus Betondecke und Stahltrapezprofil bestehenden Verbunddecken angegeben, an denen die Verbundwirkung durch Stahltrapezprofil angeschweisste Betonstahlmatten gesichert wurde. Diese Verbindungsart ist ziemlich praktisch und verhindert einen Verbundbruch. Die Berechnungsverfahren und Folgerungen beschliessen die Arbeit.

1. INTRODUCTION

In floor construction of steel skeleton buildings, there is an increased use of composite slabs with profiled steel sheeting.

In order to permit the steel deck to serve as tensile reinforcement and act compositely with the concrete, a means for positive mechanical interlock is needed. This mechanical interlocking is in most cases totally provided by the mechanical shear transferring devices [1, 2]. These are:
- Indentations or/and embossments rolled in to the deck,
- Study connectors welded on supports,
- Reinforcing steel lattice welded on the steel sheeting.

In Turkish market, steel decks' surfaces are commonly smooth. For this reason, the connection between the concrete and the profiled steel sheeting is oftenly obtained by a reinforcing lattice welded on the sheeting. This type of connection is practical and prevents generally an adherence rupture. This welded lattice, on the other hand, is also functioning as a load distributing reinforcement in transverse direction. Since the quality of connection provided by such a connection was not exactly known, it was decided to test it experimentally.

2. DESCRIPTION OF TEST SLABS

In this experimental study; a preliminary series of 6 tests and a main series of 9 tests are carried out in the positive bending moment zone to investigate the ultimate and serviceability limit states [3]. The profiled steel sheetings used in test specimens are galvanized and show three different thicknesses (t=0.75mm, t=1.00mm, t=1.20mm), same width (b=860mm) and depth (d_a=27.5mm). The typical cross section of steel sheeting is shown in (Fig. 1). The concrete was casted in such a way that the total depth of slab is nominally equal to d_t=10cm. A summary of the main series' specimens properties is given in Table 1.

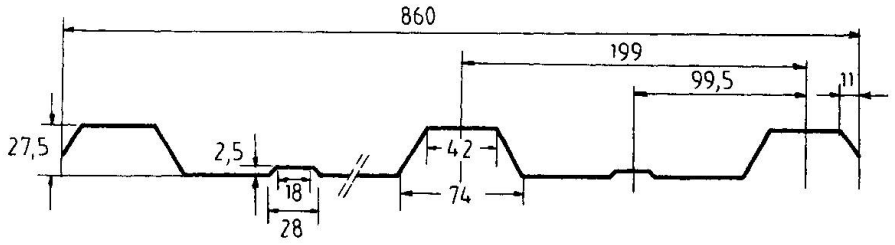

Fig. 1 Typical cross-section of the steel sheeting

Slab Element	Shear Connection Lattice	Depth of Slab Element (Measured)	Compressive Strength of the Concrete	Yield Strength of the Steel Sheeting
	mm	cm	daN/cm^2	daN/cm^2
3.A-0.75	Ø4.5/150	10.5	300	2850
3.B-0.75		10		
3.C-0.75	(150.250.4,5.4,5)	10		
4.A-1.00	Ø4.5/150	11	450	2400
4.B-1.00		9.5		
4.C-1.00	(150.250.4,5.4,5)	10		
5.A-1.20	Ø5/150	10	350	2850
5.B-1.20		10.5		
5.C-1.20	(150.250.5,0.5,0)	10		

Table 1 Summary of the main series' specimens properties

3. TEST PROCEDURE

The test specimens with a span of 300 cm, were simply supported at both ends and the test frame was designed to apply two concentrated loads at the one thirds of their span lengths (Fig. 2), such a loading providing a bending moment diagram similar to the uniform loading.

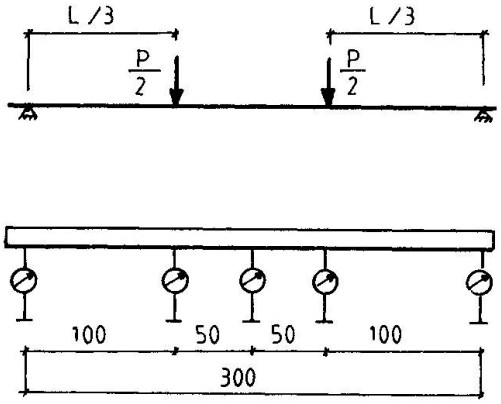

Fig. 2 Typical arrangement for testing slab elements

The load P applied to the test specimens was static in character and was increased in steps starting from zero up to the level where the failure mechanism was observed. At each increment of the loading, the deflections at the mid-span (L/2) and at one thirds of the span (L/3) along with the strains at various locations of the steel sheeting and the concrete were both measured.

The experiments were performed at the Structural Laboratories of Istanbul Technical University.

The primary test series are conducted to determine a suitable shear connection calculation which could prevent an adherence rupture.

The shearing force between the steel sheeting and the concrete can be assumed equal to the tensile capacity N_s of the steel sheeting.

$$N_s = A_s f_y$$

Where A_s is the cross-sectional area and f_y is the yield stress of the steel sheeting. It is easy to compute

$$A_{sl} > \frac{N_s}{2n_H m_H \tau_{all}}$$

Where n_H is the number of ribs of the steel sheeting, m_H is the number of transverse bars of the lattice along one shear span, A_{sl} is the cross-sectional area of this bar and τ_{all} is allowable shear stress of this bar.

The reinforcing lattice designed using this method, shear-bond failure has never been observed in the test specimens before the flexural failure.

Ultimate limit state loads of the test specimens and their serviceability limit states were both investigated. This paper presents the part of the results related to the serviceability limit states of an experimental research.

4. METHODS OF ANALYSIS OF THE DEFLECTION

In calculating the theoretical deflections for a comparison with the experimental deflections, the moment of inertia were obtained seperately for the cracked and uncracked cross-section. These two values and also their average as advised in EC4 [4] and ASCE [5], were used in calculations. In another approach, only the concrete located upon the steel sheeting profile was taken into account in the calculation of the moment of inertia.

In transforming the concrete cross-section to an equivalent steel cross-section in order to calculate the moment of inertia, the width of the concrete part was used divided with 2n, in which $n = E_s/E_c$ is the ratio of the modulus of elasticity of steel to concrete, this to take into account the creep of concrete.

The accordance, between the experimental an the computed theoretical deflections is remarkable with respect to two methods of calculations in which either the average moment of inertia of cracked and uncracked sections is used or only the moment of inertia of the concrete located upon the steel deck is taken into account.

From the practical point of view, these results are important only in between the two following application limits:

- The design load P^i_{ut} obtained by dividing the theoretical load P_{ut} with a safety factor η (1.7 in Turkish Standard TS. 4561) [6]
- Deflection limit load P_{us} (L/300 in Turkish Standard TS. 648) [7]

Table 2 shows measured deflections and computed deflections, at the mid-span, based on two different methods, for each slab element, when loaded to the design load P^i_{ut} in which theoretical deflection δ_{t1} is computed using a simple average of cracked and uncracked sections and theoretical deflection δ_{t2} is computed using the concrete located upon the steel sheeting.

Slab Element	P_{us}	P^i_{ut}	δ_e	δ_{t1}	δ_{t2}	δ_e/δ_{t1}	δ_e/δ_{t1}	P_{us}/P^i_{ut}
	daN	daN	mm	mm	mm	....	....	....
2.A-0.75	1950	1841	9.20	9.23	10.44	0.997	0.881	1.060
2.B-1.00	2250	2098	8.30	9.35	10.47	0.888	0.793	1.072
2.C-1.20	2300	3149	14.90	12.78	14.19	1.166	1.050	0.730
3.A-0.75	2100	1941	8.95	8.79	9.77	1.018	0.916	1.082
3.B-0.75	1750	1824	10.70	9.44	10.66	1.133	1.004	0.959
3.C-0.75	1850	1824	9.60	9.44	10.66	1.017	0.901	1.014
4.A-1.00	3100	2407	5.65	7.87	8.63	0.718	0.655	1.288
4.B-1.00	2340	1988	7.65	9.71	11.06	0.788	0.692	1.177
4.C-1.00	2550	2128	7.00	9.04	10.17	0.774	0.688	1.198
5.A-1.20	2300	3149	15.10	12.78	14.19	1.182	1.064	0.730
5.B-1.20	2460	3359	14.50	11.94	13.14	1.214	1.104	0.732
5.C-1.20	2300	3149	15.60	12.78	14.19	1.221	1.100	0.730

Table 2 Measured and computed deflections at P^i_{ut}

The typical load-deflection behavior for the test specimen (5.A-1.20) is shown as an example in (Fig. 3).

As in these the limits described above, the two methods described above give similar results, the second one which is simpler is concluded to be more appropriate for practical purposes.

One of the aims of this study was to observe either the ultimate limit state or the serviceability limit state was more influent. From the three different thicknesses of the folded steel sheetings used in tests, only the thickest one (t=1.20mm), resulted in ultimate design load greater than the serviceability limit state load. In the test specimens with the two other thicknesses: thin (t=0.75mm) and medium (t=1.00mm), the result in contrary.

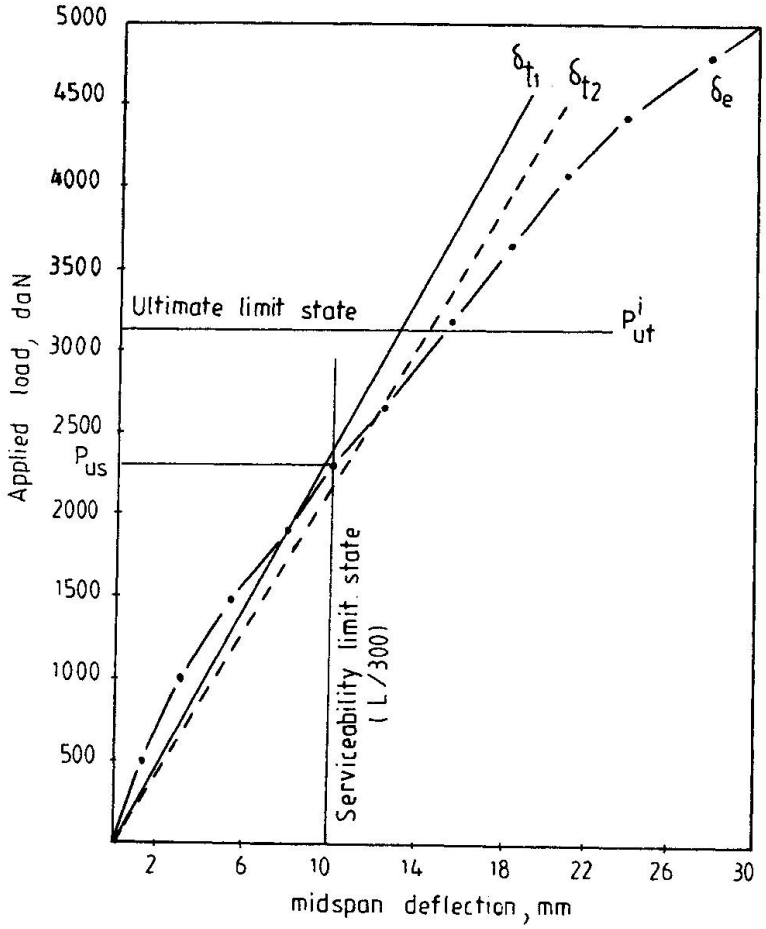

Fig. 3 Load-deflection curves for a test specimen

5. CONCLUSIONS

The accordance between the experimental and the theoretical deflections is less remarkable compared to the results reached in ultimate loads values. However, the best correlation is obtained with two methods of calculations in which either the average moment of inertia of cracked and uncracked sections, or only the moment of inertia of the concrete located upon the steel deck are used. The second approach which is simpler, is judged to be more appropriate for practical purposes.

The general evaluation of the test results show that, for the cases where, t/d ratio (thickness of the steel sheeting/nominal depth of composite slab) is

smaller than, or equal to 1 percent, the ultimate limit state is more significant than the serviceability limit state.

REFERENCES

1. SCHUSTER R.M., Composite Steel-Deck Concrete Floor Systems. Journal of the Structural Division, ASCE, pp. 899-917, May 1976.
2. JANNS J., Etude D'une Liaison Acier-Béton Pour Planchers Mixtes Avec Coffrage Collaborant. Centre de Recherches, CRIF, Bruxelles, 1982.
3. YORGUN C., The Behavior and the Load Carrying Capacity of the Composite Slabs with the Reinforcing Lattice Used as Connectors. (in Turkish), phD Thesis, Istanbul Technical University, 1992.
4. Eurocode No. 4, Design of Composite Steel and Concrete Structures. March 1992.
5. ASCE, Specifications for the Design and Construction. 1984.
6. TS 4561, Turkish Standards. 1985.
7. TS 648, Turkish Standards. 1980.

Initial and Long-Term Deformations of Prestressed Concrete Members

Déformations initiales et à long terme d'éléments en béton précontraint

Sofortige und Langzeitverformung von Spannbetonelementen

Franco MOLA
Prof. of Struct. Eng.
Politecnico di Milano
Milan, Italy

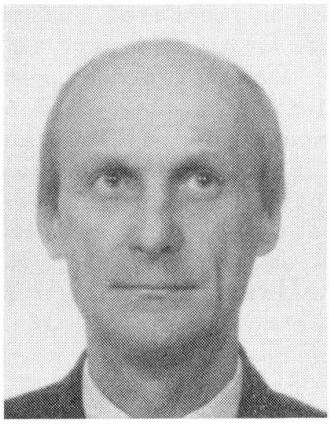

Franco Mola, born 1946, is active in research concerning creep structural analysis, instability and rehabilitation of concrete structures. Member of the Editorial Group of the FIP CEB Manual «Structural Effects of time dependent behaviour of concrete». In 1985 he was conferred the IABSE Prize in Luxembourg.

SUMMARY

A method for the analysis of pre-tensioned and post-tensioned prestressed concrete sections subjected to long-term loads is presented. Assuming for concrete an algebraic linear viscoelastic constitutive law, the relationships giving the time-evolution of the cable force and of the sectional curvature are deduced. Design formulas for the evaluation of the amount of prestressing reinforcement necessary to satisfy prescribed stress bounds in concrete in the service stage are then stated.

RESUME

Une méthode pour l'analyse des sections en béton précontraint soumises à l'action de charges de longue durée est présentée. Dans l'hypothèse de béton obéissant à une loi viscoélastique algébrique linéaire les expressions qui donnent l'évolution dans le temps de la force dans le câble de précontrainte et de la courbure de la section sont tirées. L'article se termine avec la détermination de l'armature de précontrainte nécessaire pour assurer que, dans les conditions de service, les efforts de traction dans le béton ne dépassent pas leur valeurs admissibles.

ZUSAMMENFASSUNG

Es wird ein Verfahren zur Berechnung des Langzeitverhaltens von Spannbetonelementen mit sofortigem oder nachträglichem Verbund unter Dauerlast vorgestellt. Aus der Annahme eines algebraischen, linear-viskoelastischen Materialgesetzes für den Beton lassen sich die Beziehungen für die zeitliche Entwicklung der Spannkräfte und der Querschnittskrümmungen herleiten. Abschliessend werden Bemessungsformeln genannt, mit denen die zur Einhaltung vorgegebener Betongrenzspannungen erforderliche Spannbewehrung ermittelt werden kann.

1. INTRODUCTION

The analysis of the state of stress and deformation under long-term loads represents one of the basic aspects connected to the assessment of structural safety in the service stage of P.C. elements. At the present time the Codes, [1], [2], give some general guidelines for the evaluation of long term stresses and deformations in P.C. members, but they do not develop practical procedures for the structural analysis. In particular a linear viscoelastic constitutive law is prescribed for concrete while steel is considered in the elastic range, so that if the behaviour of concrete is described by means of refined formulations the sectional analysis of P.C. elements requires the solution of a system of two Volterra integral equations by means of numerical algorithms which are not customary for the practitioners. As the service analysis of P.C. elements has in general to be performed by means of procedures exhibiting good precision levels, the development of an analytical method able to accomplish this goal without requiring too cumbersome computations and suitably utilizable by designers assumes significant interest. For this reason many simplified methods of analysis have been proposed, but they have not solved the problem in an exhaustive way, in particular they can not be immediately reduced to analytical forms in agreement with Codes Specifications or to unified hypotheses regarding the constitutive laws or the structural idealization. In the present paper a contribute to this subject is given by developing an analytical formulation for the long term sectional analysis, based on the algebraic stress-strain linear viscoelastic law proposed for concrete by Trost, [3], widely used in other author's works, [4], [5] and recommended by the Codes. Regarding the sectional geometrical and mechanical description we shall adopt the hypothesis that the prestressing cables or strands will be grouped in order to form a virtual cable having area equal to the sum of the areas of the single cables or strands and passing through the point of application of the total prestressing force. In this way it is possible to proceed by means of the force method assuming as unknown the force in the resultant cable, reaching without great difficulty simple solutions of good approximation and suitable to discuss the basic properties of the service behaviour of P.C. elements taking also into account shrinkage deformations. In particular the differences in the long term statical interaction between the cable and the section when pre-tensioned or post-tensioned elements are considered, will be pointed out and simple formulas, suitable for evaluating the amount of prestressing reinforcement will be stated, together with the analytical expressions for the control of long-term deformations. At this subject suitable moment-curvature diagrams of P.C. sections, clearly describing the interaction between the prestressing and external loads and their effect on the deformational behaviour of P.C. members will be discussed. A simple numerical example, referred to an actual P.C. element will be finally performed in order to clearly show the basic practical aspects of the proposed procedure.

2. SECTIONAL ANALYSIS OF P.C. MEMBERS

With reference to fig. 1, let us consider a P.C. pre-tensioned, (fig. 1a) or post-tensioned section (fig. 1b). Indicating by N_p the prestressing force imposed to the reinforcement, by δ_c, δ_s, the elastic influence coefficients of concrete and steel, by ϵ_s ϵ_c the corresponding deformations at time t, we can write the subsequent compatibility equation

$$\epsilon_c+\epsilon_s=N_p(a\delta_c+\delta_s)+\epsilon_{sh} \qquad (1)$$

where $\epsilon_{sh}<0$ is the shrinkage deformation. In eq. (1) the coefficient a vanishes for pre-tensioned sections (a=0) and it is equal to unity (a=1) for post-tensioned sections as in the first case the prestressing initial force N_p is applied only to steel while in the second it affects also the concrete section. According to the previously mentioned hypotheses about the materials behaviour we can write [3], [4]

$$\epsilon_c=\sigma_{co}(1+\phi)/E_{co}+(\sigma_c-\sigma_{co})(1+\mu\phi)/E_{co} \qquad (2)$$

$$\epsilon_s=\sigma_s/E_s$$

where the quantities with index o are referred to initial time, ϕ is the creep coefficient and μ is the concrete aging coefficient. Expressing the stresses by means of internal actions N, M_g and introducing eq. (2) in eq. (1) we obtain

$$N=N_R\{[\alpha(1+\Omega a^*)+\Omega b-1](1-\Omega c)+1-\beta k_{sh}\Omega c r^2/(\phi e^2)\}=N_R k_N \qquad (3)$$

where

$$N_R=\beta M_g/e;\ \beta=e^2/r^2/(1+e^2/r^2);\ \alpha=N_p/N_R;\ \Omega=(1+e^2/r^2)/(1+e^2/r^2+1/mn_s)$$

$$m=E_s/E_{co};\ n_s=A_s/A_c;\ a^*=a-1;\ c=\phi/(1+\Omega\mu\phi);\ k_{sh}=|\epsilon_{sh}|E_{co}A_c/N_R \qquad (4)$$

with A_c, r, respectively area and radius of gyration of concrete section. In eq. (3) the parameter b specifies pre-tensioned sections for b=1 and post-tensioned sections for b=0. This distinction is necessary as the external moment M_g is active on the reinforcement when it has been connected with concrete For this reason it has no effect at initial time on the reinforcement of post-tensioned elements and only successively interacts with it as a consequence of concrete creep deformations and of steel to concrete solidarisation obtained by means of the sheets grouting. Eq. (3) allows to evaluate the force in the cable at any time so that remembering the constitutive law (2) we reach the subsequent expression for the long-term sectional curvature

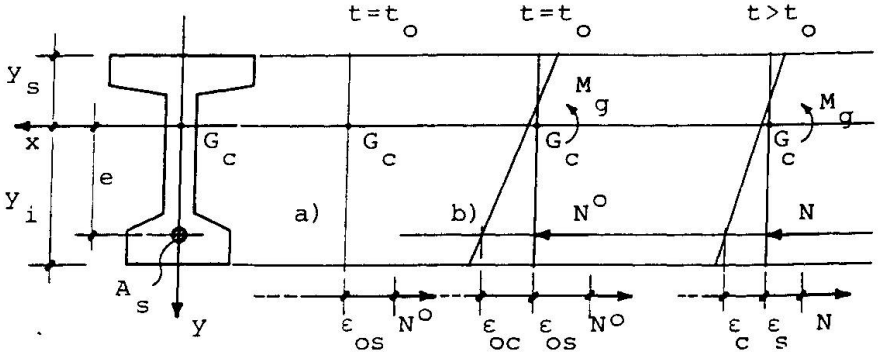

Fig.1 General features of a P.C. section

$$\Phi/\Phi^o=(1+\phi)\{1-\beta\{[\alpha(1+\Omega a^*)+\Omega b-1](1-\Omega cd)-\beta k_{sh}r^2\Omega cd/(\phi e^2)+1\}\} \qquad (5)$$

where $\Phi^o=M_g/E_{co}J_c$; $d=(1+\mu\phi)/(1+\phi)$, with J_c centroidal moment of inertia of concrete section. By means of expressions (3), (4), (5), it is possible to evaluate the sectional state of stress and deformation, assuming for the coefficient μ the expression $\mu=-k_R^{-1}-\phi^{-1}$ where $k_R<0$, $\phi>0$ are respectively the relaxation and the creep coefficient of concrete. These coefficients depend from the model assumed to describe concrete creep, in particular, for the model exposed in [5], they are reported, in graphical form, in [6]. When no data are available for μ we can however assume the subsequent approximate relation connecting creep and relaxation coefficient: $k_R=-\phi/(0.8\phi+1)$, so that for μ we deduce the approximate constant value $\mu=0.8$. As indicated in [1], this simplification can be adopted without great error in sectional P.C. members analysis.In fig. 2, referring to prescribed values of β, ϕ and for $\epsilon_{sh}=0$ the expressions (3), (5) are reported for $t=t_o$ and $t>t_o$. The corresponding diagrams are straight lines and describe the variability in time of the force in the resultant cable when varying the prestressing force. The diagrams allow to draw some interesting observations. As regards the cable force, represented at initial time t_o by the two dotted lines b_1, b_2 respectively related to pre-tensioned and post-tensioned sections, and by the two corresponding lines a_1, a_2 at time t we see that the force is greater in post-tensioned cables as they are subjected at the initial time to the total prestressing force $N_o=N_p=\alpha N_R$, (eq.(3) with $a^*=b=c=0$), while in pre-tensioned cables this initial force assumes the reduced value $N_o=N_R(\alpha(1-\Omega)+\Omega)$, (eq.(3) with $a^*=-1$, $b=1$, $c=0$). When $\alpha=0$, $t>t_o$ the line b_2, initially passing through the origin is trasformed in the line a_2 intersecting the vertical axis with a positive ordinate as a consequence of the delayed statical effect exerted by the permanent moment M_g on the cable after its solidarisation to concrete section by means of the sheet grouting. Finally we can observe that for $\alpha=1$, we reach at any time $N=N_R$, independently from the type of prestressing, so that the straight

lines a_1, a_2, b_1, b_2 have a common centre. This can be effective as for $\alpha=1$ the cable assumes the force N_R, coinciding with that produced by moment M_g on a rigid cable. In this circumstance the hypotheses of the first theorem of linear viscoelasticity become valid so that no variations in the cable force can take place. This fact evidentiates also that for $0<\alpha<1$ the force in the cable grows in time as we can state observing that lines a_1, a_2 are disposed upwards the initial lines b_1, b_2. On the contrary for $\alpha>1$ the force in the cable always decreases in time. This is the customary case of P.C. elements as values of $\alpha<1$ are connected to rather small values of the prestressing force which are not effective to guarantee a sufficient prestressing level suitable to be emploied in practical applications. Nevertheless levels of prestressing with $\alpha<1$ are often adopted for complex structures as cable-stayed bridges so that in these structures we can have an increasing of the cable force in time. The dotted lines c_1, c_2 refer to pre-tensioned and post-tensioned section adimensional curvatures at time t_o while the corresponding lines at time t are represented by lines d_1, d_2. The curvatures vary in time assuming increments which have generally the same sign of the initial curvature but in the intersecting zone of the straight lines, about for $4\leq\alpha\leq5.15$, in the present case, initial curvature and its time increment exhibit opposite signs. In other words for small prestressing forces the initial curvatures and their increments are controlled by the moment M_g and the element exhibiting downwards transverse displacements increases them in the same direction owing to concrete creep deformations.

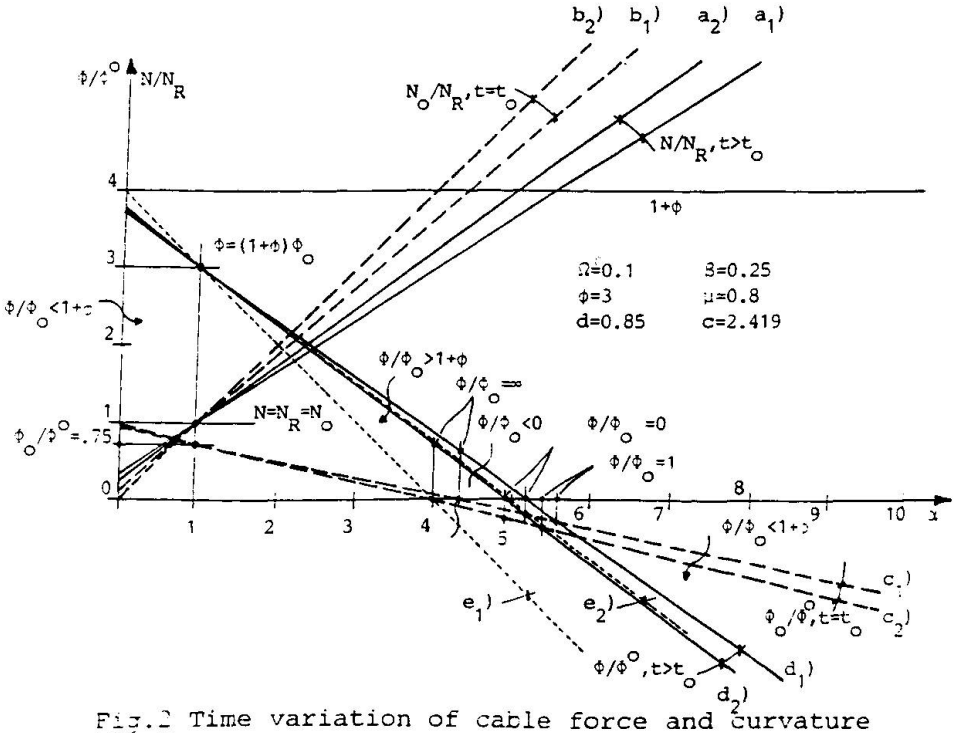

Fig. 2 Time variation of cable force and curvature

For intermediate α values the curvatures are initially negative as prestressing prevails on external load, but creep effects produced by loads are more significant so that the upwards initial displacements, exhibit downwards variations which can produce downwards, upwards or even vanishing final displacements. As a particular case we have the singular situations connected to a final value of the displacements equal to the initial ones. Finally, for high α values prestressing is always prevailing on the loads so that the upwards initial displacements increase in time in the same direction. In order to evaluate the importance connected to the choise of a reliable analytical procedure in reaching good results, in fig. 2 the two limiting lines e_1, e_2, represented for post-tensioned sections and related respectively to the simplifying hypothesis of considering constant in time the cable force with its initial or final value are reported. It is immediate to see that the first hypothesis produces too marked errors so that the cable force variability has to be accounted for in order to reach reliable results. On the other hand the second hypothesis gives very good results, but it can be applied only when the time-variability of N has be evaluated so that no substantial simplifications in computational works are introduced, and for this reason it is more convenient to

proceed by means of the general expression (5).

3. DESIGN FORMULAS AND NUMERICAL EXAMPLE

Expression (3) can be emploied in evaluating the area of prestressing steel which allows to satisfy some limit state specifications in particular to get a prescribed stress level at the bottom sectional edge when permanent and variable loads are applied. Indicating by $M_q=sM_g$ the moment produced by variable loads, remembering eq. (3), the bottom edge stress produced by permanent and variable loads together with prestressing, assuming positive compressive stress, becomes

$$\sigma_i=|\sigma_g|[-(1+s)+(k_N+\Omega s)/z] \qquad (6)$$

where:

$$|\sigma_g|=M_g/W_i;\quad z=(1+r^2/e^2)/(1+r^2/(ey_i))$$

Indicating by σ_{ct} the maximum tensile stress allowed in concrete the safety inequality can be written $\sigma_i\geq\sigma_{ct}$, or according to eq. (6)

$$k_N\geq z[1+s+p]-\Omega s \qquad (7)$$

with $p=\sigma_{ct}/|\sigma_g|$

Introducing the expression of k_N deriving from eq. (3) in eq. (7), simple algebraic calculations drive to the subsequent inequality

$$\Omega\geq\pi(1-\Omega)\{z(1+s+p)-\Omega[b(1-\Omega c)+c(1-\beta k_{sh}r^2/(\phi e^2))+s]\}/[(1+\Omega a^*)(1-\Omega c)] \qquad (8)$$

where

$$n_s=A_s/A_c=\beta r^2\Omega/[me^2(1-\Omega)];\quad \pi=me|\sigma_g|/(\sigma_s y_i);\quad N_p=\sigma_s n_s A_c$$

and σ_s represents the prestressing imposed stress to steel. Expression (8), written with equality sign, represents an implicit equation in the unknown Ω which can be solved by a trial and error method, so that we can successively evaluate by means of the expression of n_s the necessary amount of prestressing steel in order to satisfy the safety inequality (7). As we can observe the result depends from the values assumed by the parameters a^* and b, or that, by the type of prestressing imposed to the section. When the Ω coefficient has been determined, from eq. (3) we reach the value N of the cable force, so that according to the constitutive law (2) we obtain the subsequent expression for the curvature

$$\Phi/\Phi^O=(1+\phi)[1-\beta k^O_N\phi(1-\mu)/(1+\phi)-\beta k_N(1+\mu\phi)/(1+\phi)] \qquad (9)$$

where k^O_N is the initial value of the adimensional force k_N, which from eq. (3), written for $t=t_o$ becomes

$$k^O_N=\alpha(1+a^*\Omega)+\Omega b \qquad (10)$$

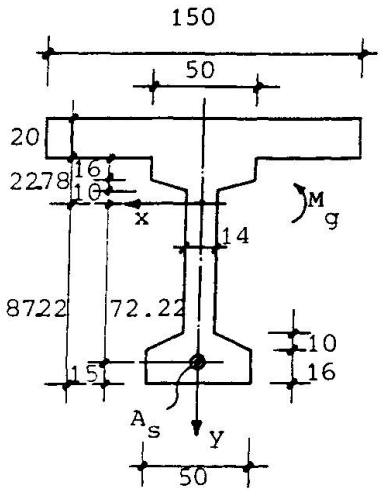

Fig.3 P.C. section of a bridge beam

In order to apply the discussed procedures to an actual case, let us consider the bridge section of fig. 3 for which we assume: $E_s=1.95\cdot10^5$ MPa; $E_{co}=3.6\cdot10^4$ MPa; m=5.417; $M_g=1500$ KNm; $|\sigma_g|=11.81$ MPa; $\sigma_s=1350$ MPa; s=1; $\epsilon_{sh}=-50\cdot10^{-5}$, $\phi=3$. With reference to the assessment of structural safety for the decompression limit state, ($\sigma_{ct}=0$), assuming a pre-tensioned reinforcement, from eqs. (9), with $a^*=-1$, b=1 , we reach $\Omega=0.09367$; $n_s=0.4956\cdot10^{-2}$; $N_p=4049$ KN; N=3080 KN; $N/N_p=0.7607$. For the curvature, according to eq. (9), we obtain $\Phi_o/\Phi^O=-0.836$; $\Phi/\Phi^O=-2.136$; $\Phi/\Phi_o=2.555$. Assuming on the contrary a post-tensioned reinforcement, $a^*=-1$, b=0 the results are $\Omega=0.08794$; $n_s=0.4623\cdot10^{-2}$; $N_p=3777$ KN; N=3080 KN; $N/N_p=0.8155$; $\Phi_o/\Phi^O=-0.819$; $\Phi/\Phi^O=-2.139$; $\Phi/\Phi_o=2.612$. We observe that the two kinds of pre-stressing are practically equivalent with respect the deformations while show a not negligible difference regarding the amount of steel reinforcement which is about 7% greater for pre-tensioned strands. This fact allows to reduce the prestressing reinforcement in post-tensioned sections as the final

force in the cable is of about 7% greater than that existing in pre-tensioned strands as they are affected by an elastic initial loss of prestressing force which is not on the contrary present, due to the prestressing technique, in post-tensioned cables.

4. CONCLUDING REMARKS

The viscoelastic analysis of P.C. sections performed assuming the simplifying hypothesis of considering the prestressing force concentrated in the resultant cable and assuming for concrete a viscoelastic algebraic law has allowed to point out significant aspects related to the long-term behaviour of these structures. Regarding this subject it has been proven that in the pre-tensioned sections the reduction of prestressing force is more marked as a consequence of the initial elastic loss which for the most usual prestressing situations, connected to high values of α, is not adequately recovered by the increasing produced by external loads. Regarding this aspect the post-tensioned sections are more profitable, but a final judgement has to be drawn also considering the friction loss which specially for cables with significant curvatures can produce high reductions of the prestressing force. Regarding the deformational aspect the two way of prestressing lead to substantially similar results but it is noteworthy to emphasize the different character of the time evolutions of the sectional deformation which can have equal or opposite sign with respect the intial curvature depending from the level of the imposed prestressing force. It is so necessary to proceed with care and precision in the analysis of long term behaviour of R.C. sections and at this subject in author's mind the proposed method represents a suitable and simple tool to reach reliable results.

REFERENCES

1. FIP/CEB Model Code 1990. CEB Bulletin d'Information No.195-196/1990.
2. EC2 - Eurocode n. 2 Design of Concrete Structures, Part. 1, General Rules and Rules for Buildings.
3. TROST, M. Auswirkungen des Superpositionprinzips auf Kriech und Relaxation Probleme bei Beton und Spannbeton, Beton und Stahlbetonbau, H. 10, 1967.
4. MOLA, F. General Viscoelastic Analysis of inhomogeneous structures and sections, Studi e Ricerche, Vol. 8, Italcementi, Bergamo, Italy, 1986 (in Italian).
5. MOLA, F., PIETRA, S., Linear viscoelastic analysis of composite steel-concrete sections, Studi e Ricerche, Vol. 8, Italcementi, Bergamo, Italy, 1991.
6. FIP/CEB Model Code for Concrete Structures. CEB Bulletin d'Information No.124 125/1978.

Statistical Distribution of Crack Widths in Reinforced Concrete Bars

Distribution statistique de l'ouverture des fissures des barres en béton armé

Statistische Verteilung der Rissbreiten an Stahlbetonstäben

István HAMZA
Eng., Arch.
Hungarian Academy of Sciences
Budapest, Hungary

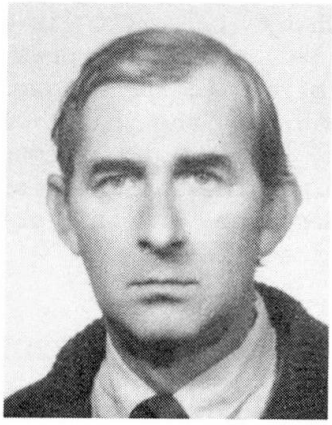

Born 1945, István Hamza obtained his engineer-architect degree at the Faculty of Architecture at the Technical University of Budapest. Since 1968 he has been working as a scientific research associate at the Department of Strength of Materials and Structures of the same University. His research field is the serviceability of structures.

SUMMARY

The characteristics of the statistical distribution of crack widths, and crack spacing were determined from a large amount of data obtained by simulating the crack formation on reinforced concrete bars under simple tension. The tensile and bond strengths were generated as random variables. The numerical results obtained were compared with experimental data and with the crack width calculated according to several standards or codes.

RESUME

En simulant par ordinateur la fissuration des barres sollicitées en traction pure, on a déterminé les caractéristiques des distributions statistiques de l'ouverture, et de la distance des fissures. Dans les essais, la résistance à la traction ainsi que celle à l'adhérence du béton ont été prises en compte comme des variables aléatoires. Les résultats numériques ont été comparés avec des données expérimentales et avec l'ouverture des fissures calculée selon différents codes.

ZUSAMMENFASSUNG

An zugbeanspruchten Stahlbetonstäben wurden die Charakteristiken der statischen Verteilung der Rissbreiten und der Rissabstände ermittelt, und zwar mittels Computersimulation der Rissbildung aus zahlreichen Daten. In den Untersuchungen wurden die Verbund- und Zugfestigkeit des Betons als zufallsverteilt betrachtet. Die ermittelten numerischen Ergebnisse wurden mit Versuchsdaten und mit gerechneten Werten der Rissbreite nach verschiedenen Normen verglichen.

1. INTRODUCTION

Recently one can notice a trend applying probability methods to determine the characteristics of service conditions, like the design value of crack widths, just as it became a practice in calculating loadbearing properties. In accordance with international recommendations the 95%-fractile of the distribution of crack widths, developing along intervals under constant stress-condition, will be considered as the characteristic value of crack width.

In the CEB-FIP Model Code [1] the 95%-fractile is obtained by multiplying the mean value of crack width by 1,7. (It is the 0,4 value of the variation coefficient of crack width, that is presumed in the multiplier.) The new CEB-FIP Model Code [2], similary to the Hungarian standard [3], calculates the characteristic crack width on the basis of maximum crack spacing. Those calculations, although they involve the elements of probability calculus, are not suitable for determining the characteristics of the statistical distribution of crack widths. Moreover, it is a question, how the calculated value relates to the actual 95%-fractile.

2. THE METHOD OF THE DISTRIBUTION CALCULATION

The characteristics of the statistical distribution of crack widths (the type of distribution, the mean value, the standard deviation, the 95%-fractile, etc.) can not be determined analytically, because of the accidental nature of cracking, thus the Monte Carlo method is applied instead. The tensile strength and the bond strength of the concrete were generated at random on axially tensed members and the development of cracks was simulated by computer. Whenever a crack has "appeared" the width of the cracks was determined at the end of the crack formation as well as at a higher and a lower level of service load. Having examined a sufficient number of members, conclusions can be drawn regarding the statistical distribution of crack spacings and crack widths.

3. THE BASIC ASSUMPTIONS OF THE CALCULATION

In the course of the examinations the tensile strength of the concrete was treated as a probability variable of normal distribution. The tensile strength - considring its mean value and standard deviation - was generated at random for each examined model. The change of tensile strength along the length of the element was disregarded.

Smooth steel bars were considered for reinforcement. Experiments showed that in the case of smooth steel the magnitude of the relative slip is irrevelant to the efficiency of the bond, it is only the direction of the bond stresses, which depends on the direction of the slip. Under these circumstances crack widths can be expressed in an explicit form. (Fig.1.; the true behavior of f_{cb} - denoted with a dotted line in the figure - can be neglected.) There was a stochastic relationship assumed between the bond strength and the tensile resistance of the concrete and its value was supposed to be $f_{cb} = \alpha * f_{ct,i}$. In this relation α is a probability variable of normal distribution the mean value of which is 1 and its variation coefficient was taken as independent of that of the tensile strength. The effects of geometrical features (the cross-section of the concrete, the diameter of the steel bar) as

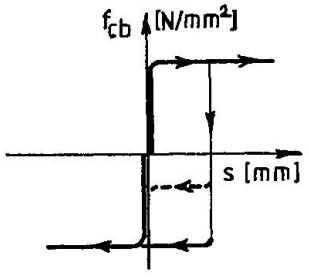

Fig.1 Bond-slip low

well as that of the elastic modulus of the concrete were neglected as being insignificant with regard to the deviation of crack widths.

In the analysis elastic stress condition was assumed and all the time-dependent effects were neglected.

4. CALCULATION OF CRACK WIDTHS

If the tensile stress reaches the value $f_{ct,i}$, the tensile strength of the concrete, Crack 1 is equally probable to appear anywhere along the length of the axially tensed member (Fig.2). Since there is no crack to the right of this one yet, the stress, strain and deformation conditions, being in differential-integral relationship with each-other, can develop freely on the bar. (This state is marked with a continuous line in the figure.) This condition can be called a primary, undisturbed crack width state, and the part of the width of Crack 1 which can be calculated from the relative slip between the concrete and the steel on its right is $s_{1r} = \epsilon_{sr,i} * l_b/2$.

In the case of the next crack (Crack 2), occuring at random with in a distance $l_b \leq l_r \leq 2*l_b$ from Crack 1, the stress and deformation conditions on its left side (see the figure) will not be independent from Crack 1. This situation can be termed as secondary, disturbed crack width state. On the left of Crack 2 - because of the direction of the displacement - there are bond stresses acting in the opposite direction, and it follows from equilibrum eguation that the change of signes takes place at $l_r/2$. In this place and on the left of it (towards Crack 1) the conditions of stress and deformation do not change; on the right side of this place (towards Crack 2) they develop as indicated by the dotted line in the figure 2. It is clear from the figure, that along this distance there is that point where the relative slip between concrete and steel is zero. The relative displacement on the left side of Crack 2 depends on the parameter $\lambda = l_r/l_b$; $s_{21} = s_{1r} * [1 - 2*(1 - \lambda/2)^2]$.

On the left side of the first and of the right side of the second crack there may occur either a primary or a secondary state of crack formation. According to these versions the width of a certain crack can be determined - using the relations above - as the sum of the right-side and the left-side relative slips.

Between two existing cracks a new one can occur if $l_r > 2*l_b$. The new crack can appear anywhere along $l_r - 2*l_b$ with the same probability. Since the tensile strength of the concrete was considered to be constant along the bar, the place of the new crack was determined by deviding the $l_r - 2*l_b$ length in proportion of a random number between 0-1 of equal distribution.

On the bar with $f_{ct,i}$ tensile strength the crack formation is final if the distance between the cracks is less than twice the bond length (l_b). If the fictitious tensile stress, which can be calculated from the external load, exceeds the tensile strength of the concrete - $\sigma_c = N_r/(A_c + A_s * E_s/E_c) > f_{ct,i}$ -, the distance between the cracks does not change, but their width increases. The change in crack width can be expressed by the increment of strain in the reinforcement : $\Delta s = \lambda * \Delta\epsilon_s/\epsilon_{sr,i}$. (See the part of the figure 2 which is drawn with a dot-dash line.) It is clear from the figure that the point which is free of relative slips moves - depending on the magnitude of the stress - towards the midpoint of the distance between the cracks. After all mentioned above it is possible to examine the distribution of the crack distance and crack widths at the end of the crack formation and at any level of the service load.

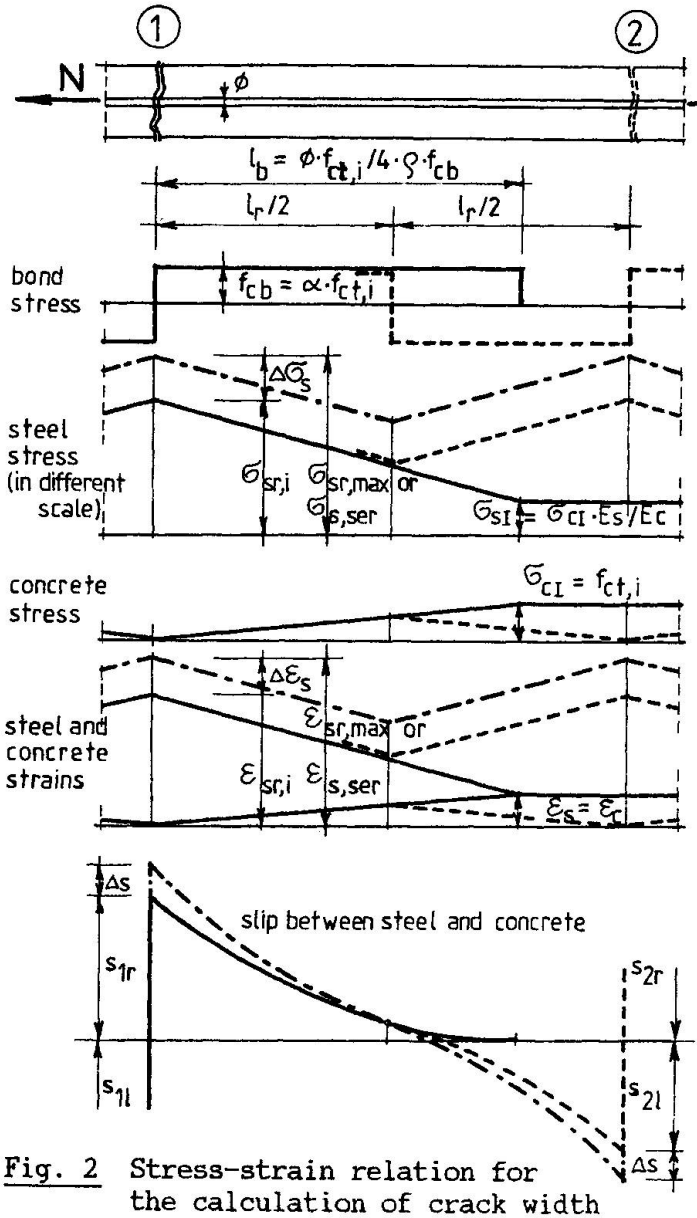

Fig. 2 Stress-strain relation for the calculation of crack width

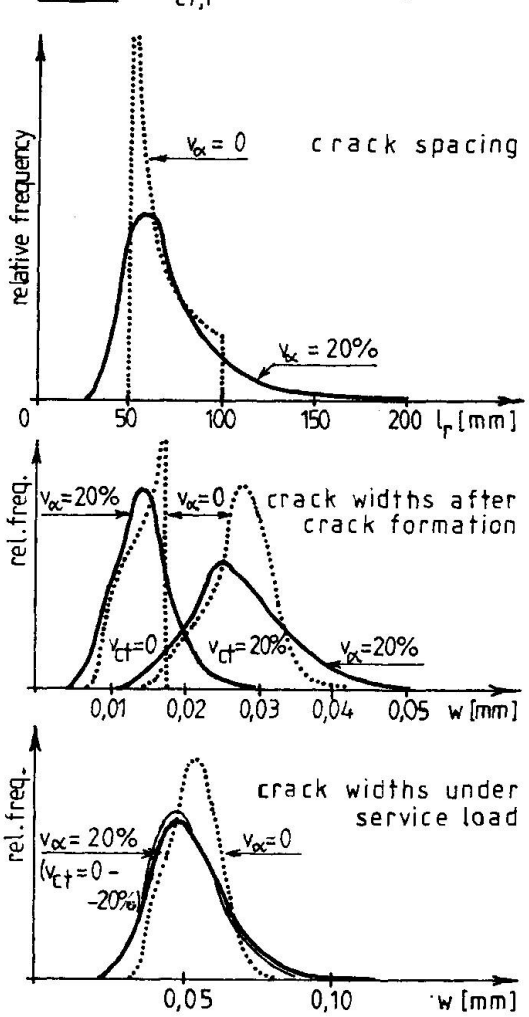

Fig. 3 The types of the distributions

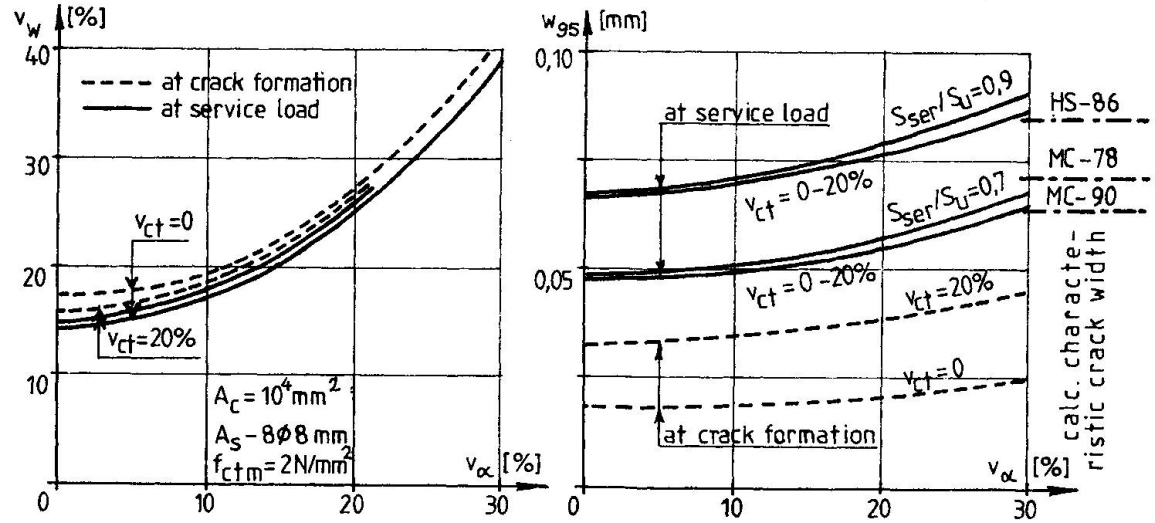

Fig. 4 The coefficient of variation and the 95%-fractile of crack widths related to the variation factors v_{ct} and v_α

The limit state of crack formation is definied by the tension determined by the maximum tensile strength ($f_{ct,max}$) that occured during the examinations, and the strain of the reinforcement ($\epsilon_{sr,max}$) corresponding to this tension. In the serviceability limit state a 0,7 ‰ and a 0,9 ‰ elongation of the steel was considered. The first value reflects the level of the service load according to the CEB-FIP Model Code, the second one reflects it according to the Hungarian standard.

5. RESULTS AND THEIR INTERPRETATION

The distribution were determined on axially tensed members of $f_{ct,m}$ = 2 N/mm² average tensile strength and A_c = 100*100 mm² cross-section, from the data obtained from cca. fifty thousand cracks.In the computer examinations the variation factc of the concrete tensile (v_{ct}) and bond strengths (v_α), just like the reinto: ement of the bar were variable parameters. (The ratio between the moduli of ' 'icity of the steel and concrete was regarded as constant with a value of 10.)

The nature of the distribution of crack spacing and crack widths is shown in the figure 3. The distribution of crack spacing is practically independent from the variation factor of the tensile strength of the concrete, but it is considerably dependent on the bond strength, that is, on the α bond factor. When the bond factor is zero the ratio of the minimum and maximum crack spacing is - as it is well-known - one to two. The character of the distribution is asymmetrical and the variation factor of crack spacing is about 21%. If the variation factor of the bond factor is other then zero the character of the distribution is logarithmically normal, the mean value of the crack spacing is practically constant, but its variation factor - of course - increases. - The statistical distribution of crack widths in the limit state of crack formation depends on the variation factor of both the tensile and the bond strength. The distributions are asymmetrical. At service load the dispersion of tensile strength hardly influences the character of the crack width distribution. Here it is the dispersion of the bond factor again, what affects the nature of the distribution. When the variation factor of the bond factor is about zero the distribution is aproximately symmetrical, in other cases it is of logarithmically normal character - it stretches towards the big crack widths.

In the limit state of crack formation and in the serviceability limit state, the figure 4 shows the variation factor (v_w) and the 95%-fractile of crack width in relation to the variation of the bond factor and the concrete tensile strength in case of 8ø8 mm reinforcement. In case of service load the variation factor is smaller than during crack formation because of the equalization of crack widths, and its value is 14%, even though both the tensile and the bond strength were assumed to be constant. The variation factor of the bond has a great influence on the variation factor of the crack width, somewhat less on its 95%-fractile, whereas the effect of the tensile strength variation factor on the two above is negligible. The slight variations in the size of the concrete cross-section and/or in the steel-diameter does not modify the variation factor and the 95%-fractile of crack widths significantly. The ratio of reinforcement and the steel bar diameter influence neither the distribution type nor the variation factor of the crack width.

Experiments show that the variation factors of tensile and bond strength are nearly the same, about 15-25%, and they are generally higher than that of the compressive strength. Table 1 shows some characteristics of cracks on elements having 8ø8 mm reinforcement, obtained by computer examinations of cases when

the variation factor of the tensile strength was 20% and that of the bond strength was 0,10,20 and 30%. (The strikingly high value of w_{max}/w_m in brackets is from the fact that the distribution of tensile- and bond-strength is not limited.)

Bond v_α [%]	Numerical results v_w[%]	w_{95}/w_m	w_{max}/w_m	Calc.values/num.res. w_k/w_{95} MC-78	MC-90	HS-86	Exp. v_w and $w_{max}/w_m \approx w_{95}/w_m$ S_{ser}/S_u ≈0,7	≈0,9	S_{ser}/S_u ≈0.7	≈0.9
0	14,7	1,25	1,48	1,48	1,33	1,25	on tensed bars		on beams	
10	17,5	1,33	1,83	1,39	1,25	1,20	38,3%-	40,6%-	27,6%-	32,7%-
20	25,3	1,46	(3,15)	1,24	1,14	1,10	-1,89	-2,11	-1,35	-1,76
30	38,2	1,66	(6,15)	1,04	0,94	0,91	21*	35*	20*	27*

Table 1 Comparison of the characteristics of crack widths (* number of cracks)

When comparing the above results with the data from our experiment on tensed and bent elements, relatively good correspondances can be observed. Hereby is presented the ratio of the characteristic value of crack width calculated according to [1],[2] and [3] to the 95%-fractile gained from computer examinations. From these values it is clear that if the deviation of bond strength rather big the 95%-fractile of crack width may exceed the calculated value, what goes to the expense of the security of the structures. It can also be observed that calculation according to [2] and [3] gives better estimations of the fractile than that according to [1].

ACKNOWLEDGEMENT

The author acknowledges the collaboration of Mr. Zoltan BUDAI for the elaboration of the computer program.

REFERENCES

1. CEB-FIP Model Code for concrete structures. 1978.
2. CEB-FIP Model Code for concrete structures. 1990.
3. Design of loadbearing structures of buildings. Reinforced concrete structures. Hungarian standard. MSZ 15022/1-86.

Transient Vibration in Light Frame Floors

Vibration passagère de planchers légers

Vorübergehende Schwingung leichter Unterzugsdecken

Anthony NASH
Consult.
Charles M. Salter Assoc. Inc.
San Francisco, CA, USA

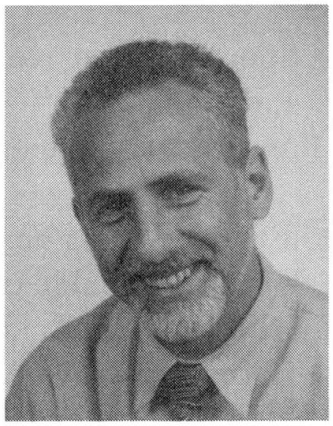

Anthony Nash is an acoustics/vibration consultant practicing in California. He has worked on noise and vibration projects for twenty years. His interest in floor vibration arises from his consulting experience with residential and commercial buildings where occupants have inquired about solutions to low frequency noise and vibration generated by footfalls.

SUMMARY

A number of long span wooden floors in existing buildings were evaluated with the so-called heeldrop test method to simulate vibration from a human footfall. The floor systems behaved differently than predicted from the dynamic model developed for heavy frame floors. The low bending stiffness of the thin floor diaphragm apparently supports a travelling wavefront that causes annoyance to people located far from the impact point.

RESUME

Plusieurs planchers en bois, de grande portée, dans des bâtiments existants, ont été étudiés à l'aide de la méthode d'essai «heeldrop». Utilisant cette méthode, on a simulé la vibration d'un pas humain. Les systèmes de planchers ont réagi différemment de ce que prévoyait le modèle dynamique réalisé pour des planchers de charpentes lourdes. La faible rigidité à la flexion du plancher mince semble permettre la diffusion d'une «onde» désagréable pour les gens situés loin du point d'impact.

ZUSAMMENFASSUNG

Eine Anzahl langbrettiger Holzdecken wurde in bestehenden Gebäuden mittels der sogenannten Fersenfall-Prüfmethode bewertet, um dabei die Schwingung infolge eines menschlichen Fussschrittes zu simulieren. Die Deckensysteme verhielten sich anders als man es von dem dynamischen Modell voraussagte, welches für schwere Decken entwickelt wurde. Die geringe Biegesteifigkeit der dünnen Deckenscheibe unterstützt offensichtlich eine sich ausbreitende Wellenfront, die für Leute, die sich weit vom Auftreffpunkt befinden, eine Störung verursacht.

INTRODUCTION

In the U.S.A., light frame wood floors are economically attractive for low-rise residential and commercial buildings. The floor framing system is usually solid lumber for clear spans up to 6 meters and open web trusses for spans above 12 meters. The framing typically supports a plywood floor diaphragm less than 30 mm thick. Although such floors can safely sustain a uniform load of 500 kg/m^2, the total service load is usually 1/10 of the design limit.

For purposes of discussing floor vibration, we shall divide floor systems into two categories — "short-span" and "long-span." Since short-span floors have been extensively treated in the literature, this paper will focus on long-span systems.

Long-span floors can be constructed using heavy or light framing. Both heavy and light frame long-span floors are capable of exhibiting annoying vibrations when excited by human footfalls. Research in this subject has concentrated on relatively massive concrete floors supported by heavy steel framing. This paper summarizes several field studies of transient vibration in light frame long-span floors.

BACKGROUND

Lenzen and others [1,2,3,4] conducted extensive laboratory and field investigations on heavy long-span floors in the 1960's and 1970's. Their efforts culminated in a quantifiable test method for rating the acceptability of floor systems where people sense the walking of others. Lenzen experimented with several techniques for simulating the effects of a human footfall. He concluded that all the significant parameters of annoyance could be derived from a test impact known as the heeldrop.* The heeldrop is analogous to the use of an instrumented hammer blow used in modal analyses of structures.

The three relevant floor parameters arising from the heeldrop are:

1) peak dynamic displacement
2) frequency of free vibration
3) damping

---

* A heeldrop is generated by an 80 kg person arching his heels up 60 mm on the balls of his feet and then free-falling onto the floor. Figure 1 is a force-time history of a standard heeldrop. The peak force is about 2200 newtons and the duration of the impulse is 50 milliseconds. The force spectrum of the heeldrop transient is well matched to the modal frequency range of long-span floors.

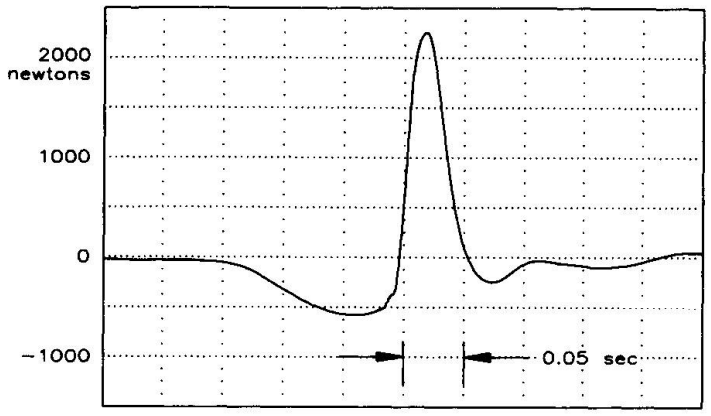

FIGURE 1: HEELDROP FORCE

Although the peak dynamic displacement is generally unaffected by the amount of damping, people are very sensitive to the duration of free vibration induced in the floor by a footfall. Long-span floors with low damping are particularly undesirable because human annoyance increases significantly with duration of the vibration transient.

Lenzen proceeded to develop a vibration annoyance scale based on the response from a standard heeldrop applied to a floor with moderate damping. Figure 2 is a chart illustrating four distinct regions of human perception for the heeldrop test. Each region is bounded by sloping lines that represent products of peak displacement multiplied by frequency (a "pseudo velocity"). In order that ordinary footfalls are sensed as "slightly perceptible," the heeldrop response should not exceed 1.25 [mm-hertz].

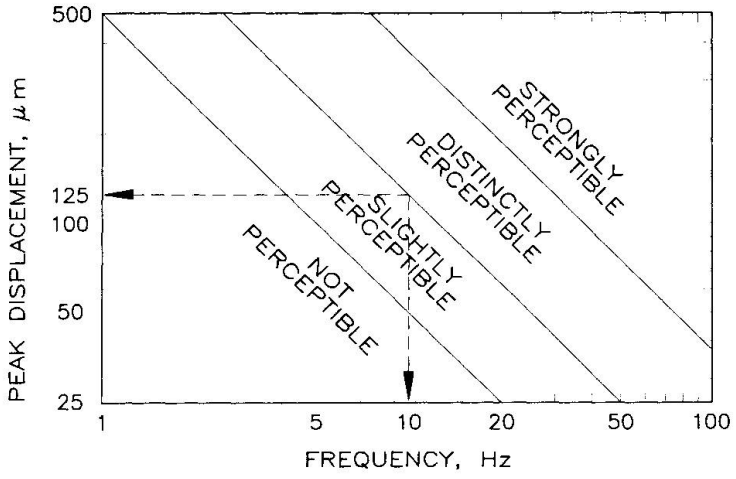

FIGURE 2: VIBRATION ANNOYANCE SCALE

The heeldrop method is useful for characterizing the global performance of a floor in terms of human annoyance. This method is analogous to firing a pistol in a large room to study sound propagation of music and speech. Impulsive excitation generally helps the engineer identify properties of a physical system such as transit speed, early reflections and decay rates. Since damping in multimodal dispersive structures is difficult to predict, the heeldrop test is a more accurate assessment of total system damping because the [viscous] human body absorbs mechanical energy whenever it is in contact with the floor.

The modal behavior of a light frame floor is sensitive to the mass contributed by the person conducting the heeldrop test, hence, the test subject affects the dynamic displacement and modal frequency distribution. In order to circumvent this problem, some researchers [5] prefer to measure the local stiffness of the floor statically or impact it with a lightweight device (e.g., a hammer).

FIELD STUDIES

In the past three years we have evaluated the characteristics of several light frame long-span wood floors. These studies were prompted by people complaining about floor vibration in certain types of buildings. The floors in these buildings were constructed with open web trusses spanning between 10 and 14 meters. Figure 3 is a photograph taken from the underside of a typical floor system. The open web trusses are seen receding into the plane of the paper. The photograph also illustrates some cross-bracing that had been installed in an earlier attempt to alleviate complaints by the occupants. Heeldrop measurements conducted on this floor placed it in the "strongly perceptible" region of the rating scheme.

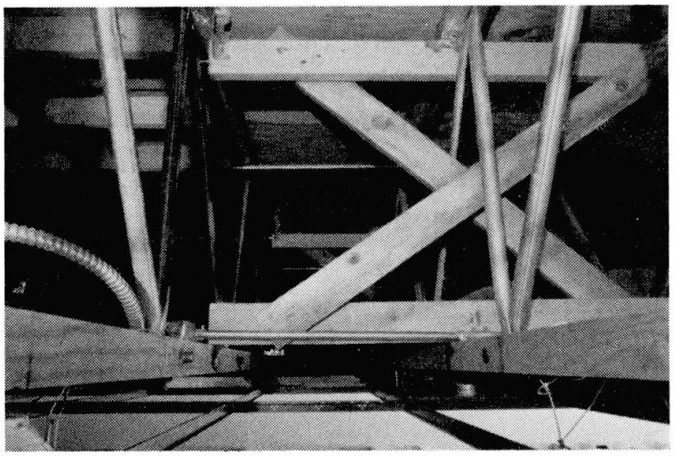

FIGURE 3: VIEW OF FLOOR FRAMING

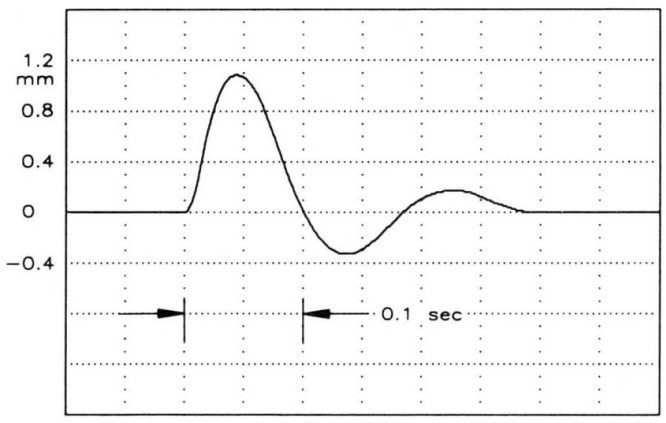

FIGURE 4: FLOOR DISPLACEMENT

Figure 4 is a typical [inverted] displacement-time history measured at the midspan of such a floor. The displacement transient is a rapidly decaying sinusoid having a peak amplitude of 1.1 mm and a free vibration frequency of 5.7 hertz. The product of peak amplitude and frequency is 6.3 [mm-hertz]. Several observers agreed that the response was indeed "strongly perceptible."

DISCUSSION

During these tests, we observed that the transient response using the heeldrop method did not compare well with the floor's steady state response measured with a 45 kg inertial vibration exciter (the peak force of the exciter was 200 newtons). The frequency of the first transverse mode of vibration differed by 10 to 30 percent between the two test methods. To evaluate damping, the exciter was also driven with sinusoidal transients at a frequency centered on the first [steady-state] mode of vibration. The apparent damping measured with this technique depended on the local position of the exciter. Figure 5 is one example of a free vibration decay after the exciter was stopped. The decay over the first 30 decibels was so rapid that the response near the source was dominated by ringing of the electronic filter used to process the accelerometer signal. This characteristic suggested that either the floor system had extremely high damping or that the mechanical energy propagated away from the source.

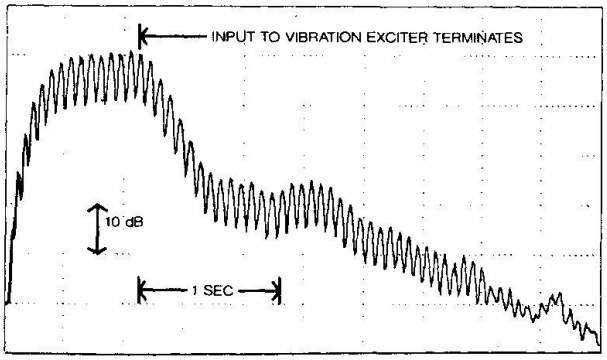

FIGURE 5: DECAY OF FLOOR VIBRATION (7.5 HZ)

Further tests using the heeldrop method tended to confirm the propagation hypothesis. Figure 6 illustrates the acceleration and displacement measured at a joist midspan 10 meters away from the impact point (which was also at a joist midspan). In this figure, the floor received a heeldrop impact at t = 0 and the response commenced t = 100 milliseconds later (propagation speed = 100 meters/second.) The reduction in peak floor displacement from the impact point to the distant measurement location was approximately 20 decibels.

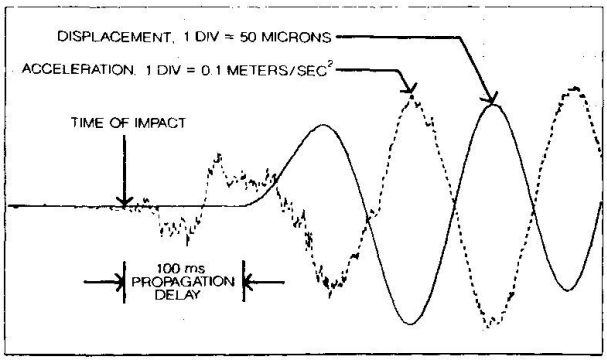

FIGURE 6: VIBRATION 10 METERS FROM HEELDROP

CONCLUSIONS

- When excited by impacts, a thin floor diaphragm with low bending stiffness behaves differently than predicted by the heavy steel frame model.

- Since adjacent joists are dynamically decoupled from the thin floor diaphragm, the relatively slow bending waves ripple outwards with high displacements, annoying people located both near and far from the impact point.

- Improving the vibration characteristics of light frame floors will require either significantly attenuating propagating wavefronts or increasing the bending stiffness of the floor diaphragm so its propagation speed is nearly infinite. An infinite propagation speed means that all joists will resist local impact forces at the same time in inverse proportion to their distance from the impact point.

We wish to acknowledge Trus-Joist MacMillan for their support during the field studies.

REFERENCES

1) LENZEN, K.H., *Vibration of Steel Joist-Concrete Slab Floors*, AISC Journal, Vol 3, No. 3, 1966, pp. 133-136.

2) ALLEN, D. L., *Vibrational Behavior of Long Span Floor Slabs*, Can. J. Civ. Eng., Vol I, 1974, pp. 108-115.

3) WISS, J.F. and PARMELEE, R.A., *Human Perception of Transient Vibrations*, ASCE Structural Journal, Vol 100, 1974, pp. 773-787.

4) MURRAY, T.M., *Design to Prevent Floor Vibrations*, AISC Journal, Third Quarter, 1975, pp. 82-87.

5) OHLSSON, S., *Floor Vibrations and Human Discomfort,* Ph.D. Thesis, Division of Steel and Timber Structures, Chalmers University of Technology, Goteborg, Sweden, 1982.

Dynamic Performance of Australian Domestic Floors

Propriétés dynamiques des planchers de bâtiments australiens

Dynamische Eigenschaften australischer Wohnhausdecken

Lam PHAM
Senior Princ. Res. Scientist
CSIRO
Melbourne, Australia

Jenny H. YANG
Experimental Scientist
CSIRO
Melbourne, Australia

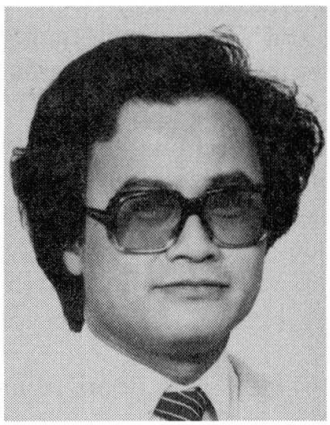

Lam Pham Ph.D., FIE Aust. has been active in research and drafting of Australian Standards in building construction. His main areas of interest are loadings (load combinations, snow and earthquake loads), applied structural reliability, steel and timber design and domestic construction.

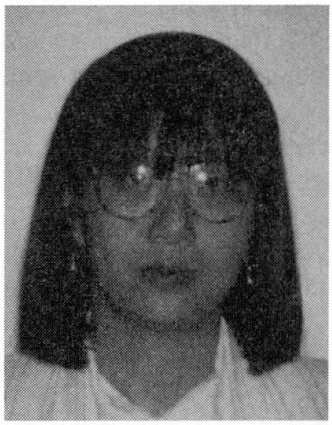

Jenni Yang M.Eng.Sc. works on building systems research and development. One of her main areas of interest is structural serviceability of domestic steel-framing construction, including the development of design criteria, finite element analysis and experimental modelling.

SUMMARY

This paper examines the dynamic characteristics of currently used Australian domestic floors of timber and steel joists with timber decking. The responses of these floors to concentrated loads and to a unit impulse are evaluated.

RESUME

L'article présente les caractéristiques dynamiques des planchers à platelage en bois et poutrelles profilées en bois ou en acier, tels qu'ils sont actuellement réalisés en Australie dans les immeubles à usage d'habitation. Il expose le comportement de ces planchers sous charge concentrée et sous l'effet d'une force impulsive unitaire.

ZUSAMMENFASSUNG

Der Beitrag untersucht die Schwingungsmerkmale von Zwischendecken aus Holz- oder Stahlunterzügen mit Holzbelag, wie sie gegenwärtig in australischen Wohnhäusern Verwendung finden. Dazu wurde das Deckenverhalten unter einer Einzellast und einer Einheitsimpulslast ausgewertet.

1. INTRODUCTION

The current design of Australian domestic light-floor systems has been based on static deflection to ensure that the floors have adequate stiffness. Current deflection limits vary for different types of floor systems or construction materials. The aim of this study is to establish design criteria for dynamic performance independent of construction materials and structural configurations. The paper evaluates, by computation, the dynamic characteristics of Australian domestic floor systems which are currently in use and are known to be satisfactory. The responses of these floors to a concentrated load and to an unit impulse are evaluated.

2. AUSTRALIAN DOMESTIC FLOOR SYSTEMS

2.1 Structural Configurations

This paper covers joist-only flooring systems which represent the majority of upper storey floors in domestic construction. Timber joists are generally either nailed or glued and nailed to the timber floorboards. Steel joists are generally either screwed or glued and screwed to the timber floorboards.

Due to various practical reasons, Australian floor systems are built over a fairly limited range of parameters. Joist spacing is usually 450 or 600 mm. The thickness of floor board is 19 mm for 450 mm joist spacing and 22 mm for 600 mm joist spacing. The range of joist spans is 2–6 m. The sizes of timber joists are given in the Australian National Timber Framing Code [1]. The sizes of steel joists are given by the product manufacturers, such as Lysaght [2] for open C sections or Spantec [3] for box sections.

In this study, three floor systems are examined: (a) timber joist floors; (b) steel joist floors using open C section joists; and (c) steel joist floors using box section joists.

2.2 Current Design Criteria

The current design criteria for Australian domestic light-floor systems is based on controlling static deflection of a single joist under the design loading. The effect of floorboards is neglected. Current deflection limits vary for different types of floor systems:

- for floor system with steel C section joists, the limiting deflection is span/750 under dead load plus live load of 1.5 kPa;
- for floor system with steel box section joists, the limiting deflection is span/500 under dead load plus live load of 1.5 kPa; and
- for floor system with timber joists, the limiting deflection is span/360 or 9 mm under live load of 1.5 kPa.

Individual floor systems designed using these criteria have been found satisfactory in actual practice. It is the purpose of this paper to find a single rational criteria which can be calibrated against these known satisfactory performance.

3. EVALUATION OF DYNAMIC PERFORMANCE

3.1 General

Various parameters have been used in literature for assessing the dynamic performance of floor systems. They include:

- frequency-weighted root-mean-square acceleration of the response caused by a footfall impact [4];

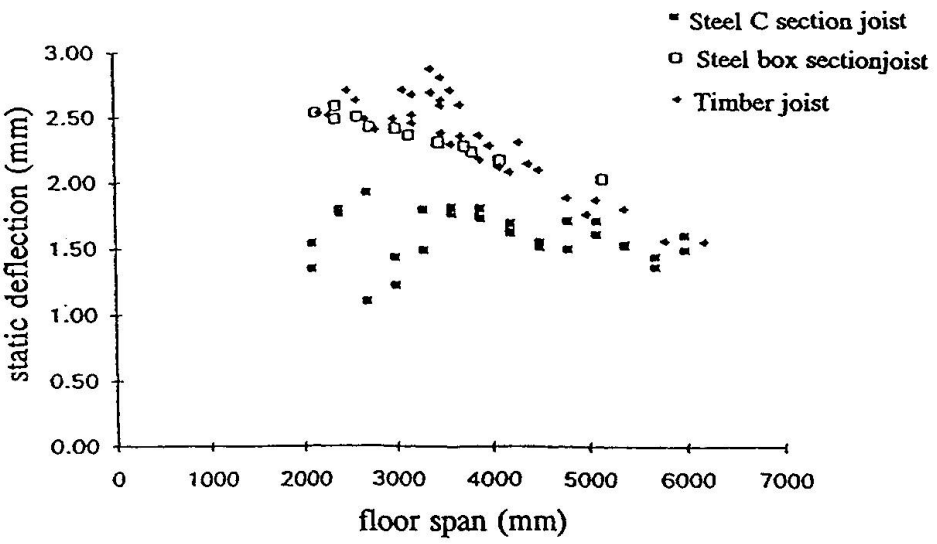

Fig.1 Static deflection of Australian floors to a point load of 1kN

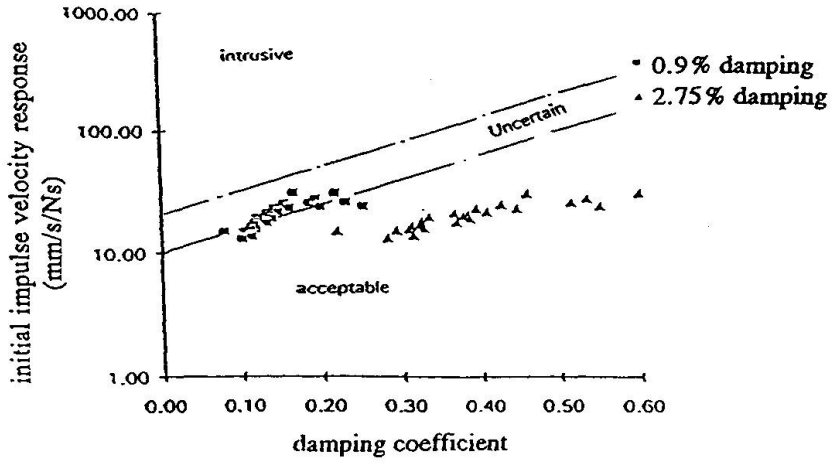

Fig.2 Impulse velocity response of Australian steel joist floors vs damping

- initial impulse velocity response under a idealised vertical force impulse of 1 Ns [5]; and
- static deflection under a concentrated force of 1kN [6].

In this paper, the initial impulse velocity response and static deflection are used to assess the dynamic characteristics of Australian floors.

3.2 Static Deflection Under a Concentrated Load

The static deflection under a concentrated load of 1 kN applied at the centre of the floor has been computed for the range of Australian floors described above. The floor system is modelled as a grid to account for the stiffness of the flooring in the direction normal to the joists, i.e. allowing the concentrated load to be shared between the adjacent joists.

The results are given in Fig.1, where it can be seen that the ranges of the deflections are:

- 1.5–3 mm for timber joist floors;
- 1–2 mm for floors with steel C section joists; and
- 2–2.5 mm for floors with steel box section joists.

It is noted that the above results are computed using the specified design properties of timber and steel as given in the Australian Standards. It is well known that specified timber design properties are generally conservative because of the inherent variability of timber. Timber floors are generally stiffer than anticipated in design.

The Swedish building code suggested a limit of 1.5 mm/kN, and the Canadian Standards suggested a limit of 0.5–1 mm maximum deflection under 1 kN. It appears that Australian floors are considerably more flexible than those in Sweden and Canada.

3.3 Initial Impulse Velocity Response of Australian Floors

Initial impulse velocity response h'_{max} under an idealised vertical force impulse of 1 Ns has been calculated using Ohlsson's formula [5]. The floors are modelled as grillages with simply supported edges. The results are discussed as follows:

3.3.1 Damping effect

Ohlsson proposed that the initial impulse velocity response should be related to the damping ratio, ζ, and the lowest natural frequency of the floor, f_1, because of their obvious effects on human response [5]. The evaluation of the damping ratio is very complicated and depends on uncertainties such as the influence of the occupant, floor coverings, partitions, furnishings. Values quoted in the literature range between 0.8 and 3%. At the design stage, the damping ratio will have to be guessed. Figure 2 shows the initial impulse velocity response plotted against damping coefficient σ_0 ($\sigma_0 = f_1.\zeta$) for the steel joist floors. It illustrates the sensitivity of the dynamic responses to different assumed damping ratios. If dynamic performance criteria is to be established based on this model then it is highly dependent on the assumed damping value.

3.3.2 Floor span

The initial impulse velocity responses have been plotted against the floor spans in Fig. 3 (with floor mass only) and Fig. 4 (with floor mass and 30 kg/m^2 live load) for both steel and timber joist floors. As seen in Figs 2 and 3, both steel and timber joist floor systems have very similar initial impulse velocity responses despite the fact that they have very different stiffnesses, as shown by their deflections under a concentrated load in Fig. 1. This is rather puzzling since it is expected that the initial impulse velocity response would have a strong correlation with stiffness.

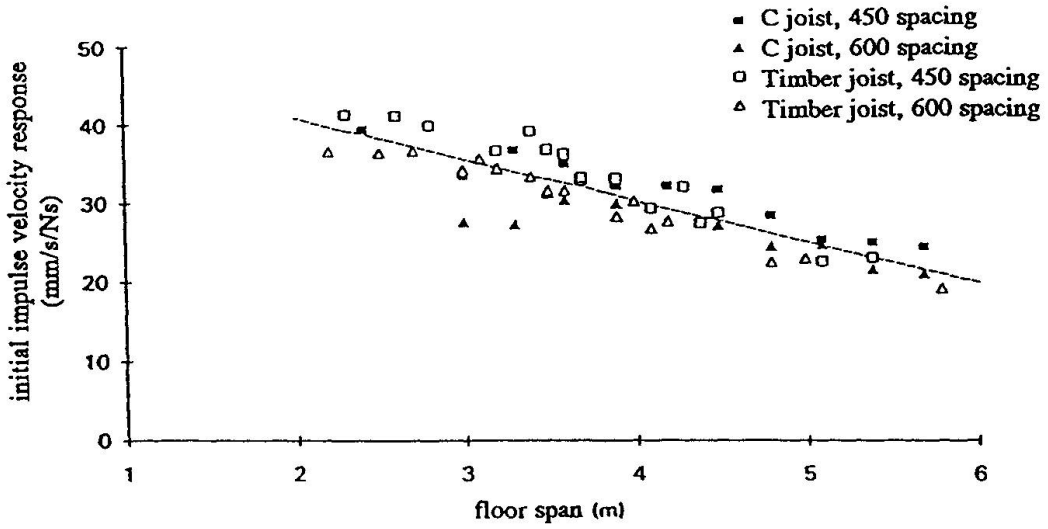

Fig.3 Impulse velocity response of Australian floors vs floor span (with floor mass only)

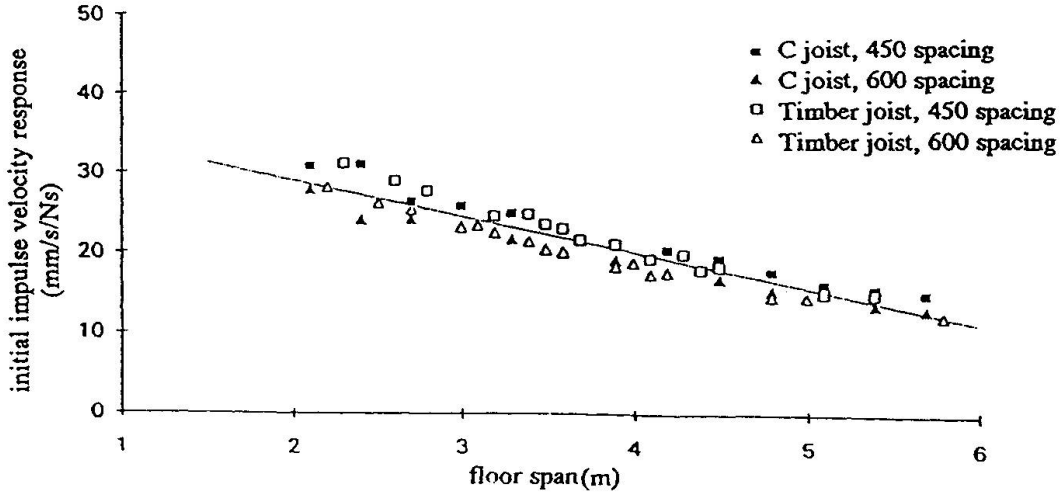

Fig.4 Impulse velocity response of Australian floors vs floor span (with floor mass plus 30kg/mm^2 live load)

The correlation between the initial impulse velocity response and the floor span is strong and appears to be independent of the construction material.

3.3.3 Other design parameters
The following points are also noted from the results:

- The natural frequencies of all floors calculated using Ohlsson's formula [5] are found to be in the range 8–40 Hz. The natural frequency decreases with increasing floor span.
- The ratio of span to width of the floor (L/B) has a relatively insignificant effect on the dynamic responses of the floors. For example, increasing L/B of a given floor system from 0.25 to 1 will change the value of h'_{max} from 13.95 to 13.45 mm/s/Ns.
- Changing the joist spacing from 450 to 600 mm slightly decreases the value of h'_{max} (see Figs 3 and 4).
- Changing the mass of the floor has a much larger effect on the values of h'max see Figs 3 and 4. Increasing the mass of the floor reduces the values of h'_{max}.

4. CONCLUSION

The computed static deflection behaviour under a concentrated load of 1 kN indicates that Australian-designed lightweight floors are more flexible than those in Sweden and Canada, but gives results that appear to be material-dependent.

For the limited range of currently accepted Australian floor systems, the initial impulse velocity response h'_{max} under an unit impulse of 1 Ns appears to be a more consistent dynamic performance indicator. It has strong correlation with floor span and is independent on the construction material of floor systems.

5. REFERENCES

1. STANDARDS AUSTRALIA, AS1684–1992, Australian National Timber Framing Code, 1992.

2. PRODUCT INFORMATION MANUAL, Lysaght Brownbuilt Industries, Australia, 1988.

3. PRODUCT INFORMATION MANUAL, SpanTec Systems Pty Ltd, Australia (Unpublished).

4. CHUI, Y.H. and SMITH, I., 'Proposed Code Requirements for Vibrational Serviceability of Timber Floors', International Council for Building Research Studies and Documentation, Working Commission W18A, Sept. 1987.

5. OHLSSON, S., 'Springiness and Human-induced Floor Vibrations', Swedish Council for Building Research, 1988.

6. CANADIAN STANDARDS, CAN 3–S16.1–M84, Steel Structures for Buildings (Limit States Design), 1984.

7. REARDON, G.F. and KLOOT, N.H., 'Low-rise Domestic and Similar Framed Structures', CSIRO Division of Building Research, 1978.

Vibration Serviceability of Ribbed Plates by Modal Synthesis

Synthèse modale de l'aptitude au service sous vibrations des dalles nervurées

Schwingungseignung von Rippenplatten durch modale Synthese

Ian SMITH
Dr. Eng.
Univ. of New Brunswick
Fredericton, NB, Canada

Lin J. HU
Dr. Eng.
Univ. of New Brunswick
Fredericton, NB, Canada

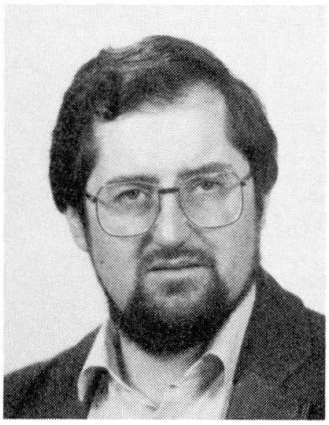

Ian Smith, born 1951, holds bachelors, masters and doctoral degrees in engineering from the Universities of Sunderland, Durham and South Bank respectively. He has spent 15 years researching structural use of wood products. Dr. Smith is professor of Forest Engineering and Director of the Wood Science and Technology Centre.

Lin. J. Hu holds bachelors and masters degrees in engineering from the University of Tsinghua, and a doctoral from the University of New Brunswick. She has spent the last 10 years researching structural vibration and computational mechanics.

SUMMARY

A generalized ribbed plate vibration model is presented, based on the free-interface modal synthesis method. Discussion centres on whether a model can reliably estimate parameters used in design criteria. A conclusion is, for example, that peak velocity of a ribbed plate can be predicted reliably using the authors' model, but not using approximate formulae proposed elsewhere.

RESUME

Les auteurs présentent un modèle généralisé, basé sur la synthèse modale des surfaces de contact, pouvant servir à étudier le comportement des dalles nervurées soumises aux vibrations. La discussion porte sur le fait de savoir si un modèle est vraiment en mesure de fournir des estimations fiables pouvant servir de critères paramétriques de dimensionnement. Le modèle proposé par les auteurs permet, par exemple, de pronostiquer avec une certaine fiabilité la vitesse de crête des vibrations d'une dalle nervurée, alors que d'autres formules approximatives proposées par ailleurs s'avèrent inapplicables.

ZUSAMMENFASSUNG

Für das Schwingungsverhalten von Rippenplatten wird ein verallgemeinertes Modell vorgestellt, das auf modaler Synthese bei freien Grenzflächen basiert. Es wird erörtert, ob überhaupt ein Modell zuverlässige Schätzwerte für die Bemessungsgrössen zu liefern imstande ist. Es ergibt sich, dass zum Beispiel die Spitzenschwinggeschwindigkeit einer Rippenplatte durch das Modell der Autoren zuverlässig vorhergesagt werden kann, während anderswo vorgeschlagene Abschätzformeln versagen.

1. INTRODUCTION

This paper explores the feasibility of applying dynamic serviceability design criteria proposed in documents such as ISO 2631 [1] and Eurocode 5 [2]. The discussion is amplified using a recently developed numerical model for vibration analysis of ribbed plates. The model accounts for various complicating factors such as plate orthotropy, shear deformation and rotatory inertia in ribs, semi-rigid connections between plate and ribs, and intermediate supports. The model is based on the free interface modal synthesis method proposed by Hou [3]. Constraint conditions are enforced at any intermediate supports by means of Lagrange multipliers. The advantage of the new model over existing models is demonstrated in detail by Hu [4]. This model is used here to evaluate the reliability of more approximate models in estimation of parameters used in design criteria.

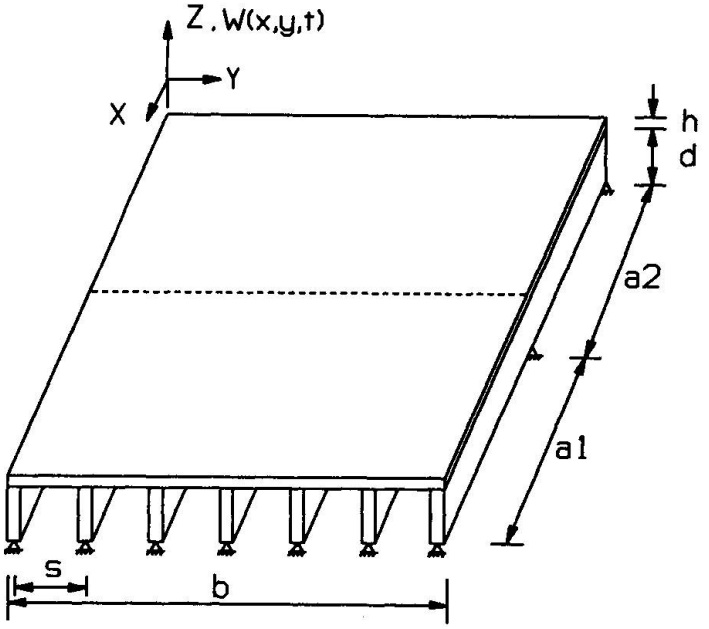

Fig. 1 A typical double-span ribbed plate arrangement

2. THEORY

A brief summary is given here of the theory on which the new model is based [4,5]. A representative rectangular double span ribbed plate is shown in Figure 1. It is assumed that transverse displacement (W) dominates the displacement of the system; small deflection theory is valid; the ribs may be rigidly or semi-rigidly attached to the plate; and intermediate rigid line supports cross the plate perpendicular to the ribs.

By modal expansion, the transverse motions of the uncoupled substructures, i.e. plate and jth rib, are

plate: $$W_p(x,y,t) = \sum_{m=1}^{M} \sum_{n=1}^{N} q^p_{m,n}(t) X^p_m(x) Y^p_n(y) \qquad (1)$$

jth rib: $$W_r^j(x,t) = \sum_{k=1}^{K} q_k^j(t) X_k^j(x) \qquad (2)$$

where the subscripts m,n define the modes selected for modelling motion of the plate; k defines the modes selected for modelling motion of the jth rib; and

q_k^j, $q_{m,n}^p$ = modal coordinate functions,

X_k^j, X_m^p, Y_n^p = mode shape functions.

The kinetic and potential energies (in plate modal coordinates) are for a ribbed plate are

Kinetic energy:

$$T = \frac{1}{2} \sum_{m=1}^{M} \sum_{n=1}^{N} (\dot{q}_{m,n}^p)^2 M_{m,n} + \sum_{j=1}^{J} \frac{1}{2} \sum_{k=1}^{K} (\dot{q}_k^j)^2 M_k^j \qquad (3)$$

Potential energy:

$$U = \frac{1}{2} \sum_{m=1}^{M} \sum_{n=1}^{N} (q_{m,n}^p)^2 \omega_{m,n}^2 M_{m,n} + \sum_{j=1}^{J} \frac{1}{2} \sum_{k=1}^{K} (q_k^j)^2 (\omega_k^j)^2 M_k^j \qquad (4)$$

where

M_k^j, $M_{m,n}$ = modal mass terms,

$\dot{q}_k^j$, $\dot{q}_{m,n}^p$ = modal velocity terms,

ω_k^j, $\omega_{m,n}$ = angular natural frequency terms.

In the analysis the modal characteristics of substructures are obtained first. Two-dimensional theory of flexural vibration of an orthotropic elastic plate is used to determine characteristics of the plate. One-dimensional Timoshenko beam theory is used for the ribs, allowing inclusion of the effects of transverse shear deformation and rotatory inertia. To simulate the semi-rigid nature of connections between plate and ribs, an effective flexural rib rigidity is used, Smith [6].

Two sets of constraint equations are needed. One set is applied to synthesize the plate and rib substructures (to form the ribbed plate) and may be expressed as

$$W_p(x,y^j,t) = W_r^j(x,t) \qquad (5)$$

This is transformed into the modal coordinate system, by substituting equations (1) and (2) in equation (5). Another set of constraint equations is needed to satisfy the zero transverse displacement requirements at intermediate rigid line supports. Let the location of the line support be at x = c. The constraint equations in modal coordinates are

$$\sum_{m=1}^{M} q^p_{m,1} X^p_m(c) = \sum_{m=1}^{M} q^p_{m,2} X^p_m(c) = \ldots \sum_{m=1}^{M} q^p_{m,N} X^p_m(c) = 0 \qquad (6)$$

To form the generalized forced vibration equations, it is assumed that a transverse force of arbitrary form acts normal to the surface of the plate. The force may be expressed as

$$P(x,y,t) = p(x,y)f(t) \qquad (7)$$

The elements of the modal force vector **Q** are

$$Q_i = \int_0^b \int_0^a X^p_m(x) Y^p_n(y) p(x,y) f(t) dxdy \qquad (8)$$

Applying Lagrange's equations in conjunction with the constraint equations, and adding a damping matrix, forced vibration equations of a ribbed plate are of the form

$$\mathbf{M}\ddot{\mathbf{q}} + \mathbf{C}\dot{\mathbf{q}} + \mathbf{K}\mathbf{q} = \mathbf{Q} \qquad (9)$$

The modal damping matrix **C** can be calibrated from experimental estimates of viscous damping ratios, Warburton [7]. A computer program implements the above under selected combinations of plate support conditions.

3. VERIFICATION

Verification testes were carried out on a series of single and double span ribbed plates built with wood I-joists [4,5]. Comparison has also been made with test results reported by Ohmart [8] who studied forced vibration response of concrete slabs with steel I-joist ribs. Figure 2 illustrates how predictions of maximum displacement amplitudes from the authors' model compare with test observations, and Ohmart's own model predictions. Systems 1 and 2 had spans of 4.47m and variable widths [8]. It can be seen that predictions with the model reported here are relatively good. As the new model has been found to predict natural frequencies and peak displacements under harmonic forces with reasonable accuracy (over a range of systems), it is concluded that velocity or acceleration predictions will be reliable.

Section 4 of this paper contains further indications of the level of agreement attained between the authors' model and test observations.

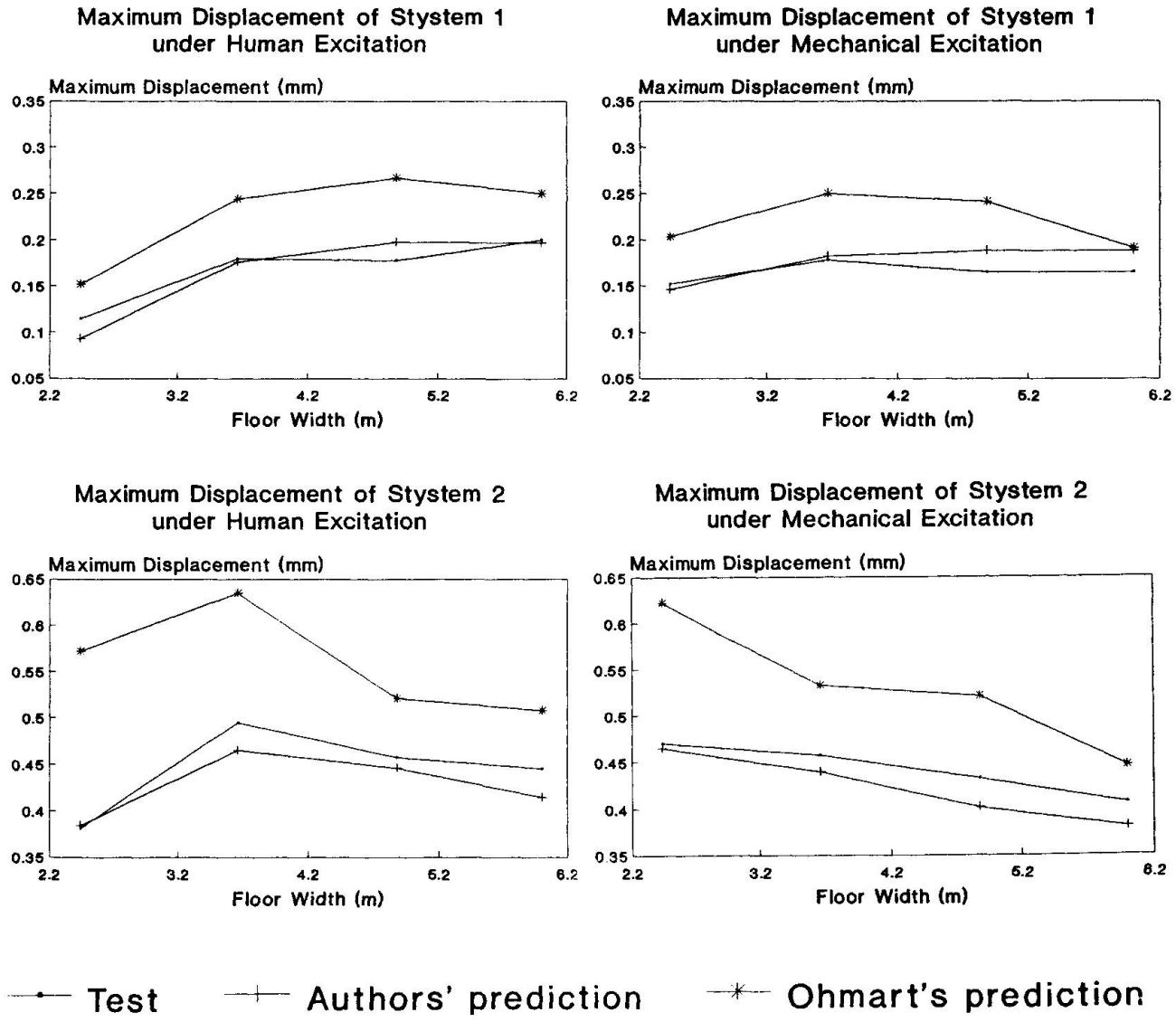

Fig. 2 Predicted vs. test maximum displacement of steel-concrete floors

4. PREDICTING VIBRATIONAL SERVICEABILITY OF FLOORS

Feasibility of applying the authors' ribbed plate model, or other more approximate models, within serviceability design of floors was investigated. Contemporary criteria require that models used in design be capable of predicting parameters such as fundamental natural frequency, N40 the number of natural frequencies less than 40 Hz and initial peak velocity [1,2]. Three types of systems have been analyzed: lumber joist system [9], wood I-joist system [4] and concrete slabs with steel I-joists [8]. Over 100 systems have been considered, but due to lack of space only an illustrative sub-set will be discussed here.

Ohlsson presents approximate design formulae for predicting fundamental natural frequency, N40 and peak velocity under a 1 Ns impulsive force [2]. These approximations are intended for predicting behaviour of systems simply supported on all edges (single span) and having natural frequencies greater than 8 Hz. Because the formulae are incorporated in draft Eurocode 5, the predictions are labelled 'Eurocode 5'. Table 1 compares test measurements with predictions by the authors' model, models developed by Ohmart [8] and Chui [9] and Eurocode 5 method. It should be noted that Ohmart only provided test and predicted frequencies for the fundamental mode. The comparison in Table 1, and other comparisons not reported here, suggests that, generally, there are large discrepancies between peak velocities predicted by Eurocode 5 formulae and by more rigorous analytical models. In the case of the Eurocode 5 formulae, N40 is used as the basis of predictions of peak velocity. Part of the discrepancies can be attributed to the inability of the Eurocode 5 formulae to reliably predict N40. It is acknowledged that for vibrational serviceability design of highly orthotropic systems, the concept of accounting for higher vibration modes is a reasonable proposition. However, the results presented here suggest that, almost inevitably, many simplifying assumptions made in the Eurocode 5 approach will be violated by practical floor systems. To ensure reliable predictions, more rigorous analysis must be employed.

Floor	Approach	Fundemamtal Frequency (Hz)	N40	Peak velocity (m/s/Ns × 10^{-2})
Chui [9]: Foor 6	Test	22.3	3	
	Chui-model	21.1	2	
	Eurocode 5	18.5	3	2.28
	Authors-model	21.6	2	2.11
Hu [4]: Floor 2	Test	11.2	6	
	Eurocode 5	10.4	5	2.0
	Authors-model	10.9	6	1.12
Floor 4	Test	13.1	5	
	Eurocode 5	13.9	5	2.18
	Authors-model	14.1	5	1.22
Floor 6	Test	17.1	4	
	Eurocode 5	24.9	5	2.69
	Authors-model	22.0	4	1.39
Ohmart[8] 1-5B	Test	18.8		
	Ohmart-model	16.8		
	Eurocode 5	13.9	3	0.159
	Authors-model	17.6	2	0.070
1-4B	Test	20.8		
	Ohmart-model	18.6		
	Eurocode 5	14.8	2	0.141
	Authors-model	19.3	2	0.067
1-3B	Test	25.9		
	Ohmart-model	22.8		
	Eurocode 5	18.0	2	0.184
	Authors-model	23.7	1	0.086
1-2B	Test	35.7		
	Ohmart-model	36.1		
	Eurocode 5	30.5	1	0.166
	Authors-model	37.5	1	0.095
2-5B	Test	15.6		
	Ohmart-model	15.3		
	Eurocode 5	16.7	2	0.196
	Authors-model	16.3	3	0.140
2-4B	Test	16.7		
	Ohmart-model	15.9		
	Eurocode 5	18.2	2	0.237
	Authors-model	16.9	2	0.142
2-3B	Test	18.5		
	Ohmart-model	17.7		
	Eurocode 5	23.2	1	0.191
	Authors-model	18.8	2	0.149
2-2B	Test	23.8		
	Ohmart-model	24.2		
	Eurocode 5	41.7	1	0.269
	Authors-model	25.6	1	0.221

Table 1 Predicted vs. test natural frequencies, and initial peak velocities under 1 Ns impulse

5. CONCLUSION

The above shows that the responses of ribbed plates, such as displacement and velocity, can be predicted reasonably accurately for a standardized impulsive force. However parameters such as N40 used by Eurocode 5 may not always be predicted accurately. Approximate formulae such as those in Eurocode 5 introduce too many assumptions to give consistently reliable predictions of initial peak velocity.

REFERENCES

1. INTERNATIONAL ORGANIZATION FOR STANDARDIZATION, Guide for the evaluation of human exposure to vibration. ISO Standard 2631, Geneva, IOS, 1978.
2. OHLSSON S.V., Serviceability criteria - especially floor vibration criteria. Proceedings of the 1991 international timber engineering conference, 2-5 September, 1991, London, United Kingdom.
3. HOU S.N., Review of modal synthesis techniques and a new approach. The Shock and Vibration Bulletin, **40**, Part 4, 25-30/1969.
4. HU L.J., Prediction of vibration responses of ribbed plates by modal synthesis. Ph.D. Thesis, University of New Brunswick, Canada, 1992.
5. HU L.J., SMITH I. and CHUI Y.H., Vibration analysis of ribbed plates with rigid intermediate line support. Journal of Sound and Vibration. (Submitted Septmber 10th, 92)
6. SMITH I., Series type solutions for built-up timber beams with semi-rigid connections. Proceedings of Institution of Civil Engineers, Part 2. **69**, 707-719/1980.
7. WARBURTON G. B., The dynamical behaviour of structures. Pergamon Press, Oxford, 1976.
8. OHMART R.D., An approximate method for the response of stiffened plates to a periodic excitation. Ph.D. Thesis, University of Kansas, USA, 1968.
9. CHUI T.H., Vibrational performance of wooden floors in domestic dwellings. Ph.D. Thesis, Brighton Polytechnic, UK, 1987.

Influence of Concrete Cracks on Floor Vibration

Influence de la fissuration sur la vibration des planchers en béton

Einfluss der Rissbildung auf die Schwingung von Betondecken

G.J. KRIGE
Civil Eng.
Univ. of Witwatersrand
Wits, South Africa

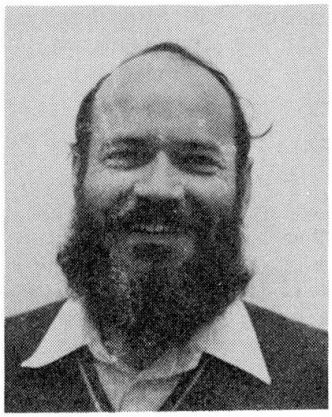

Geoff Krige has degrees from the Universities of London and the Witwatersrand. He has research and consulting interests in structural vibration and steel construction.

SUMMARY

The vibration of suspended floors, generated by various human activities, is widely recognised as an important serviceability criterion. Cracked slabs have a reduced stiffness, leading to greater static deflection and lower natural frequencies, both of which detrimentally influence vibration. Measurements of isolated slabs and complete floors, together with a theoretical analysis, are used to quantify the effect of cracking.

RESUME

Les vibrations résultant d'activités humaines sur les planchers suspendus représentent un critère d'aptitude au service largement admis. La fissuration de dalles en béton entraîne une réduction de la rigidité et, de ce fait, une augmentation des flèches sous charge statique et une diminution de la fréquence propre; ces deux derniers facteurs influencent négativement le comportement aux vibrations d'un élément porteur. Les mesures effectuées sur des dalles isostatiques et des systèmes hyperstatiques de planchers, combinées à l'analyse théorique, servent à quantifier les effets de la fissuration.

ZUSAMMENFASSUNG

Durch menschliche Tätigkeiten hervorgerufene Schwingungen sind ein anerkannt wichtiges Gebrauchstauglichkeitskriterium für abgehängte Geschossdecken. Der Steifigkeitsabfall in Betonplatten infolge Rissbildung führt zu grösserer statischer Durchbiegung und tieferen Eigenfrequenzen, was beides das Schwingungsverhalten nachteilig beeinflusst. Messungen an Einzelplatten und Deckensystemen werden zusammen mit theoretischer Analyse dazu verwendet, den Einfluss der Rissbildung zu quantifizieren.

1. INTRODUCTION

It is increasingly evident that floor vibration in office and residential buildings is an important serviceability consideration, particularly when dealing with light long span floors. Several recent studies have been reported on this topic [1,2,3,4].

Many different factors influence the vibration amplitudes which may be experienced, one of which is the stiffness of the floor structure. Typically floors are constructed in concrete or compositely. The concrete may be either conventionally reinforced or pre-tensioned. The stiffness of concrete is significantly influenced by any cracking of the concrete, whether this is due to shrinkage or stresses exceeding the tensile strength of the concrete. It is thus of interest to investigate the influence of this cracking on the vibration characteristics of the concrete portion of floors.

2. MEASUREMENTS OF BEHAVIOUR

Physical measurements of isolated concrete slabs and of completed floors in two buildings are reported. The measurements on the isolated slabs facilitate an understanding of the direct influence of cracking of concrete slabs, whilst the measurements on complete building floors give allow an overview of the broader implications of cracking of concrete.

2.1 Isolated precast slabs

Two different types of hollow precast concrete slabs have been tested in a simply supported condition using a span of 2,38 m and a central line load across the full width of the slab. This testing layout is shown in the photograph in figure 1.

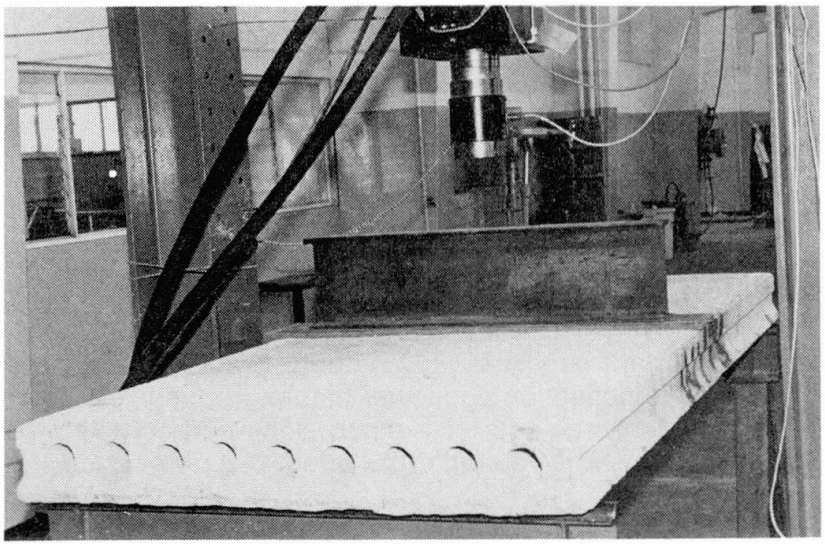

Figure 1: Photograph of Slab Testing Layout

2.1.1 Tests Conducted

In both cases, a total of three different tests was conducted. These were as follows:

(a) Dynamic test on the uncracked slab, to establish dynamic stiffness and the fundamental natural frequency.
(b) Static test to the ultimate load of the slab.
(c) Dynamic test on the cracked slab, to establish the new dynamic stiffness and fundamental natural frequency.

In the measurement work on some of the slabs, tests (a) and (c) were done at both a low level of static load, giving a stress which remained below the prestress, and at a high level of static load, giving a stress exceeding the prestress. Typical dynamic stiffness results are shown in figure 2. These dynamic stiffness values are calculated by plotting load vs deflection and calculating the slope of the resulting graph. The natural frequency is taken as that frequency at which the dynamic stiffness curve passes through 0, ie where the phase angle between load and deflection changes sign.

2.1.2 Slabs Tested

Tests on a total of three nominally identical prestressed slabs are reported. These slabs are 1170 mm wide and 155 mm deep with 10 steel tendons of 5 mm diameter

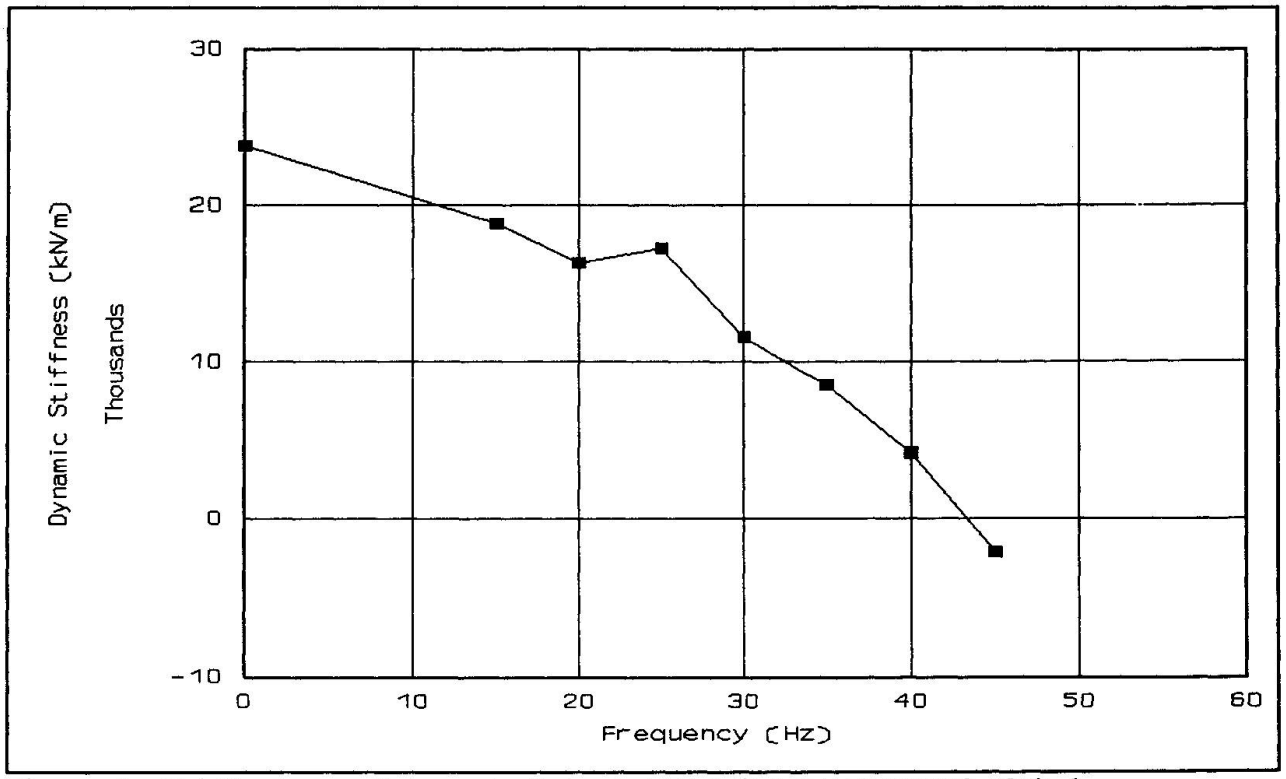

Figure 2: Stiffness vs Frequency Measurements for Prestressed Slab 1

at e depth of 130 mm. The measured mass, static stiffness, and fundamental natural frequency for each of the prestressed slabs are listed in table 1.

Tests on a total of two nominally identical plain reinforced slabs are also reported, and the results are listed in table 1. These slabs are 890 mm wide and 150 mm deep having 7 reinforcing bars of 6 mm diameter at a depth of 140 mm.

2.1.3 Influence of Vibration on Cracks

In no case is there any evidence of an influence on the crack size due to the applied vibration stresses. The vibration loads in the tests quoted have a magnitude of between 10% and 35% of the load required initially to crack the concrete. The test procedure prior to cracking of the beam requires that the beam be subjected to approximately 20000 cycles of this load, which has not shown any initiation of cracking. Subsequent to cracking the beam is subjected to approximately a further 30000 cycles, again showing no obvious extension of the crack size.

2.2 Floors in completed buildings

Vibration test on floors in two different buildings are reported here. The tests in each building are on floors of nominally identical construction, but differing in load history, and having different levels of static load. The construction of both buildings is complete. In both cases tests are reported for an unoccupied area with thin carpet finishes only, and for a fully furnished and occupied office area. There are thus differing levels of cracking. In both cases the load applied is an impulse load obtained by dropping a specified mass 200 mm onto a rubber pad. This load is designed to approximate a heel drop load, but is applied over a shorter time period of 0,02 s. The applied load and the floor acceleration at mid-span of the slab and at quarter span in both directions are recorded.

Tests on two buildings are reported. Building 1 has a continuous cast-in-situ flat floor slab which is 150 mm thick, and which has one way post-tensioning. The span between columns is 5 m in both directions. The mass dropped in these tests is 4 kg. The fully occupied area in this building is a library area with full height partitions along the column lines and heavy shelving containing books along two sides. The measured loads and peak acceleration responses are listed in table 2.

Slab Test	Condition	Mass kg/m	Stiffness kN/m		Fundamental Freq. Hz	
			Low load	High load	Low load	High load
Prestressed 1	Uncracked	338	22727	22727	40	-
	Cracked	338	-	2725	42	-
Prestressed 2	Uncracked	334	23810	-	43	-
	Cracked	334	-	4200	-	25
Prestressed 3	Uncracked	331	22571	25240	48	52
	Shallow crack	331	22105	10015	-	-
	Deep crack	331	22105	3162	46	24
Reinforced 1	Uncracked	224	8924	8924	33	-
	Cracked	224	3175	3175	22	-
Reinforced 2	Uncracked	229	11911	11911	40	-
	Cracked	229	6804	5972	28	29

Table 1: Results of Isolated Slab Tests

It is found that the 4 kg mass does not impart sufficient energy to this floor to enable any assessment of natural frequency to be made.

Building 2 has a floor which consists of 150 mm thick plain reinforced precast slabs, simply supported and spanning 5.7 m between steel beams. The steel beams are 457x152x60 kg/m I sections, which span 6.34 m. The mass dropped in these tests is 10 kg. The fully occupied area in this building is a high density general office area, with 1,2 m high partitions at approximately 3 m centres defining work areas for four people. The measured loads, natural frequencies, and peak acceleration responses are listed in table 2.

Building	Floor Occupancy	Peak Load kN	Natural Freq. Hz	Peak Accel. m/s^2
Cast-in-situ post-tensioned slab	Unoccupied	2,7	-	0,5
	Library	2,7	-	4,0
Plain reinforced precast slabs	Unoccupied	5,4	8,5	2,3
	Dense office	4,9	7,8	3,1

Table 2: Measured Full Floor Responses

Of particular interest with the measurements recorded in table 2, is to assess them against some acceptability criteria. A convenient criterion is that defined by SABS0162 [5], which permits a peak acceleration of, say 1,2 m/s^2 if a fairly high level of damping exists. It can be seen in table 2 that in both cases the acceleration amplitude is higher on the occupied floor, and in the case of the post-tensioned floor the acceleration on the unoccupied floor is acceptable, whereas that on the occupied floor is no acceptable.

3. THEORETICAL ANALYSIS

The theoretical study concentrates on a simple computer based analysis of the response of floor slabs equivalent to the prestressed slabs tested. This theoretical analysis is done using three different crack conditions and two different dynamic loads. The different crack conditions considered are:

- uncracked.
- a crack extending 55 mm above the beam soffit.
- a crack extending 105 mm above the beam soffit.

The beams are modelled as five separate elements, making up a simply supported beam as shown in figure 3, with a span of 2,38 m. All the elements are modelled with the measured mass per metre and an elastic modulus of 27 GPa. In order to introduce a more realistic span length, the analysis is repeated for an assumed span of 5,0 m. The outer two elements at each end of the beam are modelled with the full second moment of area, which is $0,335 \times 10^{-3}$ m^4. The cracking of the concrete will lead to localised variations in the stiffness, which is modelled in the central element, which has a second moment of area which is reduced to $0,090 \times 10^{-3}$ m^4 and $0,0278 \times 10^{-3}$ m^4 for the two different crack depths used. The length of the central element is assumed to be equal to the depth of the beam on each side of the crack, to allow for the full development of strains in the remaining uncracked concrete.

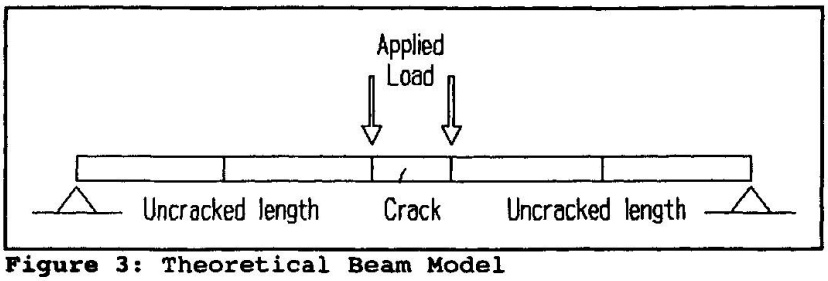

Figure 3: Theoretical Beam Model

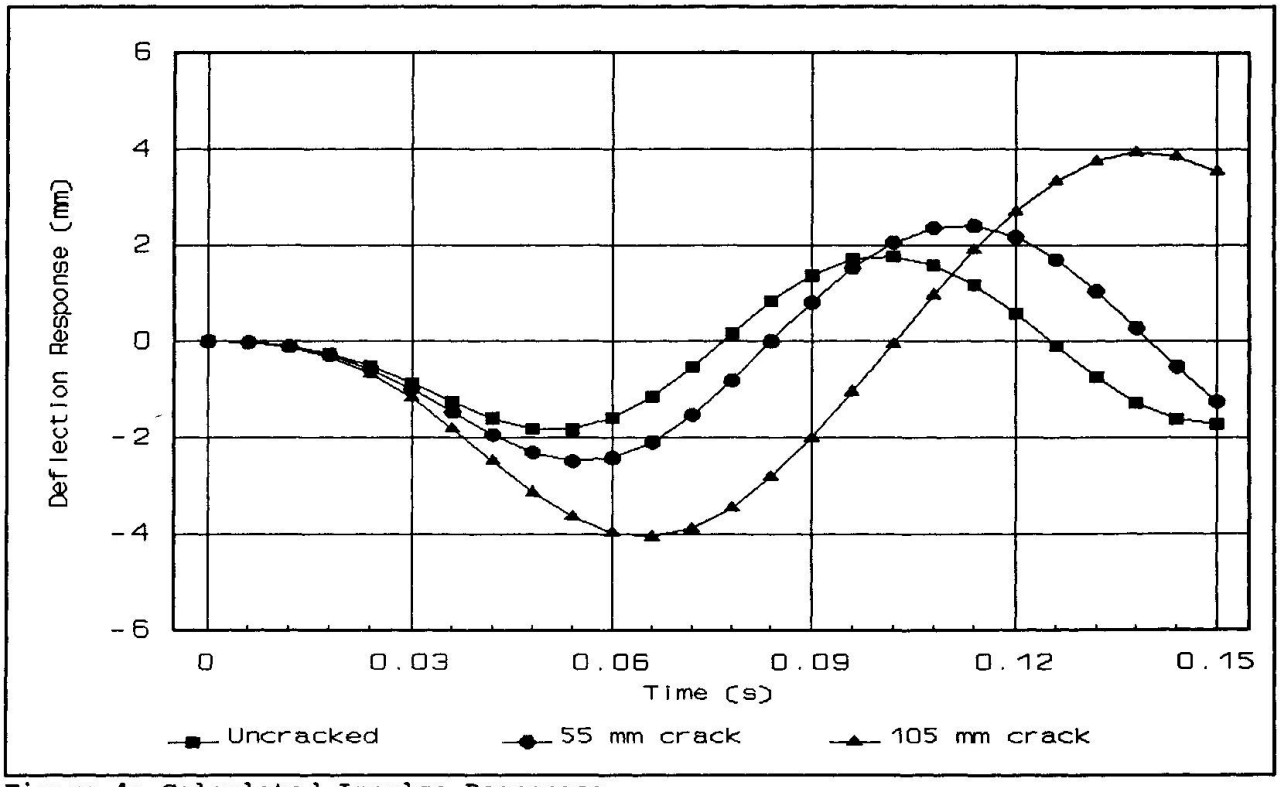

Figure 4: Calculated Impulse Responses

Two different loads are considered in this theoretical analysis:

- a load of 0,6 kN, at a frequency of 8 Hz. This assumed load is based on the work of Allen [3], which deals with loads generated by aerobics exercises, and assuming four people on the beam and the third harmonic.
- a triangular impulse load, to approximate a heel drop load, rising to a peak of 5 kN and dropping back to zero over a time period of 0,07 s. The calculated deflection vs time curves for this impulse load on the three beams, are shown in figure 4.

The results of these analyses are all listed in table 3.

4. DISCUSSION OF RESULTS

It is clear from the preceding measurements and analyses that cracking of concrete will alter the vibration amplitudes of the floor. This alteration in amplitudes results directly from the stiffness variations, and indirectly from the reduction

Load	Beam Condition	Natural Frequency Hz		Max. Disp. Response mm	
		2,38 m	5,00 m	2,38 m	5,00 m
0.6 kN at 8 Hz	Uncracked	45,4	10,3	0,018	0,429
	55 mm crack	35,0	8,9	0,034	1,231
	105 mm crack	23,4	6,7	0,088	1,131
Impulse	Uncracked	45,4	10,3	0,129	1,828
	55 mm crack	35,0	8,9	0,246	2,488
	105 mm crack	23,4	6,7	0,787	4,063

Table 3: Theoretical Results of Beam Vibration

in natural frequencies and mode shapes of the floor, which influence the manner in which the floor responds to applied dynamic loads.

Four factors emerge from this study. First, the stress fluctuations caused by the normal levels of vibration expected in a building are insufficient to cause cracking or extend existing cracks. An uncracked concrete beam thus behaves as if the full concrete section is active, resisting both compressive and tensile strains.

Second, the influence of cracks is to reduce the stiffness, thereby increasing static deflections and reducing the natural frequency. There is thus a compounding effect on the deflection, or acceleration, response to vibrations as lower natural frequencies usually result in higher dynamic amplification.

Third, the effect of prestressing is to override the influence of cracks if the general level is less than the prestress. This is shown in table 1, where it can be seen that neither the stiffness nor the natural frequencies of the prestressed beams are significantly by cracking when the general loads are low. The vibration characteristics of any form of prestressed concrete floor, are thus influenced by both the extent of cracking and the level of general loading on the floor.

Fourth, where vibration testing of floors is undertaken to establish acceptability in terms of some serviceability criteria, this testing should preferably be carried out once the floor is fully furnished and occupied. Should testing be done immediately on completion of floors, it is possible that the test results will record a rather different vibration response than may be evident at a later stage.

It is thus apparent that the vibration amplitude of cracked concrete floors may be significantly more than that of uncracked concrete floors, so it is recommended that dynamic design procedures should consider concrete floors to be cracked, even when the vibration stress amplitude is insufficient to cause cracking. This is particularly true in the case of lightly prestressed concrete floors, where the normal working stress levels may be sufficient to exceed the prestress.

5. REFERENCES

1. FOSCHI R.O. and GUPTA A., Reliability of Floors under Impact Vibration. Canadian Journal of Civil Engineering, No 14, 1987.

2. MURRAY T., Floor Vibration in Buildings - US Practice. Trends in Steel Structures for Mining and Industry. SAISC/IABSE Conf., August 1991.

3. ALLEN D.E., Floor Vibrations from Aerobics. Canadian Journal of Civil Engineering, No 17, 1990.

4. WYATT T.A., Design Guide on the Vibration of Floors. Steel Construction Institute, 1989.

5. SABS0162, The Structural Use of Steel. South African Bureau of Standards, Pretoria, 1992.